DIAGNOZA - GENEZA - PROGNOZA => PODSTAWA KAŻDEJ DECYZJI

POLSKIE TOWARZYSTWO DIAGNOSTYKI TECHNICZNEJ
PTDT

afiliowane przy

Wydziale Nauk
Technicznych
Polskiej Akademii Nauk

Diagnostyka

ISSN 1641-6414

Nr 4(56)/2010

WYDAWCA:
Polskie Towarzystwo Diagnostyki Technicznej
ul. Narbutta 84
02-524 Warszawa

REDAKTOR NACZELNY:
prof. dr hab. inż. **Ryszard MICHALSKI**

SEKRETARZ REDAKCJI:
dr inż. **Sławomir WIERZBICKI**

CZŁONKOWIE KOMITETU REDAKCYJNEGO:
dr inż. **Krzysztof LIGIER**
dr inż. **Paweł MIKOŁAJCZAK**

ADRES REDAKCJI:
Redakcja Diagnostyki
Katedra Budowy, Eksploatacji Pojazdów i Maszyn
UWM w Olsztynie
ul. Oczapowskiego 11
10-736 Olsztyn, Poland
tel.: 89-523-48-11, fax: 89-523-34-63
www.diagnostyka.net.pl
e-mail: redakcja@diagnostyka.net.pl

KONTO PTDT:
Bank PEKAO SA O/Warszawa
nr konta: 33 1240 5963 1111 0000 4796 8376

NAKŁAD: **500 egzemplarzy**

Wydanie dofinansowane przez Ministra Nauki i Szkolnictwa Wyższego

Spis treści / Contents

SINGULAR SPECTRUM ANALYSIS AS A SMOOTHING METHOD OF LOAD VARIABILITY

Czesław CEMPEL, Maciej TABASZEWSKI

Instytut Mechaniki Stosowanej, Politechniki Poznańskiej
Ul Piotrowo 3, 60-965 Poznań
fax. 61 665 2307, email: Maciej.Tabaszewski@put.poznan.pl

Summary

Application of SVD to fault extraction from the machine symptom observation matrix (**SOM**) seems to be validated enough, especially by data taken from many real diagnostic cases. However, frequently we have situation of varying machine load during the production process, where by observed primary symptoms are influenced greatly. This concerns generalized symptoms too, so decision making process and forecasting is disturbed. But we can apply some new data smoothing procedure called singular spectrum analysis (SSA), to eliminate load influenced symptom fluctuation, and obtain the machine wear trend only. This seems to be true, as it was shown in the paper, but special care should be taken to choose smoothing approximation order properly.

Keywords: condition monitoring, singular value decomposition, singular spectrum analysis.

ANALIZA WIDMA SZCZEGÓLNEGO JAKO METODA WYGŁADZANIA ZMIENNOŚCI OBCIĄŻENIA

Streszczenie

Zastosowanie rozkładu SVD do wydobycia informacji o uszkodzeniu z symptomowej macierzy obserwacji (ang. **SOM**) wydaje się być wystarczająco uzasadnione, szczególnie dla danych pochodzących z wielu rzeczywistych przypadków diagnostycznych. Jednakże w wielu przypadkach mamy do czynienia z sytuacją zmiennych obciążeń maszyny podczas procesu produkcji, silnie wpływających na obserwowane symptomy. Dotyczy to także symptomów uogólnionych, co utrudnia proces podejmowania decyzji i prognozowania. Możemy jednak zastosować pewną nową procedurę wygładzania nazywaną analizą widma szczególnego (ang. SSA), aby wyeliminować obciążenia wpływające na fluktuacje symptomu i otrzymać tylko trend zużycia maszyny. Wydaje się to być prawdą, jak zostało pokazane w pracy, jednak z zachowaniem szczególnej uwagi w poprawnym wyborze rzędu przybliżenia w procedurze wygładzania.

Słowa kluczowe: diagnostyka, rozkład na wartości szczególne, analiza widma szczególnego.

1. INTRODUCTION

The idea of symptom observation matrix (**SOM**) in multidimensional condition monitoring of machines is well established and brings several advantages [1]. Usually it is basing on $p > r$ rectangular matrix, with (r) symptoms $\boldsymbol{S}_r$ in columns, measured along the system life θ, what gives p symptom readings (matrix rows). It allows placing all physically different symptoms[1] measured in a phenomenal field of the machine in a one **SOM**, and to process them in order to obtain projection of observation space to the fault space of machine. Of course, at the beginning we usually observe more symptoms (columns of **SOM**), than there is expected number of faults in a machine.

The preprocessing of **SOM** may be different (see for example [2]), but for condition monitoring it was found that column normalization and extraction by symptom initial value is the best solution, bringing all symptoms to their dimensionless form. Then, the application of SVD to the dimensionless form of **SOM** gives needed projection of observation space to the fault space. The resultant matrices of SVD decomposition allow calculating of two important matrices. The first is **SD** matrix, which give us generalized fault symptoms $\boldsymbol{SD}_i$ of machine, and in theory they are independent each other. From this matrix we can calculate so called total damage symptom, as the sum of all $\boldsymbol{SD}_i$ generalized fault symptoms. This is mainly in order to calculate the symptom limit value S_l, or to make the forecast of the total damage symptom. The second **AL** matrix allows us to assess the contribution of primary measured symptoms $\boldsymbol{S}_r$ to a newly formed generalized fault symptoms $\boldsymbol{SD}_i$. In this way we can just say which of primary symptom is redundant, giving no substantial information contribution, and as such can be rejected from further calculations

[1] Symptom, measurable quantity covariable (*or assumed to be*) with the system condition

and/or future measurements [3]. But should we only reduce the dimensionality of **SOM** by rejecting redundant symptoms? Maybe the addition to **SOM** some information which is inherent in observed machine will give much better results, or we should do both operations on every **SOM**? Some years ago, the present author has added intuitively life time symptom of the machine, as the first symptom before **SOM** processing, increasing this way the rank of the matrix and amount of its information asset. As it was shown in the last paper of first author [4] this increase of information asset allow us to detect earlier the evolving second fault in a machine, and in some cases it can be done on an automatic way.

However basing on the condition monitoring data of real objects we are encountering frequently the variability of machine load, which influences on the readings of almost all symptoms, in some cases. This concerns the generalized symptoms $\boldsymbol{SD}_i$ as well, what disturbs our fault detection ability and assessment of its severity too. But it seems, even in this case of load variability, there is possibility to smooth out the chosen generalized symptom in order to base diagnostic decision on the data showing stable machine wear trend. Such an opportunity brings the application of special method called Singular Spectrum Analysis (SSA), used lately with a success in physics [5] and economic forecasting [6]. We will try to adopt this method to our diagnostic needs in this paper, in a similar way as it was already shown in our last paper [7].

Concerning **SOM** decomposition, in reality there is no big choice of decomposition method; principal components analysis (PCA), which uses SVD as it can be shown [8], and both are well diagnostically interpretable [9], [10], [11]. The well known QR decomposition seems to be not usable in multidimensional diagnostics[2], according to unpublished study of the first author. Here only the main diagonal of the upper triangular matrix **R** of this decomposition can be compared to the first generalized symptom $\boldsymbol{SD}_1$, the higher upper diagonals are shortened and do not carry readable diagnostic information.

2. OPTIMIZATION OF MULTI SYMPTOM MACHINE OBSERVATION

It was described earlier, our information about machine condition evolution is contained in p x r **SOM**, where in r columns and p rows of the successive readings of each symptom are presented. Usually they are made at equidistant system life time moments θ_n, n=1,2,...p. In pre-processing operations the columns of **SOM** are centred and normalized to the three point average of initial readings of every symptom. This is in order to make the **SOM** dimensionless, and to diminish starting disturbances of symptoms. This allows also to present the evolution range of every symptom from zero up to few times of the initial symptom value S_{0r}, (measured in the vicinity of $\theta = 0$).

After such preprocessing we obtain the dimensionless **SOM** in the form [1]:

$$\mathbf{SOM} = \mathbf{O}_{pr} = \left[S'_{nm}\right], \quad S'_{nm} = \frac{S_{nm}}{S_{0m}} - 1. \tag{1}$$

This is the way of **SOM** preprocessing when we do not include life symptom (***LS***). As it is seen from above this new symptom should be normalized and also adjusted to given form and values of observed symptoms. This additional symptom can not have to small values or to large values, because in this way it will, or will not, influence our calculation and final result. If machine observation starts from its good condition, than usually symptoms starts also from small values, and at the end of life we have maximal symptom values. Hence one way of scaling life symptom ***LS*** may include multiplying by the average of last readings of all symptoms. Let the counting of symptom readings in **SOM** will be i = 1,2 … n, and for r symptoms one can write:

$$\boldsymbol{LS} = \frac{i}{rn}\sum_{m=1}^{r} S_{n,m} \tag{1a}$$

where i =1,2, … n, $S_{n,m}$ means the last readings of symptom number m.

Now, adding ***LS*** symptom as a first column to the old **SOM** we have a new $\mathbf{SOM}_L$, which includes explicit machine life information to our diagnostic calculations and decision. Having this we can apply the Singular Value Decomposition (SVD) [8][13][17] to our dimensionless **SOM** (1) and (1a), to obtain singular components (vectors) and singular values (numbers) of **SOM**, in the form:

$$\mathbf{O}_{pr} = \mathbf{U}_{pp} \cdot \mathbf{\Sigma}_{pr} \cdot \mathbf{V}_{rr}^{\ T}, \tag{2}$$

where: T is matrix transposition, $\mathbf{U}_{pp}$ is p dimensional orthonormal matrix of left hand side singular vectors $\mathbf{V}_{rr}$ is r dimensional orthonormal matrix of right hand side singular vectors, and the diagonal matrix of singular values $\mathbf{\Sigma}_{pr}$ is defined as below:

$$\begin{aligned} &\mathbf{\Sigma}_{pr} = diag\left(\sigma_1, \sigma_2, ...\sigma_l\right), \\ &\sigma_1 > \sigma_2 > ... > \sigma_u > 0, \\ &\quad and \\ &\sigma_{u+1} = \sigma_l = 0, \\ &l = \max(p, r), \quad u \le \min\ (p, r), \quad u < r < p. \end{aligned} \tag{3}$$

Going back to SVD itself it is worthwhile to say, that every non square matrix has such decomposition, and it may be interpreted also as the product of three matrices [13], namely:

$$\boldsymbol{O}_{pr} = (\boldsymbol{Hanger}) \times (\boldsymbol{Stretcher}) \times (\boldsymbol{Aligner}^T). \tag{4}$$

This is a very metaphorical description of SVD transformation, but it seems to be an useful analogy

[2] Hence, the QR method maybe the base for quick looking of main fault only.

for the inference and decision making in condition monitoring. The diagnostic interpretation of formulae (4) can be obtained very easily. Namely, using its left hand side part, we are stretching our **SOM** over the life (observations) dimension, obtaining the matrix of generalized symptoms **SD** as the columns of the matrix. And using the right hand side part of (4) we are stretching **SOM** over the observed (primary) symptoms dimension in the form of matrix **AL**, assessing in this way the contribution of each primary measured symptom to the generalized fault symptom $\boldsymbol{SD}_i$,i=1,2,...u.

$$\begin{aligned} &\mathbf{SD} = \mathbf{O}_{pr} \cdot \mathbf{V}_{rr} = \mathbf{U}_{pp} \cdot \mathbf{\Sigma}_{rr} \,; \\ &\textit{and} \\ &\mathbf{AL} = \mathbf{U}^T_{pp} \cdot \mathbf{O}_{pr} = \mathbf{\Sigma}_{rr} \cdot \mathbf{V}^T_{rr} \end{aligned} \tag{5}$$

We will calculate the above matrices and use them for better interpretation of monitoring results (**SD**) and optimization of the dimension of the observation space (**AL**).

As the rows of **SOM** matrix were formed along the machine lifetime, so the columns of **SD** matrix have the discrete argument of life time θ, and we can write their fault space interpretation as below:

$$\boldsymbol{SD_t}(\theta) \propto \boldsymbol{F_t}(\theta), \tag{6}$$

$$Norm\,(\boldsymbol{SD_t}) \equiv ||\,\boldsymbol{SD_t}\,|| = \sigma_t,\ t = 1,2\ ...,u$$

For the assessment of total machine damage we can calculate the sum of all generalized symptoms:

$$\begin{aligned} \boldsymbol{SumSD}_i(\theta) &= \sum_{i=1}^{z} \boldsymbol{SD}_i(\theta) = \\ &= \sum_{i=1}^{z} \sigma_i(\theta) \cdot \boldsymbol{u}_i(\theta) \propto \boldsymbol{F}(\theta) \end{aligned} \,, \tag{7}$$

where; $\boldsymbol{u}_i$ is a column of $\mathbf{U}_{pp}$.

This concept of diagnostic inference, for individual fault $\boldsymbol{F_t}(\theta)$ (eq. 6), and total fault damage $\boldsymbol{F}(\theta)$ (eq. 7) has been proven in several papers [1][14] and we will use it here in further consideration.

The above results, based on generalized fault symptoms, have been obtained only from the first matrix **SD** of (5). And the second matrix **AL** gives us the relative measure of information contribution to each generalized symptom, as given by particular primary symptom measured during the **SOM** gathering. This is one way of assessment of the primary symptom redundancy, but we need some other global indicators of eventual rejection of the redundant symptom. We can use modified Frobenius norm of **SOM** and the generalized volume of the fault space created by **SOM** [3]. What is important here, these two measures are based on singular values of **SOM**, which in turn can be treated as the faults advancement measure (see (6-7)). Hence we can write the **SOM** measures [3]:

$$\begin{aligned} &Frob1 = \quad \Sigma\, \sigma_i \,; \\ &\quad \text{and} \\ &Vol1 = \Pi\, \sigma_i \,, \end{aligned} \tag{8}$$

where: i = 1,2,...u.

Looking for the way of value creation method of the above, one can say that if some primary symptom will be really redundant (small σ_i) its rejection should change *Frob1* measure only a little, and in contrary it should increase much the fault space volume *Vol1*. We will notice how it behaves with real examples of symptom rejection for **SOM** of diagnosed machines.

3. MULTIDIMENSIONAL CONDITION DETECTION OF MACHINE WITH VARYING LOAD

As a first example of application of our idea we will take a hard diagnostic case - a huge fan for coal milling working at one of Polish thermo power station. Here the root mean square vibration velocity (V_{rms}) has been used as a symptom of condition, and initially altogether 11 symptoms at different places of fan mill aggregate structure were constantly monitored, over 60 weeks of a lifetime θ. We will process this case twice, first with inclusion of life time symptom to $\mathbf{SOM}_{\boldsymbol{L}}$ (1a) and secondly **SOM** without life time symptom.

How unstable and noisy the fan running environment is, one can notice from the left top picture of the fig.1. It is seen further (middle left picture), that the symptom normalization and addition of life time symptom ***LS*** (straight line) do not change much the noisy behaviour of primary and generalized symptoms after **SVD** (bottom left picture).

Looking at the middle right picture of fig.1, where matrix **AL** is presented, one can notice that symptoms No 8,9,10, do not give substantial contribution to the two dominating generalized symptoms, and probably can be rejected as redundant at the second approach. With this respect please note the value of Frobenius modified measure *Frob1=33.82* and the volume of the fault space *Vol1=0.10*, at upper right picture. One can also note here, that there are two generalized symptoms with high information contents (picture top right), and due to that two symptom limit values are assessed: namely S_{lc} for the total damage symptom, and S_{l1} for the first generalized symptom (bottom pictures).

Using the same software we can make forecast the future symptom value of generalized symptom ***SD1*** by means of new method called grey system theory created by Deng [15], and adopted to condition monitoring by us in a previous paper [12]. As it seen from fig. 2 due to varying load of the fan the error of forecast is high, of 46% order, and the application of rolling window (picture bottom left) does not improve the forecast greatly, as it usually does. Hence we need some smoothing method which can reject the varying load undulations, and preserve the trend of machine wear only.

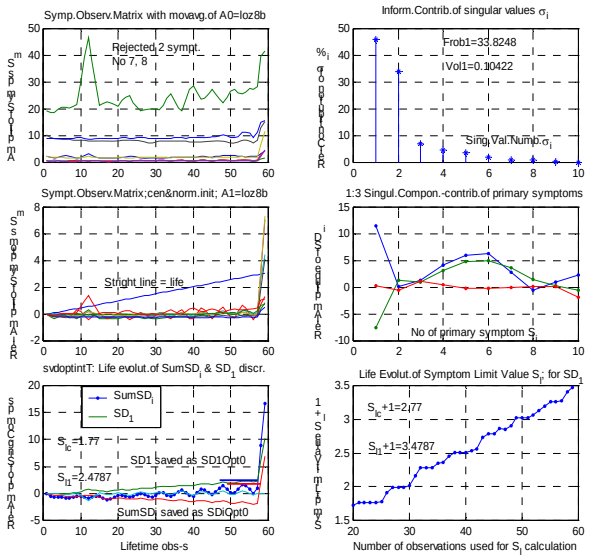

Fig. 1. Vibration condition monitoring (V_{rms}) of the coal mill fan observed at bearings of fan and electric motor

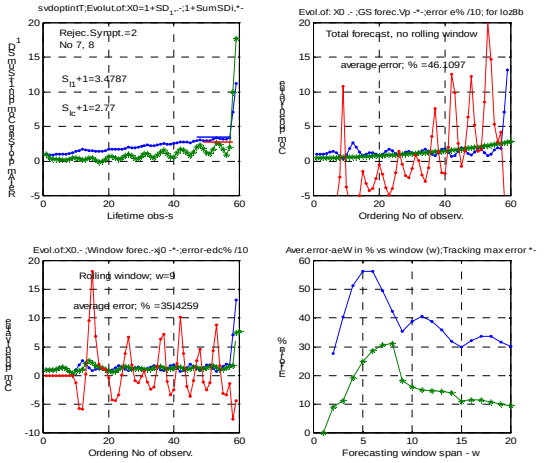

Fig. 2. Grey system theory forecast with and without rolling window for the fan mill data with varying load as on fig. 1

There are some cases of condition monitoring that are much worse, as it is shown on the fig.3 for the case of rolling bearing testing with pulsating load (loz12r). There was here 19 symptoms measured altogether, and after rejection of 3 most redundant at the first approach, the situation was not much improved, as it can be seen from the fig. 3. When approaching to obtain the forecast of next symptom value by means of GST method of rolling window (see fig. 4), the obtained result is similar to obtained previously, when forecasting the future symptom value 46% error without rolling window, and 35% with rolling window applied. Again one can see we need some method to filter varying load effects in a symptom reading. But it seems, even in this case of load variability, there is possibility to smooth out the chosen generalized symptom in order to base diagnostic decision on the data showing stable machine wear trend. Such an opportunity brings the application of SSA.

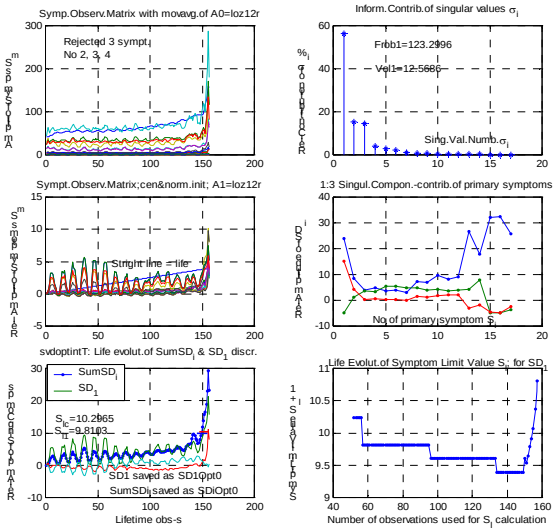

Fig. 3. Condition monitoring of a rolling bearing at the testing rig with the varying load

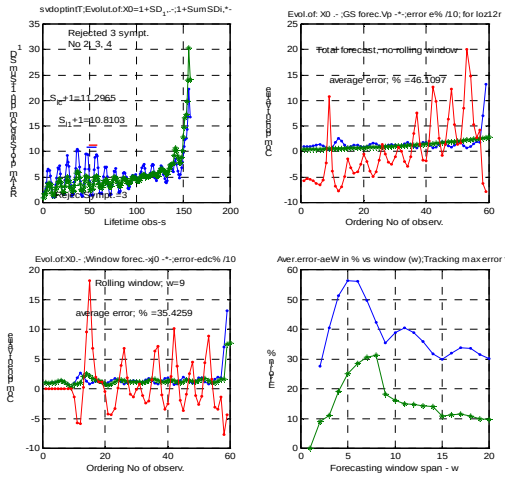

Fig. 4. GST forecast of a symptom value (first generalized symptom), with and without rolling window, for the ball bearing test rig (see Fig. 3)

4. TRAJECTORY MATRIX OF GENERALIZED SYMPTOM AND ITS DECOMPOSITION

The SSA method itself consists of four steps [16], [6]. In the first step, called embedding, the one dimensional time series denoted here by **S** is recast into *L* dimensional time series composed in trajectory matrix **X**, (**TM** see (9)). As a second step the **TM** is decomposed by SVD into a sum of orthogonal matrices of rank one. This gives us a new set of time subseries, where each component can be

identified; as a trend, quasi periodic component, or noise. By truncating the unwanted components in the third step we can preserve trendlike component into matrix **D** (see (10)) for further processing. The last step is reconstruction of de-noised time series by a special procedure called diagonal summation over matrix **D** (see (11)).

Let us denote the original total damage symptom (***TDS*** vector) by $\boldsymbol{x} = [x_1, x_2, \ldots x_N]$, and for a chosen embedding dimension L we obtain the trajectory matrix, as below:

$$\mathbf{X} = \begin{bmatrix} x_1 & x_2 & x_3 & \ldots & x_{N-L} \\ x_2 & x_3 & x_4 & \ldots & x_{N-L+1} \\ x_3 & x_4 & \ldots & \ldots & \ldots \\ \ldots & \ldots & \ldots & \ldots & \ldots. \\ x_L & \ldots & \ldots & \ldots & \ldots..x_N \end{bmatrix} \tag{9}$$

Such a matrix, is by definition, a Hankel matrix, as it is $X_{i,j} = x_{i+j-1}$, so all elements of a particular left hand diagonals are equal. This can be seen even from the definition, as above (9).

The subsequent SVD of trajectory matrix **X** allows as to decompose it into a sum of orthogonal matrices (subseries) which can be arbitrarily grouped as two sums; the trend matrix **D** and the noise as below:

$$\mathbf{X} = \sum_{i=1}^{q} \sigma_i \boldsymbol{u}_i \boldsymbol{v}_i^T + \sum_{i=q+1}^{N} \sigma_i \boldsymbol{u}_i \boldsymbol{v}_i^T = \mathbf{D} + \mathbf{Noise} \tag{10}$$

where, as before, σ_i is the singular value, and vectors $\boldsymbol{u}_i$, $\boldsymbol{v}_i$ are elements of secondary SVD of **X** matrix, similarly as it was in relation (2-3). The level of approximation q of trajectory matrix (*de-noising*) should be chosen arbitrary, usually q=1 or 2 is enough, depending on the structure of the data.

The fourth step of SSA is a diagonal averaging over the first matrix **D** of (10), it means summation of all elements in given diagonal and division over the number of these elements. And in this way we obtain a low order approximation of input vector denoted here as $\hat{\boldsymbol{S}}$ with the same number of elements N as input series $\boldsymbol{x}$. This can be done as below:

$$\begin{cases} \hat{S}_r = \dfrac{1}{r}\displaystyle\sum_{i=1}^{r} D_{i,r-i+1} & \text{for } r \le k \\ \hat{S}_r = \dfrac{1}{k}\displaystyle\sum_{i=1}^{k} D_{i,r-i+1} & \text{for } k < r \le L \\ \hat{S}_r = \dfrac{1}{k-r+L}\displaystyle\sum_{i=1}^{k-r+L} D_{r-L-i,L-i+1} & \text{for } r > L \end{cases} \tag{11}$$

where k – number of rows of matrix **D**, and r = 1,2, … L+k-1

Starting from this de-noised symptom and using the already elaborated Matlab program **gsago.m** for GST forecasting we can make de-noised series $\hat{\boldsymbol{S}}$ with much better forecast than before, but the amplitude scaling may be a little different, due to the rejection of some number of noisy components of input vector (approximation order q).

Let us return now to the total damage symptom of ball bearing on a testing rig (Loz12r) shown on Fig.3 (see bottom left picture) and saved as *SDiOpt0* after SVD decomposition. Next figure 5 presents us the results of SSA processing outlined above (9-11) and calculated by special program **singspectrel.m**, applied already in a modified version in a published paper [7].

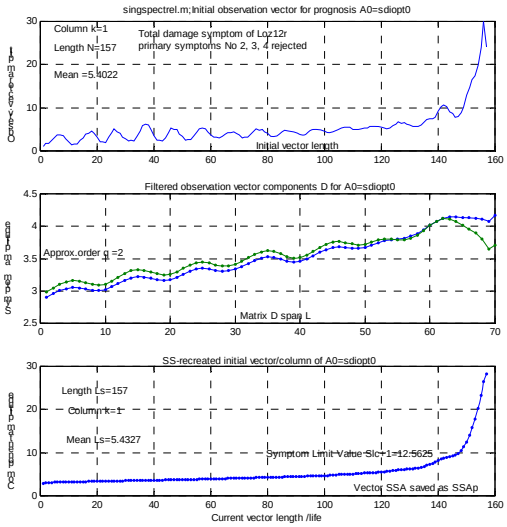

Fig. 5. Denoised total damage symptom of a rolling bearing testing rig with pulsating load

The order of approximation taken in de-noising operation was taken as q=2, and this seems to be good when we take a look for a lower picture of Fig.5. Here no significant symptom oscillation can be observed, and also no significant reduction of symptom amplitude after reconstruction is observed, when we compare upper and lower pictures.

Going to obtain the forecast of total damage symptom we will apply again the GST procedure and calculate also the symptom limit value S_l. The results of such calculations are shown on Fig.6, which seems to be self explaining. As one can notice there, the forecast of total damage symptom is amazingly good having the average error of order of 0.6%, which seems to be very small in comparison to previous result of 35% error, as it is seen on figure 4. Hence, the application of Singular Spectrum Analysis, as the smoothing method seems to be good validated in this case.

But the same operation made for generalized symptom ***SD1*** gives much worse smoothing and prognostic result with q=2, one should apply here the lower approximation order q=1, what in turn makes the amplitude of symptom more than twice smaller as the input amplitude of ***SD1***. This seems to be not good for the condition inference and needs special rescaling of symptom after its recreation by SSA procedure.

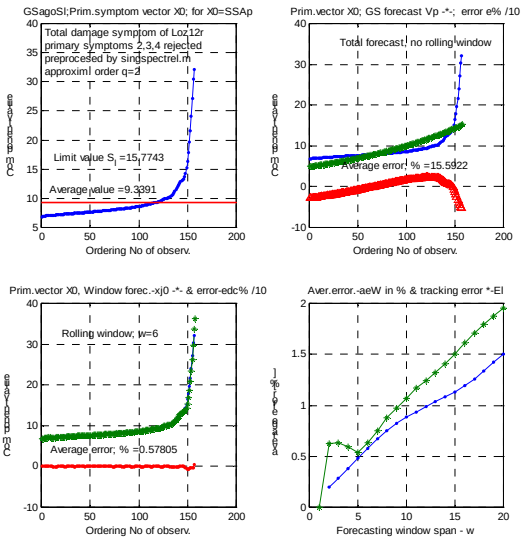

Fig. 6. GST forecast of de-noised total damage symptom for loz12r

5. CONCLUSIONS

Varying load of machines with condition monitoring is a frequent case, and that was the reason in one of our paper [14] we have proposed rescaling of observed symptoms. This time we propose not to rescale symptoms, but to filter or smooth, the SVD decomposition results by a special method called SSA, used with a success in physics and econometrics. Special diagnostic oriented software have been prepared for that purpose, and it has been shown that using it and choosing the approximation order *q* carefully we can obtain wear trend like behaviour of generalized symptoms of monitored machine.

ACKNOWLEDGMENT

The paper was written due to financial support of Ministry of Science and Higher Education of Poland, grant No 1751/B/T02/2009/37.

REFERENCES

[1] Cempel C., Tabaszewski M.; *Multidimensional condition monitoring of the machines in non-stationary operation*; Mechanical Systems and Signal Processing; Vol. 21, 2007, str. 1233-1247.

[2] Cempel C.; *Optimization of Symptom Observation Matrix in Vibration Condition Monitoring*; Proceeding of ICRMS09, Chengdu-China; July 2009, str. 944-960.

[3] Cempel C., Tabaszewski M.; *Optimization of dimensionality of symptom space in machine condition monitoring*; Mechanical Systems and Signal Processing; 24 (2010), str. 1129-1137;

[4] Cempel C.; *Externalization of internal machine information to increase diagnostic accuracy and quality*; paper submitted to IMEKO 11 Conference, Cracow October 2010.

[5] Vautard R., Yiou P., Ghil M.; *Singular spectrum analysis: A toolkit for short, noisy chaotic signals*; Physics, 58, str. 95-126.

[6] Hassani H., Heravi S., Zhigljavsky A.; *Forecasting European industrial production with singular spectrum analysis*; International Journal of Forecasting, 25 (2009), str. 103-118.

[7] Cempel C., Tabaszewski M.; *Double singular value decomposition (SVD) as the way to improvement of vibration condition monitoring, sent to*; Mechanical Systems and Signal Processing, November 2009.

[8] Golub G. H., VanLoan Ch. F.; *Matrix Computation*; III-rd edit, J Hopkins Univ. Press, Baltimore, 1996, p. 694.

[9] Tumer I. Y., Huff E. M.; *Principal component analysis of tri-axial vibration data from helicopter transmission*; 56th Meeting of the Society of Machine Failure Prevention Technology, 2002.

[10] Jasiński M., *Empirical models in gearbox diagnostics* (in Polish); PhD Thesis, Warsaw University of Technology, Warsaw, December 2004.

[11] Korbicz J., et al, (*eds.*), *Fault Diagnosis – Models, Artificial Intelligence, Applications*; Springer Verlag, Berlin - Heidelberg, 2004, p. 828.

[12] Cempel C., Tabaszewski M.; *Application of grey system theory in multidimensional machine condition monitoring* (in Polish), Diagnostyka, No 2, (47) 2007, str. 11-18.

[13] Will T., Hanger matrix, two-thirds theorem, Internet; http://www.uwlax.edu/faculty/will/svd/svd/index.html, June 2005; (*see also: SVD ingredients*, Mathematica, *April 2004*).

[14] Cempel C., Tabaszewski M.; *Multidimensional vibration condition monitoring of non-stationary systems in operation,* Proceedings of 12 International Congress on Sound and Vibration, (*on CD- paper No 496*), Lisbon, July 2005.

[15] Deng J-L.; *Introduction to grey system theory*, The Journal of Grey System, 1989,Vol. 1, No 1, str. 1-24.

[16] Carniel R., Barazza F., Pascolo P.; *Improvement of Nakamura technique by singular spectrum analysis*; Soil Dynamics and Earthquake Engineering; 26, (2006), str. 53-63.

[17] Kielbasinski A., Schwetlik H.; *Numeric Linear Algebra*; WNT Press Warsaw 1992; p. 502.

AN APPLICATION EXAMPLE OF A MULTIASPECT DIAGNOSTIC MODEL*

Damian SKUPNIK

Silesian University of Technology, Department of Fundamentals of Machinery Design, 18A Konarskiego str., 44-100 Gliwice, Poland
e-mail: Damian.Skupnik@polsl.pl

Summary

The paper shows an application example of a multiaspect diagnostic model, i.e. a special kind of a model that consists of at least two submodels which are applied together but they can be identified separately most often by means of the different methods and criteria. In the presented example each submodel concerns the one in five predefined aspects (viewpoints). The example concerns a technical object which makes possible diagnostics of the continuous processes and exemplifies a physical miniaturization of an industrial installation used e.g. in chemical industry. The chosen results of diagnosis obtained from the multiaspect diagnostic model were shown and discussed.

Keywords: technical diagnostics, diagnostic model, multiaspect model.

PRZYKŁAD ZASTOSOWANIA WIELOASPEKTOWEGO MODELU DIAGNOSTYCZNEGO

Streszczenie

Artykuł przedstawia przykład zastosowania wieloaspektowego modelu diagnostycznego, który składa się z co najmniej dwóch stosowanych łącznie modeli składowych, przy czym modele te identyfikowane są oddzielnie najczęściej za pomocą różnych metod i kryteriów. W prezentowanym przykładzie każdy model składowy dotyczy jednego z pięciu zdefiniowanych wcześniej aspektów (punktów widzenia). Przykład dotyczy obiektu technicznego, dla którego możliwe jest diagnozowanie procesów ciągłych i stanowi fizyczną miniaturyzację instalacji przemysłowej stosowanej, np. w przemyśle chemicznym. Przedstawiono i przedyskutowano wybrane wyniki uzyskane z wieloaspektowego modelu diagnostycznego.

Słowa kluczowe: diagnostyka techniczna, model diagnostyczny, model wieloaspektowy.

1. INTRODUCTION

For many modern and complicated technical objects working out of a diagnostic model is uphill task. Identification of a single diagnostic model which would relate to the whole object, could be very difficult or even impossible. The practice shows that instead of using one global model better results are obtained by means of so-called local models (e.g. [Cholewa & Kiciński 1997]). If the outputs of local models are joined properly, e.g. by means of an aggregation operator, a multimodel will be built. Generally speaking the multimodel is a model that consists of at least two submodels which are applied together but they can be identified separately most often by means of the different methods and criteria [Wojtusik 2006].

In the presented example each submodel is designed on the basis of knowledge acquired from one point of view, i.e. taking into account one aspect. It means that a multiaspect approach consists in adoption at least two different points of view on the considered technical object. The set of aspects important from technical diagnostics point of view, the way of representation of the considered aspects and other details of the multiaspect approach were shown in [Skupnik 2008, Skupnik 2009b].

2. RESEARCH OBJECT

As a research object *FESTO S7 EduTrainer Compact Siemens S7-300 CPU313C* was chosen. This object exemplifies a physical miniaturization of an industrial installation used e.g. in chemical industry or food industry and makes possible diagnostics of the continuous processes.

2.1. The main elements of the object

Fig. 1 shows structure of the considered object. System control (not shown in the fig. 1) makes possible control one in four of process variables (i.e. temperature of water in the tank T1, level of water in the tank T2, pressure of air in the tank T3 and water flow intensity in the place where flow sensor FS is located) by suitable configuration of opening or closing manual valves Vi (i = 1, 3, 4, 5, 7, 8, 9, 10).

* Research partly financed by the Ministry of Science and Higher Education (research project No. 4T07B04230).

2.2. Operation of the object

Operation of the object is controlled by the program developed by the author and executed by the programmable logic controller. After checking that the object is in the initial state the pump P is activated for 20 seconds and relative pressure of air in the tank T3 is increased to 200 mbar (atmospheric pressure is the level of reference). In order to achieve and stabilize the required pressure the proportional-integral-derivative controller was used (the values of tuning parameters were following: proportional gain k_p=1; integral gain t_i=1 s; derivative gain t_d=1 s). In the result of the operation the portion of water is pumped to the tank T3 from the tank T1 (fig. 2). Just before the 20th second the operator should close the valve V8. The pump P is turned off when time is up and the operation of the object is paused for 5 seconds. The operator should close the valve V3 during the break.

After the break the ball valve V2 is opened and the tank T1 is filled by water from the tank T2 (fig. 3).

The height of water pillar in the tank T2 is measured by the ultrasonic sensor US. The ball valve V2 is closed when the water pillar in the tank T2 equals 100 mm. Then the operation of the object is paused for 5 seconds. During the break the operator should open the manual valve V4. After the break the pump P is activated for 30 seconds and the water in the tank T1 is mixed (fig. 4). When time is up the pump P is turned off and the operation of the object is ended.

3. THE WORKED OUT MULTIASPECT DIAGNOSTIC MODEL (MDM)

The multiaspect diagnostic model was designed according to the method which had been presented in [Skupnik 2009a]. In the considered example all submodels were represented in the form of belief networks (Bayesian networks).

Generally speaking a belief network is a directed acyclic graph which nodes represent random variables and directed edges represent probabilistic relationships between the variables. The relationships are defined by means of conditional probability tables. The set of conditional probability tables makes possible calculating joint probability. Thus the whole network represents joint probability distribution for the all variables in an economical way [Jensen 2001].

Inference in a belief network consists in calculating unknown values of some variables on the basis of known values of remaining variables. If for example variables of a Bayesian network concern symptoms and technical states of an object then for given symptoms the network can be used to compute the probabilities of the presence of the considered technical states.

In the presented example each belief network represents the probabilistic relationships between technical states and symptoms in relation to one viewpoint (aspect). There are maximum five submodels for each functional state because according to the method presented in [Skupnik 2009a] should be enough to consider the following aspects:

- the functional state aspect (FSA);
- the elements activity aspect (EAA);
- the elements activity constraints aspect (EACA);
- the elements timing aspect (ETA);
- the elements history aspect (EHA).

In the operation of the research object one may distinguish three functional states. Thus in this case the multiaspect diagnostic model consists of the 15 submodels. Its structure and the idea of its application is shown in the fig. 5.

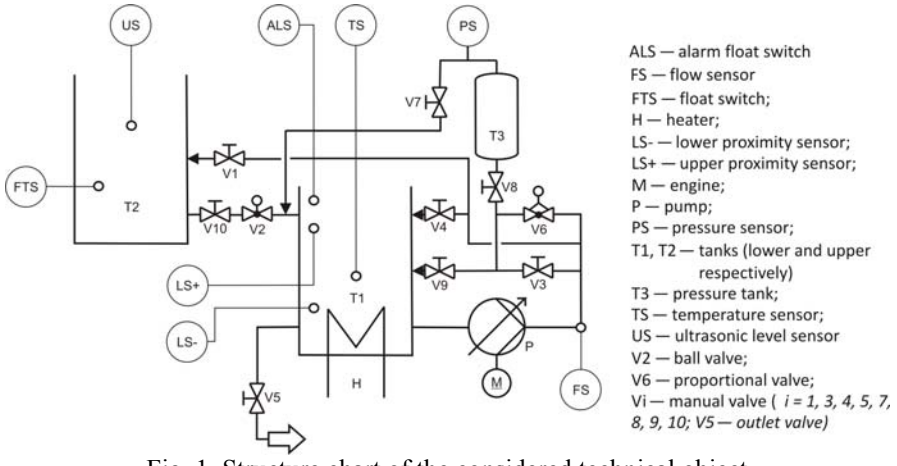

Fig. 1. Structure chart of the considered technical object

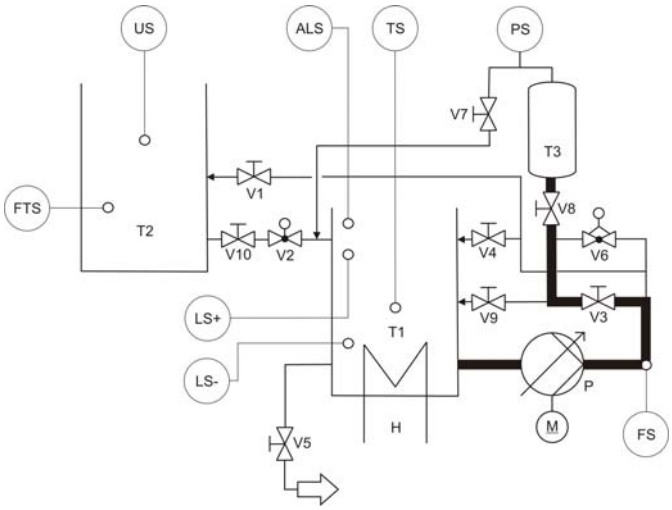

Fig. 2. Compression of air in the tank T3 by water flowing from the tank T1 to the tank T3 (bold curve shows the flow of water)

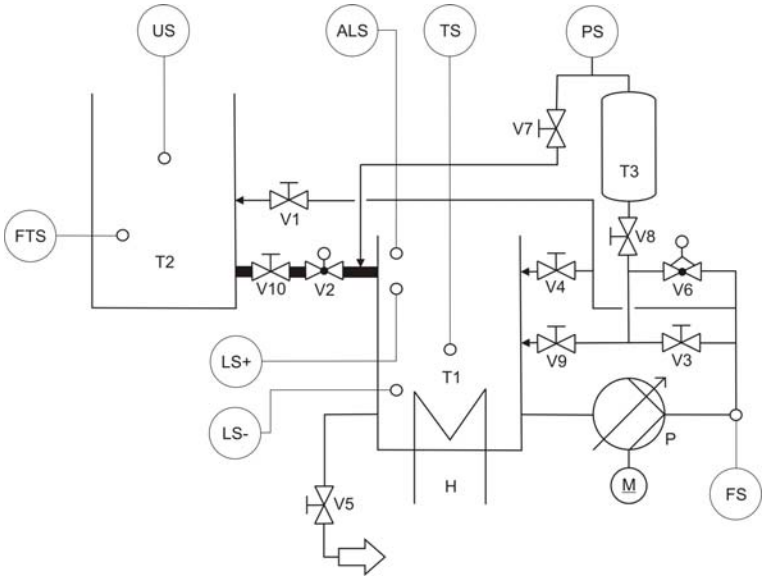

Fig. 3. Filling the tank T1 by water from the tank T2 (bold line shows the flow of water)

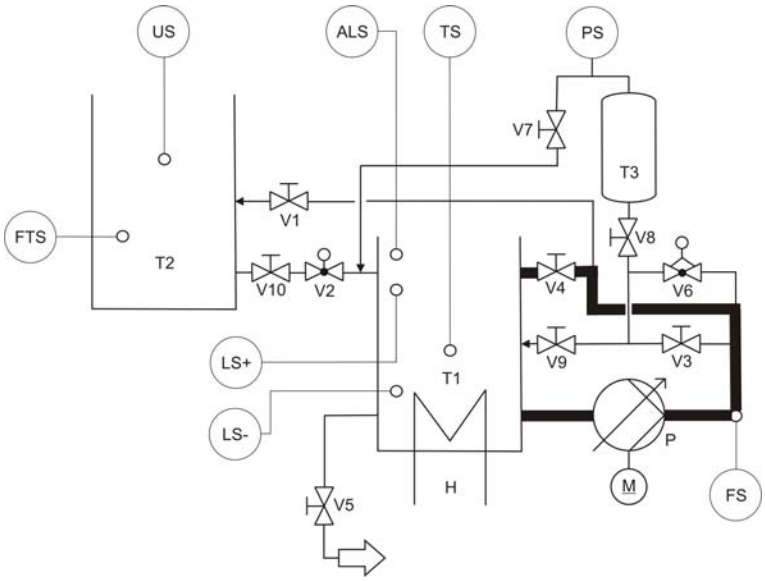

Fig. 4. Mixing the water in the tank T1 (bold curve shows the flow of water)

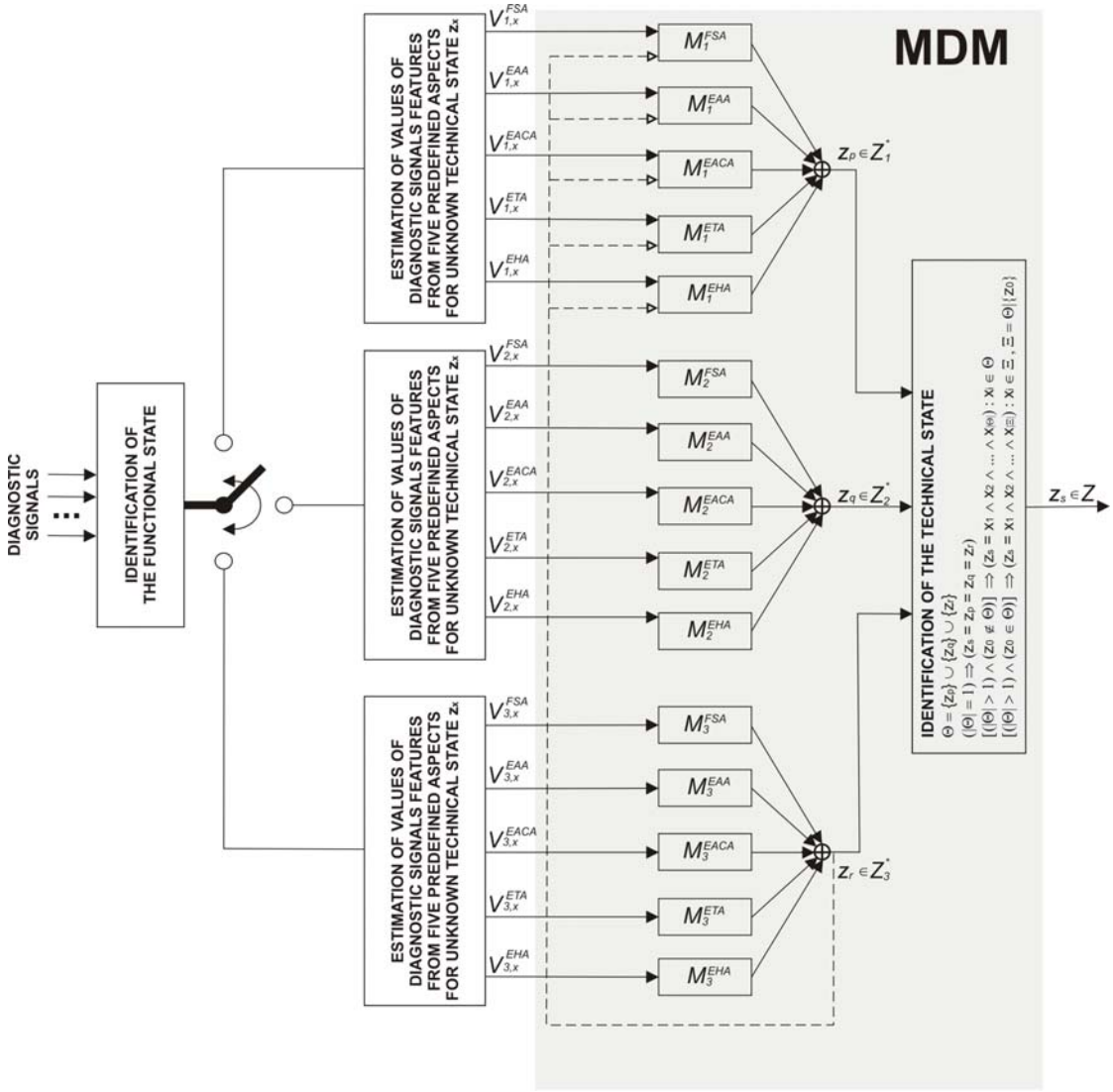

Fig. 5. The structure of the multiaspect diagnostic model (MDM) and the idea of its application where:

- $V_{j,x}^{FSA}, V_{j,x}^{EAA}, V_{j,x}^{EACA}, V_{j,x}^{ETA}, V_{j,x}^{EHA}$ - subsets of values of diagnostic signal features which are calculated in the functional state aspect, elements activity aspect, elements activity constraints aspect, elements timing aspect, elements history aspect respectively, for the j functional state and unknown technical state z_x;
- $M_j^{FSA}, M_j^{EAA}, M_j^{EACA}, M_j^{ETA}, M_j^{EHA}$ - aspect diagnostic models (submodels) represented in the form of belief networks for the j functional state;
- Z_j^* - subset of the considered technical states for the j functional state;
- $Z = \bigcup_{j=1}^{3} Z_j^*$ - set of the all considered technical states.

The structures of the models $M_j^{FSA}, M_j^{EAA}, M_j^{ETA}$ were designed automatically by means of K2 algorithm and identification of the models was done with use of the junction tree algorithm. Both the structures and identified parameters were obtained on the basis of the set of data acquired in the result of active diagnostic experiments. The models M_j^{EACA}, M_j^{EHA} were designed by the author in the subjective way.

Taking into account the chosen form of the aspect diagnostic models, i.e. Bayesian networks, it was decided that as an aggregation operator $\oplus$ Dempster's rule of combination [Dempster 1967],

$$m_{12}(\varnothing) = 0$$

$$m_{12}(A) = m_1 \oplus m_2(A) = \frac{\sum_{B \cap C = A \neq \varnothing} m_1(B) m_2(C)}{1 - \sum_{B \cap C = \varnothing} m_1(B) m_2(C)} \qquad (1)$$

can be used. Thanks to it, it is possible to compute output of the multiaspect diagnostic model but it should be emphasised that in some cases the rule may lead to irrational conclusions. Interesting discussion about this problem was published e.g. in [Zadeh 1986].

4. APPLICATION OF THE MULTIASPECT DIAGNOSTIC MODEL

Some results obtained from the multiaspect diagnostic model were presented in tab. 1÷8 (the last column called "**MDM**"). The first column of each table concerns the correct degrees of belief. The columns 2÷6 show degrees of belief obtained from the submodels, where: $M_j^{FSA}, M_j^{EAA}, M_j^{EACA}, M_j^{ETA}, M_j^{EHA}$ concern the functional state aspect, the elements activity aspect, the elements activity limitations aspect, the elements timing aspect the elements history aspect respectively in the *j* functional state.

4.1. Example 1 – leakiness of the tank T3

Tab. 1 contains degrees of belief about technical state of the tank T3 when it was leaky and remaining elements of the object were in usable technical state. One may notice that in this case only one submodel, i.e. M_1^{FSA}, gives useful information because it points unambiguously the right technical state. It is impossible to draw a conclusion about technical state of the tank T3 taking only into account the results obtained from the rest of the submodels. Application of Dempster's rule of combination in order to aggregate degrees of belief obtained from the all submodels makes possible computation, the output of the MDM. As it shown the result is completely consistent with the values of the correct beliefs.

4.2. Example 2 – partly blocked the canal between the tank T1 and T3

Tab. 2 contains degrees of belief about technical state of the canal between the tank T1 and T3 when it was partly blocked (the other elements of the object were in usable technical state). In this case there is a contradiction between results obtained from the submodels M_1^{FSA} and M_1^{EAA} or M_1^{EAA} and M_1^{ETA}. In spite of this fact the output of the MDM is again completely consistent with the values of the correct beliefs.

Tab. 1. Degrees of belief about the technical state of the tank T3 when it was leaky

Correct beliefs	M_1^{FSA}	M_1^{EAA}	M_1^{ETA}	M_1^{EALA}	M_1^{EHA}	**MDM**
0	0	0.4933	0.5156	0.5	0.5	**0**
1	1	0.5067	0.4844	0.5	0.5	**1**

Tab. 2. Degrees of belief about the technical state of the canal between the tank T1 and T3 when it was partly blocked

Correct beliefs	M_1^{FSA}	M_1^{EAA}	M_1^{ETA}	M_1^{EALA}	M_1^{EHA}	**MDM**
0	0	0.8235	0	0.2	0.2	0
1	1	0.1765	1	0.2	0.2	1
0	0	0	0	0.2	0.2	0
0	0	0	0	0.2	0.2	0
0	0	0	0	0.2	0.2	0

4.3. Example 3 – failure of the pump P

Tab. 3 contains degrees of belief about technical state of the pump P when it was faulty and the rest of the elements of the object were in usable technical state. As one can see this case is similar as in the example 2 but here none of the submodels point unambiguously the right technical state. Moreover there is a contradiction between results obtained from the some submodels. In consequence on the basis of degrees of belief obtained from the MDM one cannot draw a conclusion about technical state of the pump P without any doubts. However it should be noticed that the obtained result does not mislead.

4.4. Example 4 – completely blocked the canal between the tank T1 and T3

As it was mentioned above, in the operation of the research object one may distinguish three functional states. Lets consider the case when the canal between the tank T1 and T3 is completely blocked and the other elements of the object are in usable technical state.

On the basis of results obtained from the aspect models in the first functional state (tab. 4 and 5) one may draw a false conclusion that the pump P was probably faulty and the canal between the tank T1 and T3 was almost for sure in a good technical state.

However for the third functional state it was stated without any doubts that the pump P was in working order (tab. 6). Thus it was sensible to assume that the pump P had also been efficient in the first functional state.

The earlier conclusions for the first functional state were modified and accuracy of the diagnosis became higher after the information had been entered into the aspect models, which concerned the first functional state (tab. 7 and 8).

Tab. 3. Degrees of belief about the technical state obtained when the pump P was faulty

Correct beliefs	M_1^{FSA}	M_1^{EAA}	M_1^{ETA}	M_1^{EALA}	M_1^{EHA}	**MDM**
0	0.5451	0.1837	0.6770	0.5	0.5	0.3610
1	0.4549	0.8163	0.3230	0.5	0.5	0.6390

Tab. 4. Degrees of belief about the technical state of the canal between the tank T1 and T3 when it was completely blocked (before recalculation)

Correct beliefs	M_1^{FSA}	M_1^{EAA}	M_1^{ETA}	M_1^{EALA}	M_1^{EHA}	**MDM**
0	0.4618	0.5714	0.6178	0.2	0.2	0.9646
0	0.1865	0.1225	0.1324	0.2	0.2	0.0179
1	0.1137	0.2041	0.0808	0.2	0.2	0.0111
0	0.1243	0.0817	0.0882	0.2	0.2	0.0053
0	0.1137	0.0203	0.0808	0.2	0.2	0.0011

Tab. 5. Degrees of belief about the technical state of the pump P (before recalculation)

Correct beliefs	M_1^{FSA}	M_1^{EAA}	M_1^{ETA}	M_1^{EALA}	M_1^{EHA}	**MDM**
1	0.5451	0.1837	0.6770	0.5	0.5	0.3610
0	0.4549	0.8163	0.3230	0.5	0.5	0.6390

Tab. 6. Degrees of belief about the technical state of the pump P for the 3-rd functional state

Correct beliefs	M_3^{FSA}	M_3^{EAA}	M_3^{ETA}	M_3^{EALA}	M_3^{EHA}	**MDM**
1	1	1	1	0.5	0.5	1
0	0	0	0	0.5	0.5	0

Tab. 7. Degrees of belief about the technical state of the canal between the tank T1 and T3 when it was completely blocked (after recalculation)

Correct beliefs	M_1^{FSA}	M_1^{EAA}	M_1^{ETA}	M_1^{EALA}	M_1^{EHA}	**MDM**
0	0.2630	0.0001	0.5786	0.2	0.2	0.0002
0	0.2169	0	0.1240	0.2	0.2	0
1	0.1877	0.9999	0.1074	0.2	0.2	0.9998
0	0.1447	0	0.0826	0.2	0.2	0
0	0.1877	0	0.1074	0.2	0.2	0

Tab. 8. Degrees of belief about the technical state of the pump P (after recalculation)

Correct beliefs	M_1^{FSA}	M_1^{EAA}	M_1^{ETA}	M_1^{EALA}	M_1^{EHA}	**MDM**
1	1	1	1	0.5	0.5	1
0	0	0	0	0.5	0.5	0

The possibility of modification of the conclusions in the worked out multiaspect diagnostic model is represented in the fig. 5 by means of the broken lines.

5. SUMMARY

Many modern technical objects consist of several subsystems (e.g. mechanical, electric, control, etc.) and works according to the established procedures in changeable conditions. It seems that for this kind of objects an application of a multiaspect diagnostic model to recognize a technical state is a good idea. The main advantage of this approach is based on the fact that a change of a technical state observed from one point of view may be reflected, even more clearly, in the other point of view. Thus in that case the hard task of recognizing a technical state is solved by solving a few simpler tasks. Unfortunately, there is a serious difficulty which consists in aggregation the results obtained from the aspect models.

Even though, it seems that application of a multiaspect diagnostic model makes possible determination of new procedures connected with designing of supervision systems or improvement (simplification) of existing procedures, especially in relation to complicated technical objects. In other words a multiaspect approach may be used in formulating new methods intended for constructing diagnostic models or supplement of the methods which relate to analysis of residual processes (e.g. vibrations, noise etc.).

REFERENCES

1. Cholewa W., Kiciński J. (Eds.): 1997: *Technical diagnostics. Inverse diagnostic models* (in Polish). Publishing House of Silesian University of Technology, Gliwice.
2. Dempster A. P.: 1967: *Upper and lower probabilities induced by a multivalued mapping*. The Annals of Statistics, 28, pp. 325-339.
3. Jensen F .V.: 2001: *Bayesian Networks and Decisions Graphs*. Springer, New York.
4. Skupnik D., 2008: *A multiaspect approach to the modelling in technical diagnostics* (in Polish). Diagnostyka 2(46), pp. 117-120.
5. Skupnik D.: 2009a: *The method of constructing a multiaspect diagnostic model* (in Polish). In: Gardulski J. (Ed.): XXXVI all-Polish Symposium "Diagnostyka Maszyn", Wisła, 2-7 March 2009.
6. Skupnik D.: 2009b: *Application of UML in constructing the multiaspect diagnostic models*. Accepted to print in "MOTROL - Motorization and Power Industry in Agriculture".
7. Wojtusik J.: 2006: *Diagnostic multimodels for rotating machinery* (in Polish). Book of Department of Fundamentals of Machinery Design, No. 128, Gliwice.
8. Zadeh L.: 1986: *A simple view of the Dempster-Shafer theory of evidence a*nd its implication for the rule of combination. The AI Magazine, 7, pp. 85-90.

SELECTION OF PIEZOCERAMIC SENSOR PARAMETERS FOR DAMAGE DETECTION AND LOCALIZATION SYSTEM

Andrzej KLEPKA, Łukasz AMBROZIŃSKI

Department of Robotics and Mechatronics AGH - University of Science and Technology,
Al. Mickiewicza 30, 30-059 Kraków, tel. 12 6173128
andrzej.klepka@agh.edu.pl, lukasz.ambrozinski@agh.edu.pl

Summary

Damage detection method based on Lamb waves propagation phenomena are increasingly used as a tool for Structural Health Monitoring (SHM) and Nondestructive Testing and Evaluation (NDT/E). Phenomena connected with wave propagation and interaction with damages are very complex and complicated. In many cases depends on sensors/actuators location, electronic system design, sensor shape, frequency range of excitation or sensors properties. Actuator/sensor selection based only on specification sheet can be insufficient, so time and frequency analysis have to be applied to signals acquired when an examined transducer was attached to a plate. In this paper sensor study on the transducer used for Lamb waves generation and acquisition has been presented. Robustness of the array consisting of chosen transducers has been verified with the scanning vibrometer.

Keywords: lamb waves, damage detection, piezoceramics transducers, phased array technique.

DOBÓR PARAMETRÓW PRZETWORNIKÓW PIEZOCERAMICZNYCH DO SYSTEMU DETEKCJI I LOKALIZACJI USZKODZEŃ

Streszczenie

Metody detekcji uszkodzeń oparte o zjawiska propagacji fal Lamba są coraz częściej używane w systemach SHM oraz do nieniszczących metod badań i oceny stanu konstrukcji. Zjawiska związane z propagacją fali oraz jej interakcji z uszkodzeniami są złożone i skomplikowane. W wielu przypadkach zalezą od rozmieszczenia nadajników/odbiorników, układu elektronicznego i jego parametrów elektrycznych, kształtu elementu piezoceramicznego, zakresu częstotliwości wymuszenia czy właściwości samego przetwornika piezoceramicznego (PZT). Wybór elementów PZT tylko na podstawie danych zawartych w specyfikacji nie zawsze jest wystarczający. Konieczne jest przeprowadzenie analiz układu składającego się z badanej struktury oraz przetwornika. W artykule przedstawiono analizę czujników wykorzystywanych do wymuszania struktury oraz do akwizycji sygnałów odpowiedzi. Poprawność przeprowadzonych testów została zweryfikowana z wykorzystaniem wibrometru laserowego.

Słowa kluczowe: fale lamba, detekcja uszkodzeń, przetworniki piezoceramiczne, technika phased array.

1. INTRODUCTION

A variety of means can be used as Lamb waves actuators and sensors such as ultrasonic probes, lasers, piezoelectric element, interdigital transducers, optical fibers. Brief description of transducers can be found in [2]. A selection of the transducer used in a system depends on many factors like a size and a shape of a monitored element, its material properties and signal processing applied to a damage detection algorithm. In this paper a SHM system based on piezoelectric transducers used to the damage detection method based on the phased array technique was presented. Giurgiutiu in [1] showed that piezoelectric active wafers can be used in this method with good results.

Lamb waves are dispersive and multimode – many modes can exist at one frequency. It means, that Lamb waves excited by PZT contains multiple modes. However when excitation frequency is limited below so called cut-off frequency only two: A_0 and S_0 modes exist. Moreover it is possible to enhance one mode and reduce the other by mode tuning technique based on a transducer size and an excitation frequency selection [3].

Phased array technique is very often used as a non-destructive damage detection method based on ultrasound waves. Main idea of that method is to steer of wavefront shape, generated by a matrix of

piezoelectric transducers [5,6,12]. The selection of transducer size, and the excitation frequency is essential for the phased array technique. Time delays calculation for each transducer is based on the phase velocity and transducers spacing so exact material properties of examined structure are necessary to calculate the phase and the group velocity. The excited wavelength should be at least twice as long as transmitters spacing, in another case the side lobes and additional false ghost damages could be disclosed. The size of a PZT determinates the lowest wavelength and the highest excitation frequency.

2. HARDWARE

In all experiments Phased Array Non Destructive Testing System (PAS-8000)(fig. 1) was used. The system enable sinusoidal signal generation with frequencies between 40 – 500kHz. Additionally many types of windows can be applied (square, triangle or Hanning). 8 channels wave used for signal sending with simultaneous phase shifting generation between generated signals. Data acquisition was performed by PAQ-16000D at 2.5 MHz sampling frequency.

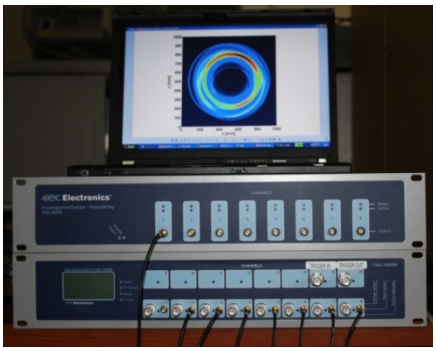

Fig. 1. PAS-8000 and PAQ-16000 used in experiments.

3. SENSOR STUDY

3.1. Time and frequency domain test

As mentioned above many factors affect the wave propagation so transducers attached to the aluminum plate were tested rather than unbounded ones. Three types of multilayer Noliac PZTs transducers were examined: a ring actuator CMAR03 of the diameter 12 mm and two plate actuators: CMAP07 and CMAP12 of the size 5x5x2 and 2x2x2 respectively. All transducers were made of material NCE57 with frequency constant 1950 m/s, so resonance frequencies corresponding to the largest transducer dimension was calculated as 166 kHz, 390 kHz and 975 kHz for CMAR03, CMAP07 and CMAP12 respectively.

Examined transducers were placed on the 2 mm thick plate in a pitch-catch setup (Fig.).

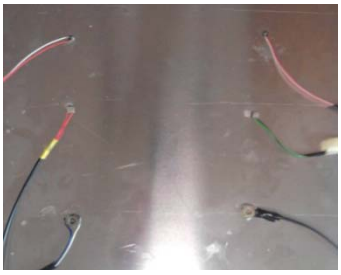

Fig. 2. Three types of Noliac PZTs transducers:

Wax was used as a coupling agent. The actuator-sensor distance was 150 mm. In the first step transducers were excited with a broadband square pulse. Frequency responses presented in the Fig. 3. reveal resonance frequencies calculated above.

a)

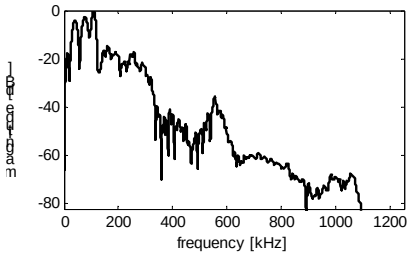

b)

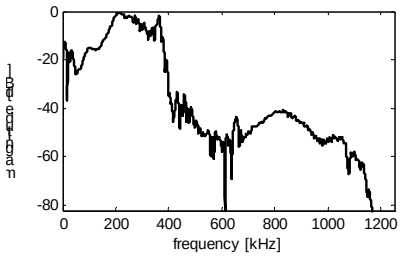

c)

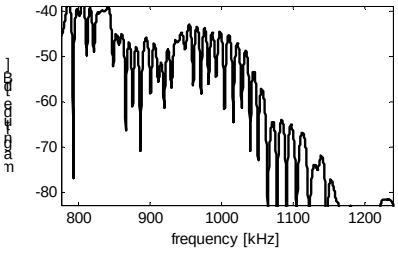

Fig. 3. Frequency responses of transducers excited with a broadband square signal a) CMAR 03 b) CMAP07 c) CMAP12.

In the second step transducers were excited with a tone-burst signal – 4 cycles of sinusoid with the centre frequency 100 kHz, modulated with Hanning window. Comparisons of the excitation pulse to the time responses, presented in the 4, reveals that the best representation of the excited signal can be found in the signal acquired with the CMAP 12. The CMAP 7 response distinctly contain high frequency components, for the CMAR03 it was impossible to isolate the excited pulse. In the next

experiments only CMAP 7 and CMAP 12 have been used.

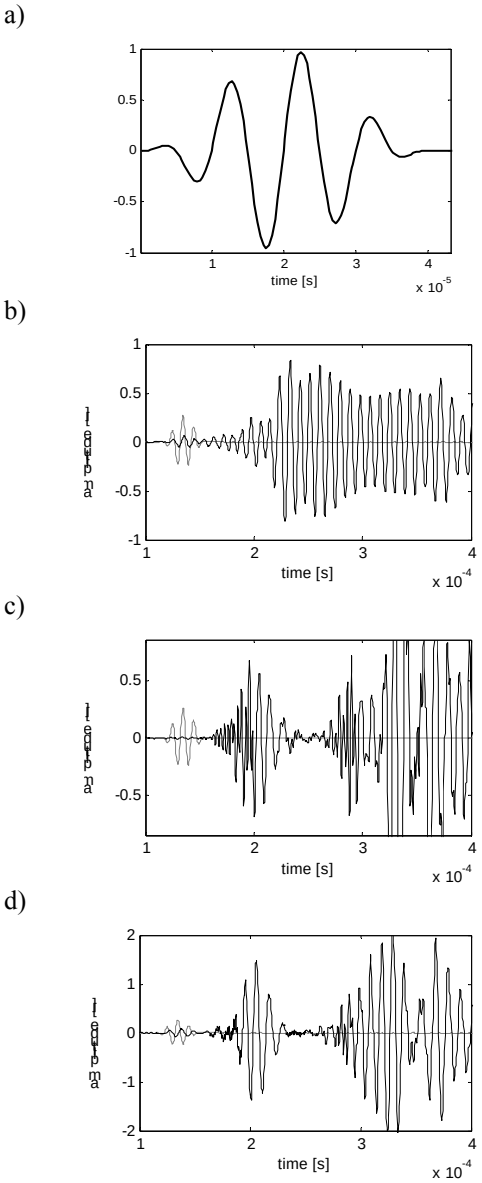

Fig. 4. Time responses acquired at 100 kHz narrowband pulse excitation a) excitation signal b) CMAR 03 c) CMAP07d) CMAP12.

3.2. Dispersion curves validation

In the phased array technique time delays calculation based on the phased velocity of excited mode. To validate the analytically calculated curves by comparing them with the experimental ones and to assess the sensitivity of the transducer to the particular Lamb mode, the 2D Fourier transform method for the measurement of propagating multimode signals was used [4]. In Fig. 5a. can be seen that the S_0 mode is hardly recognizable for signals acquired by CMAP07 at lower wavenumber-frequency range. In the response from CMAP12 A_0 (Fig. 5b.)mode is even more dominant for whole frequency range.

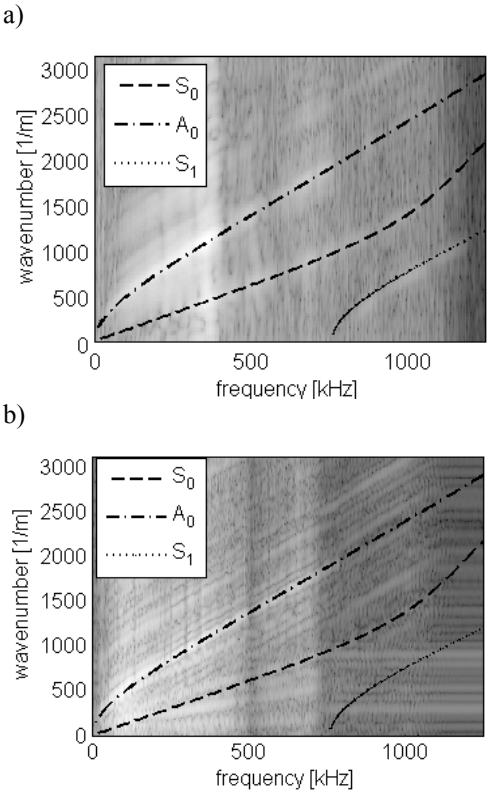

Fig. 5. Theoretical and measured wavenumber vs. frequency plot obtained for signals acquired by a) CMAP07, b) CMAP12.

When a mode with different wavenumber is generated with a PZT element an additional beam is formed in the unintentional direction. Generated signal contains multiple frequency components with significant amplitude. It may affect more unwanted beams. The least of the tested transducers (CMAP12) allows for narrowband excitation without high frequency components, moreover in the tested plate it generated enhanced A_0 with reduced S_0 mode.

3.3. Experimental results for Damage imaging technique

Damage localization algorithm is based on time domain responses analysis of the structure. The responses are acquired from the distributed actuators – sensors grid, placed on the structure. First step in this method is estimation of the group velocity for given plate geometry. It can be done in two ways: solving dispersion equation or measure the group velocity experimentally. Position in time domain of the incident wave and scatters from edges can be estimated using time of flight parameter[13].

Damage localisation process consist in representing investigated area as an image, where

values of the pixel $S(i,j)$ are calculated using equation [13]:

$$S(i,j) = \sum_{m}^{N} A_m f_{wg}(t_{mij}) f_m(t_{mij}), \quad (1)$$

$$t_{mij} = \frac{R_m^a + R_m^s}{c_g}, A_m = \frac{10}{max|f_m|}$$

where $S(i,j)$ – value of the given pixel, R_m^a, R_m^s is the distance from damage to actuator and sensor respectively, f_m – envelope of the recorded signal, c_g – group velocity of the wave, f_{wg} – is windowing function. Typical structure response signal is presented in figure 6.

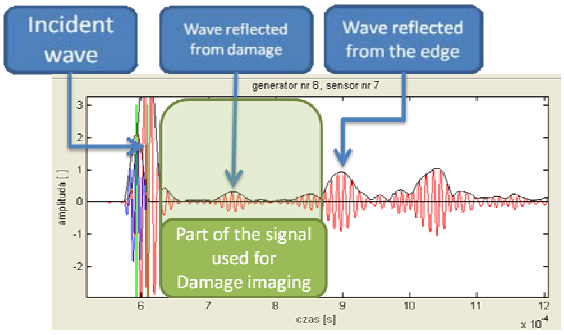

Fig. 6. Example of structure response signal with damage.

For each actuator–sensor path one image can be obtained. The final result is achieved by summing images from all paths. Comparison of results obtained with use CMAP 7 and CMAP 12 transducers are presented in figure 7. As can be noticed that in case of use CMAP 12 transducers damage area is showed correctly. In case CMAP 7 transducer, results are not clear.

3.4. Experimental results for phased array

The second method is based on the phased array technique. This technique creates the possibility of forming and steering the front wave generated from a set of transducers. The beam forming is realized by delay generation during excitation of particular transducers, using equation [6,10,11].

$$t = \frac{l_x \cdot \sin(\alpha)}{c} \quad (2)$$

a)

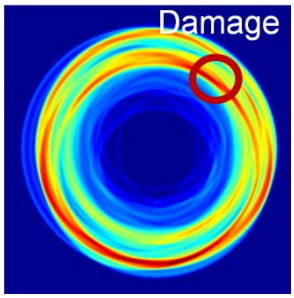

b)

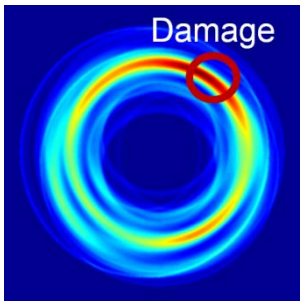

Fig. 7. Comparison of damage identification process with use different types of PZT: a) CMAP 7, b) CMAP 12

where l_x is the distance between transducers, c is phase velocity, α is the angle between the actuator line and wave front. The acquisition process is performed with the same delay as during excitation of the structure. Due to the complexity of the phenomena appearing during the interaction between waves and the damage, some methods of signal processing have been proposed, such as wavelet filtration and envelope estimation.

Main parameters of the phased array technique are distance between transducers and angle resolution (width of the main lobe). If the some restriction connected with wave length, sensor or actuators placement or frequency component of the excitation signals are not fulfill, the result of the identification algorithm which based on the response signal processing can be incorrect. In case when side lobes have dominant influence, the effects like ghost damages or false damage can appear (Fig.8)

Eight CMAP12 plate actuators of the size 2x2x2 mm were used to built an linear array. The distance between PZTs centers was equal to 5 mm. The array was set in the centre of an aluminum plate with size 1000x1000x2 mm. As a coupling agent a wax was used. Disadvantages of this coupling method is irregular wax layer for all transducers. In the end the amplitudes of the signal sending to the plate can be different for particular elements. Before the experiment a calibration procedure was performed. Each actuator one by one generated signals captured by one PZT element. Output amplitude gains for all channels were adjusted so the linear and Hamming apertures was achieved. This problem is not investigated in the

current paper but detailed information about apodization and effective aperture can be found in[7 – 9,12].

Time delays calculation was based on theoretical dispersion curves presented in Fig. 5.

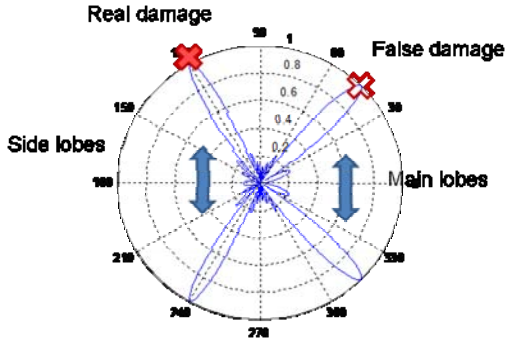

Fig. 8."False damage" effect.

Fig. 9. Experimental setup for phased array testing.

During experiment assumed excitation frequency equal to 100kHz. It is correspond wavelength equal 13.57mm. This parameters provided "half wavelength" condition fulfill (half of the wavelength should be grater then transducer spacing). The steering direction was 120 degrees. To validate the performance of steering the wavefront a scanning laser vibrometer POLYTEC PSV 400 was used (Fig. 9). The signals generated by the array were captured by the vibrometer. The device enabled noncontact measurement of the out of plane perturbation velocity. Examined points were distributed in a circle shape so distances between the measurement points and the source of the wave were equal. Time signals were acquired in the arc shaped grid points, the maximum value of the first arrival wave packet has been used to create the beam patterns. Two methods of an apodisation have been used during the experiment.

The results of the experiment can be seen above. The highest vibration amplitude was appeared in the desired direction. Fig. 10a,b presents measured beam pattern in polar plot. It represents the normalized maximum amplitude in all directions for a specified array configuration. A theoretical beam pattern was added to Fig 10c,d. It showed good agreement with a measured signal and theoretical calculation. A slight difference of steering angle is caused by a small error in the theoretical disperse curves estimation. The array used in experiments was linear so an additional, symmetric beam is expected at direction 240 degrees.

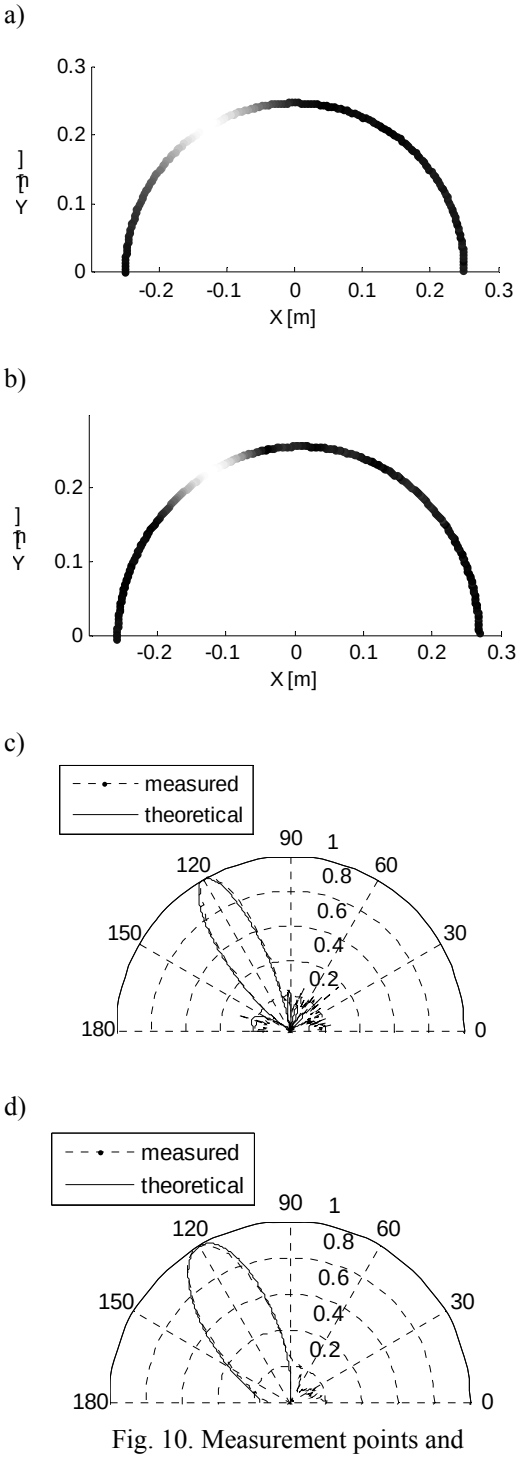

Fig. 10. Measurement points and amplitude values- a) linear apodization b) Hamming apodization. Theoretical and experimental normalized results of wave amplitudes in measured direction. - c) linear apodization d) Hamming apodization

4. CONCLUSIONS

Performed test showed that shape and dimensions of transducer can have significant impact of damage detection algorithm results. The smallest transducers have better properties but their power sometimes can be unsatisfactory.

The geometrical resonant frequency can be determined, but their influence on results during narrowband excitation can be significant. Resonant frequency of the PZT elements can have influence on results in spite of frequency of excitation is selected definitely outside the resonance.

Selection of proper transducers and their parameters is key for Phased Array technique and apply together with apodization technique allow to decrease of sidelobs, enable better directionality and prevent „false damage" and „ghost damage" effects.

ACKNOWLEDGMENTS

Research funding from the Polish research project MONIT (No. POIG.01.01.02-00-013/08-00) is acknowledged by the authors.

BIBLOGRAPHY

[1].Giurgiutiu V. "Structural Health Monitoring with piezoelectric wafer active sensors" Elsevier Inc. 2008.
[2].Zhongqing Su, Lin Ye, YeLu. "Guided Lamb waves for identification of damage in composite structures: A review" Journal of Sound and Vibration 295 (2006) 753–780.
[3].Giurgiutiu V (2005), "Tuned Lamb wave excitation and detection with piezoelectric wafer active sensors for structural health monitoring." *Journal of Intelligent Material Systems and Structures* 16, 291–305.
[4].Alleyne D. and P. Cawley (1991), "A two-dimensional Fourier transform method for the measurement of propagating multimode signals" Journal of the Acoustical Society of America 89(3) pp.1159-1168.
[5].M. Veidt C. T. Ng S. Hames and T. Wattinger "Imaging Laminar Damage in Plates using Lamb Wave Beamforming" Advanced Materials Research Vols. 47-50 (2008) pp 666-669
[6].T. Stepinski, P. Wu, E. Martinez, "Ultrasonic inspection of copper canisters using phase arrays" NDTnet 1998 March, Vol.3 No.3.
[7].L. Moreau B. Drinkwater P. Wilcox "Ultrasonic Imaging Algorithms With Limited Transmission Cycles for Rapid Nondestructive Evaluation" Transactions on Ultrasonics, Ferroelectrics, and Frequency Control, vol. 56, no. 9, September 2009
[8].M. Nikolov V. Behar "Analysis and Optimization of Medical Ultrasound Imaging Using the Effective Aperture Approach" Cybernetics and information technologies Volume 5, No 2, Sofia 2005
[9].L. Mažeika R. Kažys A. Maciulevičius "Optimization of transducer arrays parameters for efficient excitation of Lamb waves" ISSN 1392-2114 Ultragarsas (ultrasound), Vol.62, No.4, 2007.
[10]. Su Z. and L. Ye (2009): "Identification of Damage Using Lamb Waves From Fundamentals to Applications" *Springer-Verlag Berlin Heidelberg,* pp. 65.
[11]. Z. Su, L. Ye, *"Identification of Damage Using Lamb Waves"* Lecture Notes in Applied and Computational Mechanics, Vol. 48, 346 p. 2009 [978-1-84882-783-7].
[12]. S. C. Wooh, Y. Shi *"Optimum beam steering of linear phased arrays"* Wave Motion 29 (1999) 245-265.
[13]. Q. Wang, S. Yuan *"Baseline-free damage imaging method for lamb wave based structural health monitoring"* IV ECCOMAS Thematic Conference on Smart Structures and Materials.

Andrzej KLEPKA Ph.D. is an assistant proffessor at the Department of Robotics and Mechatronics of AGH University of Science and Techmnology. His scientific interests focus on signal processing, nonlinear systems and Structural Sealth Monitoring

Łukasz AMBROZIŃSKI M.Sc. is PhD student at the Department of Robotics and Mechatronics of AGH University of Science and Techmnology. His works are connected with damage detection and localisation and Structural Health Monitoring.

NUMERICAL STUDY OF THE FATIGUE DELAMINATION GROWTH CONSIDERING THERMAL PHENOMENA

Andrzej KATUNIN

Department of Fundamentals of Machinery Design, Silesian University of Technology
Konarskiego 18A, 44-100 Gliwice, Poland, email: andrzej.katunin@polsl.pl

Summary

The wide applicability of polymer-based laminates in the engineering practice causes the development of methods of their diagnosing. One of the most crucial faults in polymer-based laminates is their delamination. The problem becomes more complicated while thermal effects (e.g. self-heating and frictional heating) are taken into consideration. In the present study the numerical model of fatigue growth of the delamination in linearly viscoelastic polymer-based laminate was developed. The obtained results show, that the neglecting of the thermal effects in delamination process with some loading parameters for such structures can cause large inaccuracies in delamination growth evaluation and prediction.

Keywords: polymer-based laminates, self-heating, delamination growth, laminate diagnostics.

ANALIZA NUMERYCZNA ZMĘCZENIOWEGO PRZYROSTU DELAMINACJI Z UWZGLĘDNIENIEM ZJAWISK CIEPLNYCH

Streszczenie

Szerokie zastosowanie laminatów polimerowych w praktyce inżynierskiej wywołuje potrzebę rozwoju metod ich diagnostyki. Jednym z najbardziej krytycznych uszkodzeń w laminatach polimerowych jest delaminacja. Problem staje się bardziej skomplikowany, gdy pod uwagę biorze się efekty cieplne (samorozgrzanie, rozgrzanie od tarcia). W niniejszej pracy zaproponowano model numeryczny zmęczeniowego przyrostu delaminacji w liniowo-lepkosprężystym laminacie polimerowym. Otrzymane wyniki wskazują, że pominięcie efektów cieplnych w procesie delaminacji z pewnymi parametrami obciążenia dla takich struktur może powodować duże niedokładności w oszacowaniu i predykcji przyrostu delaminacji.

Słowa kluczowe: laminaty polimerowe, samorozgrzanie, przyrost delaminacji, diagnostyka laminatów.

1. INTRODUCTION

The wide applicability of polymer-based laminates, especially in automotive and aircraft applications, determines the necessity of development of diagnostic methods for the laminates. One of the most crucial faults is the delamination. The most valuable information during diagnosing such structures is the relation for an evaluation and prediction of the delamination growth and, based on this, estimation of the lifetime of the structure. In this case, when the cyclic loading is applied to the structure standard formulations of fracture mechanics based on the beam theory and its modifications cannot be applied. Results of previous works [1] show that the delamination growth depends on several factors: layer orientation, between which the delamination occurs, position on the thickness, type of boundary conditions, etc. During cyclic loading such laminates reveal viscoelastic state, which cause hysteretic behaviour. According to this, the self-heating effect caused by dissipated energy appears. Due to the problem complexity there is no strict theoretical formulation of the thermoviscoelastic fracture. The interesting approach was proposed in [2], which based on rheological-dynamical analogy, but generally the phenomenon was investigated numerically [3-5] using various numerical techniques: cohesive zone model (CZM), virtual crack closure technique (VCCT) or virtual crack extension technique (VCET).

The previous research [1] shows, that the layers orientation may have great influence on the delamination propagation. The steady self-heating in the delamination propagation process is negligible, because of low values of temperature increase. The non-steady self-heating and its influence on the fatigue delamination growth was investigated in this paper.

In the present study the fatigue delamination growth with thermal effects influence for ELS (End-Loaded Split) plate was considered. The critical energy release rates on the delamination front were calculated numerically using J-integral formulation. Then, the process of the delamination was modeled using VCCT with direct crack growth. The non-steady self-heating was presented by analytical

formula and inputted to the numerical model as temperature-, frequency- and coordinates-dependent volumetric heat flux. The frictional heating was modeled basing on stick-slip Coulomb model. After numerical analysis the energy release rates and temperature distributions for the investigated configuration of boundary conditions were obtained and compared.

2. PREPARATION OF THE NUMERICAL MODEL

The numerical simulation was prepared using MSC.Marc/Mentat® commercial FE software. We considered ELS 24-layered plate (Fig.1) made of glass fiber reinforced epoxy resin with the length *l* of 0.125m, width *b* of 0.025m and thickness *h* of 0.00528m. Such configuration was subjected for mode II delamination.

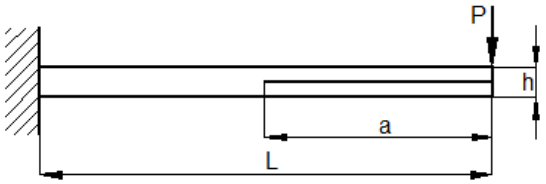

Fig. 1. Configuration of ELS plate

The layers orientation and material properties of the laminate were the same as in [1]. Each layer was modeled as deformable body with contact constraints except the initial delamination area. The model was meshed using 3000 three-dimensional eight-node thermomechanical elements. The viscoelasticity was modeled basing on Williams-Landel-Ferry (WLF) hypothesis and experimental data obtained from dynamic mechanical analysis [6] and represented as Prony series. The reference temperature (which coincides with glass-transition temperature) was 378 K and WLF constants C_1 and C_2 were 54.4745 K and 377.288 K, respectively [6]. Then the thermomechanical material properties were applied [7]. In this study one assumes the isotropy and temperature independence of above-mentioned properties. On the opposite sides of the plate mechanical boundary conditions of fixture on the one and loading force of 40 N on the other were applied.

The preliminary analysis of the critical energy release rates for different location of the crack front was performed using J-integral approach. The delamination in mid-plane (between 12th and 13th layer) was modelled as contact deactivation. Obtained values of critical energy release rates were presented in Fig. 2.

Then, the model of fatigue delamination growth was prepared. The above-mentioned parameters were defined the same as for previous model. The force was applied in sinusoidal cycles with the amplitude of 40 N. The initial delamination was assumed to 0.08 L and the delamination propagation was modeled using VCCT, where the crack growth resistance was defined as results presented in Fig.2. The direct crack propagation mode was chosen. The delamination propagation direction was defined using user subroutine (UCRACKGROW) compiled in Intel® Fortran Compiler®.

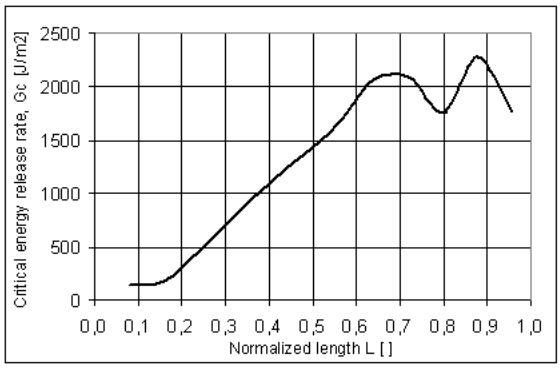

Fig.2. Critical energy release rates for investigated delamination growth

The initial temperature of the plate was assumed as 298 K. The friction in the delaminated area was modeled using Coulomb stick-slip model with the coefficient of friction equaling 0.15 (assumed following [8]). Due to the impossibility of modeling the self-heating, it was defined using the analytical formula proposed in [9]:

$$\Delta\theta(x,y) = 6w^2(x,y)\varepsilon_{\max}^2\omega D''(\omega,\theta)\lambda^{-1}\cdot \sum_{m,n=1}^{\infty}\frac{\operatorname{sinc}\mu_m \operatorname{sinc}\gamma_n \cos\xi_m x\cos\xi_n y}{(1+\operatorname{sinc}2\mu_m)(1+\operatorname{sinc}2\gamma_n)(\xi_m^2+\xi_n^2)}\cdot \left(1-\kappa t\xi_{mn}\right) \quad (1)$$

where: x and y are Cartesian coordinates, θ is the temperature, w is the deflection function, ε_{max} is the maximal deflection, ω is the angular frequency, λ is the thermal conductivity, D'' is the loss rigidity, κ is the thermal diffusivity, t is the time, μ and γ are subsequent roots of the boundary-value equations,

$$\xi_m = \frac{\mu_m}{l},\ \xi_n = \frac{\gamma_n}{b} \text{ and } \xi_{mn} = \xi_m^2 + \xi_n^2. \quad (2)$$

This expression was defined using multiple independent variable table as volumetric heat flux thermal boundary condition. The temperature dependence of D'' (which was obtained experimentally using dynamic mechanical analysis [6]) for loading frequency of 200 Hz was fitted using the 4th order polynomial function ($R^2 = 1$):

$$D''(400\pi,\theta) = 75.91\theta^4 - 14468.23\theta^3 + 1023044.75\theta^2 - 314824472.23\theta + 588479316.65. \quad (3)$$

The analysis was defined as thermomechanical one with delamination growth. The analysis was continued until total delamination of the laminate for three cases: under self-heating and frictional heating, under frictional heating only and without considering any heating.

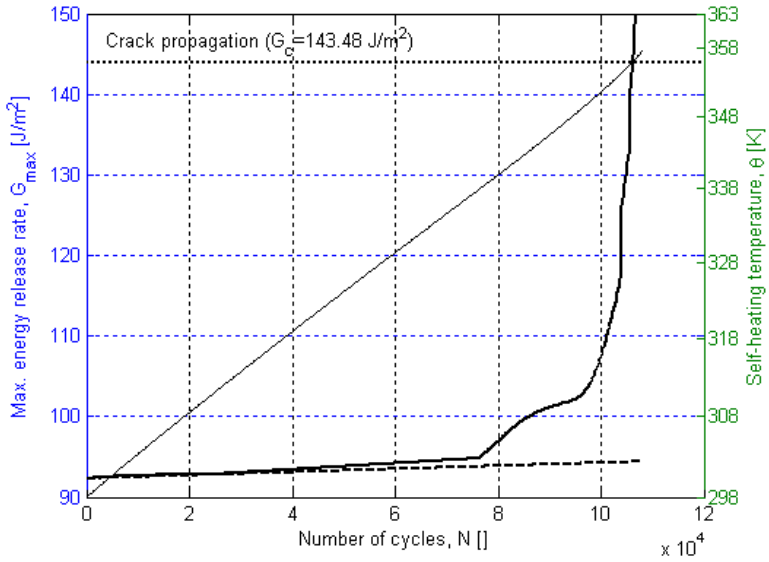

Fig. 3. Comparison of energy release rates for fatigue with and without consideration of the self-heating

3. RESULTS AND DISCUSSION

Numerical analyses were performed for $2 \cdot 10^5$ cycles for each investigated case. In Fig.3. were presented obtained results for maximal energy release rate G_{max} along the delamination front for cases with and without self-heating. During the delamination growth its front is irregular (Fig.4), therefore the maximum value of the energy release rates were considered. Also the temperature θ in the delamination front was presented for the case with self-heating (thin solid curve). As it can be noticed, the crack propagation occurred after $1.068 \cdot 10^5$ cycles with self-heating temperature of 357.48 K (intersection of bold solid and bold dashed curves), while in the case without taking into consideration the self-heating effect the energy release rate has still small value for the same number of cycles.

The observed nonlinearities of the energy release rate between $7.5 \cdot 10^4$ and 10^5 cycles appeared due to the relaxation process. After the first delamination, values of energy release rate in new delamination fronts were higher than critical ones, therefore the delamination propagated instantly in the whole area after few cycles. Fig.5. presents the energy release rates in new delamination fronts with the indication of critical energy release rates on the dimensionless normalized length of the plate.

The obtained characteristics of the energy release rate during delamination growth (Fig.5) are in good agreement with numerical and experimental results presented in other works [10].

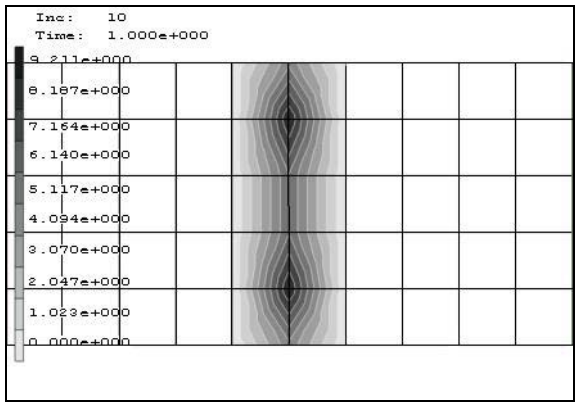

Fig. 4. Exemplary energy release rates distribution along the delamination front

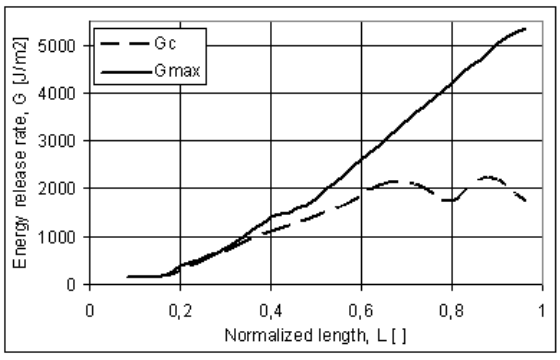

Fig. 5. Comparison of critical energy release rates and energy release rates during delamination growth

In case with frictional heating only values of the energy release rate practically were not differ than in case with self-heating. The temperature grown from the initial one to 304.6 K after $2 \cdot 10^5$ cycles and the maximal energy release rate was 101.52 J/m^2. Therefore, results for this case were omitted in Fig.3. However, in case of delamination bridging at the delamination front position value greater than in

present case it may has greater influence on the structure heating up due to greater displacements in the delaminated region and also may cause the delamination growth.

The presented dependence of temperature and fatigue delamination growth shows, that the rapid increase of the energy release rates started at approximately 310 K. It shows, that the stiffness degradation of polymer-based laminates depends not only on loading parameters, but also on rheological characteristics.

4. CONCLUSIONS

In this work the numerical model of fatigue delamination growth in polymer-based laminates with thermal phenomena was developed. The research shows, that omitting self-heating in prediction of the delamination growth may cause large inaccuracies, especially when the laminate structure is subjected to intensive loading. The self-heating of the structure causes the stiffness decrease of the laminate and increase of the energy release rate along the delamination front. Moreover, the heating of the laminate causes the non-stationarity of the delamination propagation, which was observed in the present analysis.

For the numerical model validation the fatigue experiments will be carried out under laboratory conditions. After experiments it will be possible to use the Paris law in modeling the fatigue delamination growth. Then, the numerical model will be tuned by inserting i.a. temperature-dependent thermomechanical constants and coefficients from the experiments. After final calculations the empirical dependencies between fatigue, delamination growth and self-heating will be investigated. In the present work only the bending vibrations of the plate were discussed. Future research in the above-presented area consider other types of an excitation, e.g. self-heating and delamination growth under the torsional vibrations.

ACKNOWLEDGEMENTS

Results presented in this paper have been carried out within the framework of the research grant No. N N504 282137 financed by Polish Ministry of Science and Higher Education.

REFERENCES

[1] Katunin A.: *Numerical study of delamination propagation in polymer-based laminates during quasi-static loading*, Scientific Problems of Machines Operation and Maintenance, 44, 3(159), 2009, pp. 49-62.

[2] Milašinović D.D.: *Rheological-dynamical analogy: modeling of fatigue behavior*, International Journal of Solids and Structures, 40, 2003, pp. 181-217.

[3] Rahul-Kumar P., Jagota A., Bennison S. J., Saigal S., Muralidhar S.: *Polymer interfacial fracture simulations using cohesive elements*, Acta Metallurgica, 47, 15, 1999, pp. 4161-4169.

[4] Turon A., Costa J., Comanho P. P., Dávila C.G.: *Simulation of delamination in composites under high-cycle fatigue*, Composites: Part A, 38, 2007, pp. 2270-2282.

[5] Muñoz J. J., Galvanetto U., Robinson P., *On the numerical simulation of fatigue driven delamination with interface elements*, International Journal of Fatigue, 28, 2006, pp. 1136-1146.

[6] Katunin A., Hufenbach W., Kostka P., Holeczek K., *Frequency dependence of the self-heating effect in polymer-based composites*, Archives of Material Science and Engineering, submitted.

[7] Katunin A., *O modelowaniu temperatury samowzbudnej w laminacie*, II Konferencja Naukowa „Metody komputerowe – 2008", Gliwice 2008, s. 21-24.

[8] Licari J. J., *Coating materials for electronic applications – polymers, processes, reliability, testing*, William Andrew Publishing/Noyes, 2003.

[9] Katunin A., *On the self-heating effect of the polymer-based laminate rectangular plates in non-steady state under harmonic excitation*, ECCM2010, Proc. of the 4th European Conference on Computational Mechanics, Paris, 2010.

[10] Caimmi F., Pavan A.: *An experimental evaluation of glass-polymer interfacial toughness*, Engineering Fracture Mechanics, 76, 18, 2009, pp. 2731-2747.

Andrzej KATUNIN is a scientific assistant in the Department of Fundamentals of Machinery Design of Silesian University of Technology at Gliwice, Poland. His main areas of research are thermal phenomena in polymer-based laminates, laminates diagnostics, fatigue and life prediction of laminates, wavelets theory and applications.

THE DIAGNOSIS OF EGR SYSTEM'S FAILUERS DEPENDED ON DETECTION AND MEASURE OF VIBROACUSTIC VIBRATIONS

Andrzej KAZMIERCZAK, Krzysztof MIKSIEWICZ, Radosław WRÓBEL

Politechnika Wrocławska, radoslaw.wrobel@pwr.wroc.pl

Summary

The authors presents a new in – vitro way of diagnosis in automotive vehicle which depend on detection and measure of vibroacustic vibrations of the diesel engine. It seems that the Exhaust Gas Recirculation circuit that does not work properly shouldn't have an influence on vibrations generated by an engine. However, authors indicate that this statement is wrong. EGR system has an influence on engine's vibration, what was described in the article. On that way, detection of vibrations must be accomplished with high quality diagnostic systems. Therefore, vibrometric laser scanner Polytec had been used. To achieve full diagnostic results multidimensional vibration's function has been researched, where the torque moment has been used as an extra parameter. Measured vibrations were subjected to digital signal processing like windowing, fast Fourier transform, filtration by finite impulse response which also undergone to windowing . The results of measure and processing perform in form of 3D plots, which indulge in speed estimate of the usefulness of presented method. Moreover authors presents principle of working EGRs' systems of different generations, its evolution and history. A EGR is a popular system of recirculation of the automotive vehicle emission. The principle of working depends on the forcing in the part of outlet gas to the combustion chamber. Majority of the users of automotive vehicles with EGR systems claim that system has negative effect on the performance of the car. Nonetheless that opinion is subjective, because the generally available research on the subject doesn't exist. However, EGR system, as the most of automotive vehicle is being subjected to physic's rules - it uses up. The polluted flowing valve of circuit has an influence on stability of engine's work, and what follows on a performance of a car.

Keywords: laser Doppler vibrometry, EGR, digital signal processing.

DIAGNOSTYKA USTEREK UKŁADU EGR NA PODSTAWIE DETEKCJI I POMIARÓW DRGAŃ WIBROAKUSTYCZNYCH

Streszczenie

Autorzy prezentują nową metodę diagnostyczną (in-vitro), wykorzystywaną w diagnostyce pojazdów samochodowych, polegającą na detekcji i pomiarze wartości drgań o charakterze wibroakustycznym. Wydaje się, że niesprawność układu recyrkulacji spalin nie powinna mieć wpływu na drgania, generowane przez silnik spalinowy. Autorzy dowodzą, że twierdzenie taki jest błędne. W tym wypadku koniecznym jest wysokiej jakości układ diagnostyczny. Dlatego użyto głowicę laserową firmy Polytec. Na podstawie badań otrzymano wielowymiarową funkcję wiroakustyczną, w której dodatkową zmienną jest wartość momentu obrotowego. Zmierzone drgania zostały poddane operacją cyfrowego przetwarzania sygnałów, takic jak okienkowanie, FFT, filtracji z użyciem filtrów o skończonej odpowiedzi impulsowej, które zostały poddane dodatkowo operacją okienkowania. Rezultaty pomiarów i przetwarzania zostały zaprezentowane w postaci obrazowania 3D, które w wypadku tej metody diagnostycznej wydają się najlepsze. Ponadto autorzy prezentują rozwój układów EGR różnych generacji. Zasada pracy tego układu polega na wtłoczeniu do komory spalania części gazów wylotowych. Duża część użytkowników tego systemu twierdzi, że jego działanie ma negatywny wpływ na osiągi pojazdu. Nie można jednak stwierdzić czy twierdzenie to jest właściwe gdyż dotychczas brakuje badań prowadzonyc w tym kierunku. Pomimo tego pewne jest, że zanieczyszczony zawór układu EGR na pewno będzie miał wpływ na osiągi pojazdu.

Słowa kluczowe: laserowa wibromeria Dopplerowska, EGR, cyfrowe przetwarzanie sygnałów.

1. INTRODUCTION

Since the 1960s, when rapid degeneration of the environment was first noticed, ways of reducing the emission of dangerous substances by automotive vehicles have been sought. The dangerous compounds are hydrocarbons (HC), nitrogen oxides (NO_x) and carbon dioxide (CO_2). The dangerous emissions can be reduced by [1]:

1. improving the fuel,
2. improving lubrication,
3. maintaining higher thermal stability,
4. perfectly insulating the system,
5. using catalytic systems.

Among the systems which have a bearing on engine thermal economics by reducing lean mixture temperature there is the Exhaust Gas Recirculation (EGR) system whose principle of operation consists in forcing some of the exhaust gas back into the combustion chamber [2].

The first experiences with EGR systems date back to the 1970s. The operation of the system was then limited to steady feeding the exhaust gas to the combustion chamber when the vehicle user turned on the system by means of a proper switch. That system only partially fulfilled its functions which included [3]:

1. lowering the combustion temperature of the lean mixture,
2. oxidizing harmful substances,
3. accelerating fuel vaporization.

As one can easily guess, the first vehicles with the EGR, which, thanks to General Motors, appeared on the American market in 1973 contributed little to emission reduction. It was mainly the fault of the human being who would decide when the EGR was and was not to work. In the late 1970s the system was improved by introducing a primitive diagnostic system whose integral part was a temperature sensor located on the cooler. It would turn on the EGR (provided the decision unit, i.e. the human being, had switched on the whole system) only at specified engine (coolant) temperatures. The next generations of the system were equipped with timing circuits which would switch off the EGR for a few seconds after the throttle was fully opened.

In 1983 research on the 4th generation EGR which is human-independent, i.e. it takes its own decisions about switching the system on or off, started. Besides taking the right switching decision, the system also decides what percentage of the exhaust gas can be turned back to the combustion chamber. The modern EGR takes a decision to switch on the system only if the following conditions are fulfilled [3]:

1. the engine temperature is higher than 77˚C,
2. the temperature under the bonnet is above -6˚C,
3. the engine has been working for at least 3 minutes at the above temperatures,
4. the crankshaft rotational speed is 1952-2400 rpm for the manual gearbox,
5. the crankshaft rotational speed is 2248-2688 rpm for the automatic gearbox,
6. the exhaust gas overpressure is 667-2667 Pa,
7. the fuel temperature does not differ from the one specified by the vehicle manufacturer (T_o) by -8% to +7%,
8. the voltage generated by the throttle opening sensor is in a range of 0.6-1.8V,
9. the driving speed is higher than 40 km/h.

2. DEVELOPMENT OF EGR

EGR systems are highly complex, particularly as regards their electronics and sensor system. However, when one examines the evolution of the EGR one can notice similarities to other emission reducing system. This is illustrated in fig. 1.

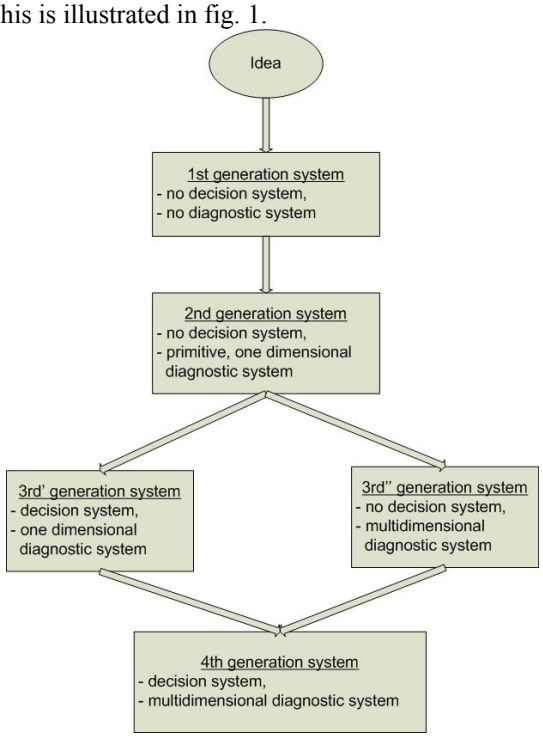

Fig. 1. Evolution of emission reducing systems

The emission reduction idea led to the development of the 1st generation EGR which is a simple implementation of this idea. Its control is limited to switching the system on by the human being at a proper moment, similarly as in other systems, e.g. in the 1st generation LPG system. The 2nd generation systems are equipped with a temperature sensor to aid the human being in decision taking.

The systems installed in cars have evolved in two ways, depending on system complexity and popularity. If the system is simple and there is a demand for it, a hybrid is usually created by adding a processor diagnostic system which eliminates the human being from decision taking. The diagnostic system takes decisions on the basis of one- or two-dimensional information coming from sensors (e.g. temperature and crank sensors). This is the case in LPG systems. The EGR has evolved in the other way, i.e. the decision still belongs to the human being who can switch the system off, but he/she is aided by systems consisting of many sensors (the 3rd generation system).

The synthesis is the 4th generation system. Here the human being does not take any decisions. Everything proceeds automatically, but so as not to disturb the operation of the engine or adversely affect driving safety and ergonomics.

3. OPERATION OF EGR

Although the idea seems to be simple, since it consists in pumping some of the exhaust gas back to the combustion chamber, its implementation is not so obvious. Two groups of systems [5] are distinguished:

1. pneumatically controlled,
2. electronically (processor) controlled.

As a rule, the operation of electronically controlled systems is based on a decision unit in the form of a (micro-) processor system. The decision whether to switch the system on and about the amount of exhaust gas which is to be forced back into the combustion chamber belongs solely to the integrated circuit which takes the decision on the basis of the information coming from the sensor CAN bus.

The EGR, belonging to the group of negative pressure-controlled sensors [2], is employed in both supercharged and unsupercharged engines. Generally speaking, in all the EGR systems known so far the valve is opened by a negative-pressure servomotor and closed by an elastic element [5]. Subpressure is produced by a double-purpose pump called a tandem pump, which is a combination of a fuel pump and a subpressure pump in one housing (fig. 2). The subpressure value is adjusted by an electrovalve (fig. 3) controlled by the information contained in the rectangular signal. In this case, this is pulse-duty factor k_w (fig. 4):

$$k_w = \frac{t_i}{T} \tag{1}$$

where: t_i – pulse duration, T– the period.

Fig. 2. Negative-pressure pump (fuel pump is on other side)

When the pulse-duty factor is close to 0, the electrovalve is closed. The degree of valve opening is directly proportional to the value of the factor and the maximum opening is reached at k_w=1.

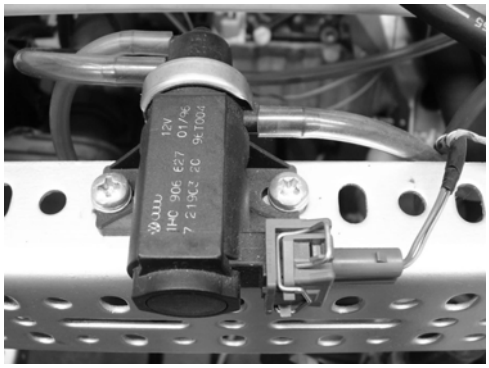

Fig. 3. EGR system electrovalve

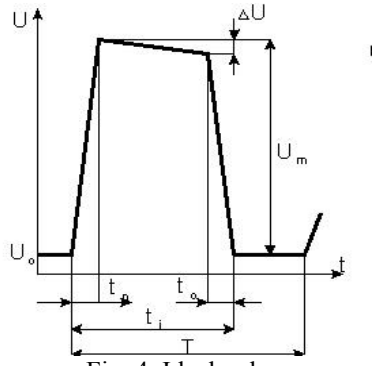

Fig. 4. Ideal pulse

The control system allows switching on the ERG only in certain engine operating conditions (described in chapter 1). But never the entire exhaust gas is forced back into the combustion chamber. The amount of exhaust gas which is forced in depends on [5]:

1. the mass of the air sucked in by the engine,
2. the volume of the air sucked in by the engine,
3. the throttle opening angle,
4. the absolute pressure in the intake manifold,
5. the exhaust gas overpressure in the exhaust system.

4. EGR FAILURES

In the literature on the subject and also on Internet forums the EGR and the need for its existence are often discussed. Unfortunately, many users who know how the EGR system works switch it off to improve the performance of their vehicles and prevent failures in the intake systems [4]. As a result, the EGR valve in the supercharged engine gets gummed up, as shown in fig. 5. Carbon deposit accumulation may totally block the EGR electrovalve and thereby damage the lambda probe, which leads to serious consequences.

The EGR valve can also be blocked when the negative-pressure system is untight or the pulse length control system is damaged. Negative-pressure system leakage is a typical failure of systems controlled in this way. The problem here is that the pipes feeding negative pressure to the EGR system are located close to the hot engine parts. Damage to a negative pressure feeding pipe results in, among other

things, engine stalling both when the engine is cold and hot.

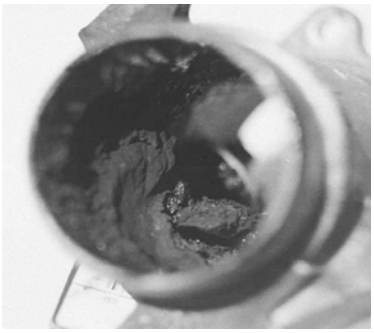

Fig. 5: Gummed up intake valve of EGR [4]

Besides the failures mentioned above, the systems of sensors which aid the processor unit in taking the ERG system switch on decision may fail. The sensors include [6]:

1. A coolant temperature sensor (CTS), which is an NTC (Negative Temperature Coefficient) thermistor. The typical resistances of this sensor are shown in the table below (tab. 1).

Tab. 1. Resistance values against coolant temperature sensor temperature

No.	R[Ω]	t[˚C]
1.	177	99
2.	467	70
3.	1459	40
4.	3520	20
5.	9420	0
6.	28680	-20
7.	100700	-40

2. A throttle position sensor (TPS), which is a potentiometer measuring voltage drop.
3. An oxygen sensor (OS), which is located in the throttle system and measures air volume. It usually works in tandem with a rate generator coupled with an a/d converter.
4. An intake air temperature (IAT) sensor, which, similarly as the coolant temperature sensor, is an NTC thermistor. As opposed to the thermistor which measures coolant temperature, a semiconductor thermistor with a different dopant is used in this case. This affects the resistance values versus temperature (tab. 2).
5. A crank sensor (CS).
6. A manifold absolute pressure (MAP) sensor.

Tab. 2. Resistance values versus intake air temperature sensor temperature.

No.	R[Ω]	t[˚C]
1.	185	99
2.	450	70
3.	1800	40
4.	3400	20
5.	7500	0
6.	25000	-20
7.	100700	-40

A failure of any of the systems mentioned above will cause a malfunction of the EGR system.

EGR faults have special a special symbol in the EOBD (OBDII) code, i.e. the value 4 in the 3rd field of the fault code [5].

A new method of diagnosing the EGR system, based on the multidimensional function of compression-ignition engine vibration, is presented below.

5. MEASUREMENT METHODOLOGY

Since 2008 the CAN bus can be the only diagnostic medium in automotive vehicles. Furthermore, since 2001 each new European vehicle has been equipped with the European On Board Diagnostics (EOBD) system which enables the real-time diagnosis of 849 faults [7].

The presented here EGR diagnostics methodology does not require direct access. The proposed system diagnoses many faults through a dedicated analysis of combustion engine vibrations. It would seem that the exhaust gas recirculation system has no effect on the (vibroacoustic) vibrations generated by the engine. However, it turns out that such diagnostics is possible.

Figure 6 shows a measuring rig which includes an engine (1), an electrorotary brake (2) and a vibrometeric head (3) which records vibrations.

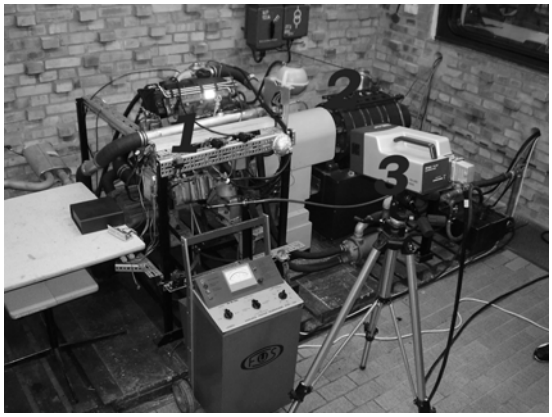

Fig. 6. Measuring rig: engine (1), electrorotary brake (2), vibrometeric head (3)

Tested object: compression-ignition engine

A compression-ignition Volkswagen, 1.9TDi engine was used for the tests. The engine is with direct injection effected by a system of injection units, a turbocharging system with adjustable charger guide blades and a turbocharging air cooling system, and an intercooler.

The engine performance specifications are as follows:

1. maximum power – 74 kW (101 KM) at 4000 rpm,
2. maximum torque – 250 Nm at 1900 rpm.

Figure 8 shows the external performance of the tested engine.

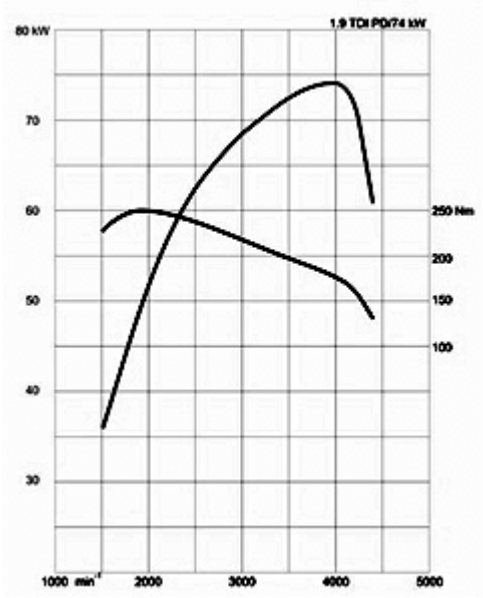

Fig. 7. Tested engine performance [14]

Engine test bench brake

The engine test bench was equipped with a Alpha 240 electrorotary brake made by AVL [8]. Its specifications are as follows [9]:

1. maximum power – 240 kW,
2. maximum torque – 600 Nm.
3. maximum speed – 10000 rpm.
4. inertia – $0.368 \frac{J}{kg * m^2}$.

Figure 8 shows the brake's characteristic P=f(ω) [9].

Vibrometric system for measuring vibrations

The vibrations generated by the engine were measured by a scanning vibrometric system PSV made by Politec. The system includes:

1. a controller (OFV-5000),
2. a decoder module,
3. a vibrometric head (PSV400).

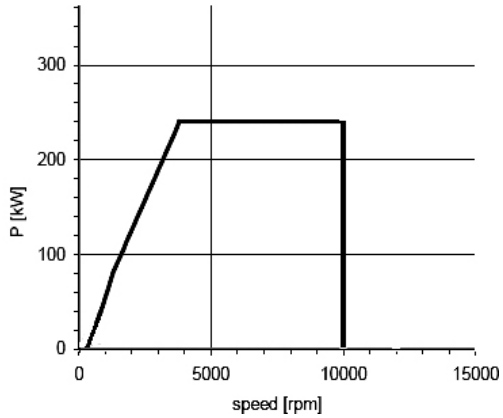

Fig. 8. Power characteristic of test brake

The vibration measurement parameters are shown in table 3.

Table 3.
Vibration measurement parameters

No.	Parameter	Value
1.	Kind of measurement	Speed vector
2.	Averaging	Off
3.	Number of samples	4096
4.	Sampling frequency	2048 Hz
5.	Measurement duration	2 s
6.	Filter	No
7.	Directivity	+Z
8.	Barrier frequency	20 kHz
9.	Vibration range	640 μV/m

Figure 9 shows the adopted diagnostic circuit.

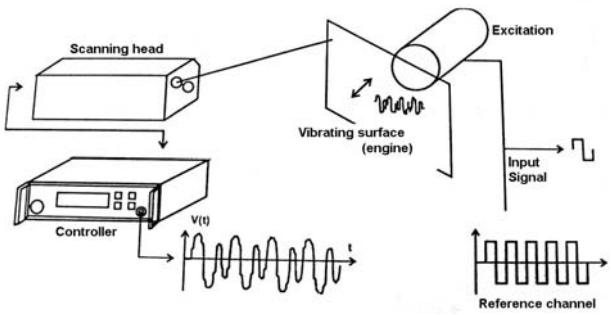

Fig. 9: Adopted diagnostic circuit

One should mention that it was not necessary to use a reference channel with a trigger arm in the investigations. This means that garage diagnostics without additional specialist equipment will be possible.

6. DIGITAL PROCESSING OF VIBRATION SIGNAL

Without proper signal processing direct measurements do not yield explicit results. In addition, the proposed method requires multidimensional measurements, i.e. of a series of vibrations in the torque domain.

6.1. Operations on signal in time domain

The aim of all the signal digital processing operations performed during the investigations was to change the shape of the signal spectrum in a replicable way using standard methods. The first operation is signal windowing. In this case, windowing in the time domain since it is limited to the multiplication of the discrete vibration signal and the discrete window spectrum. Naturally, one could use a window in the frequency domain, but this would require the convolution of the two discrete signals.

A rectangular spectrum would have an ideal windowing sequence for damping uncharacteristic (from the investigation point of view) parts of the spectrum and simultaneously amplifying its characteristic parts. The ideal window would not distort the signal and prevent spectral leakage (an effect in which a part of the signal component, not situated by the frequencies for which the analysis is made, appears in all the output discrete signal values after transformation to the frequency domain [12]).

Since it is impossible to obtain a rectangular frequency characteristic a compromise is necessary. The compromise consists in the use of the best (from the investigation point of view) windowing sequence.

It has been experimentally found that a flap-top window is a good solution. This window is characterized by a low resolution at high dynamics [10]. Also its amplitude rendering accuracy is quite high. The values of this kind of window are calculated from the following formula (1) [10]:

$$\omega(t) = 1 - 1.93\cos(\frac{2\pi t}{T}) + 1.29\cos(\frac{4\pi t}{T}) - 0.388\cos(\frac{6\pi t}{T}) + 0.0322\cos(\frac{8\pi t}{T}) \quad (2)$$

where: $0 \le t \le T$ and ω(t)=0 for values from outside the domain.

Figure 10 shows the window's spectrum in the time and frequency domains.

6.2. Transformation to frequency domain

After windowing the signal is transformed to the frequency domain, using the fast Fourier transform with a base of 2. The way in which the FFT algorithm is introduced has been known since 1965 and it is widely described in the literature [10, 11, 12]. The fast Fourier transform used for discrete signals is expressed as follows:

$$X(k) = \sum_{j=1}^{N} x(j)\omega_N^{(j-1)(k-1)} \quad (3)$$

where: $\omega_N = \exp(\frac{-2\pi i}{N})$; N – the number of samples, k– the current sample of the frequency domain,

j – the current sample of the time domain.

Thanks to the algorithm the calculations can be significantly speeded up and a modern PC does the job in a few seconds.

6.3. Filtering in frequency domain. Remez algorithm

One of the features of the discrete signal after the Fourier transformation, i.e. the time domain shift theorem, was used in the investigations. It follows from the definition of the Fourier transformation that a shift of the signal in the time domain by the value x is equivalent to multiplying the signal spectrum by the complex number $e^{-j\omega x}$ [13]. The multiplication result has no effect on the shift of the spectrum in the frequency domain. Generally, the dependence can be written as:

$$x(t - t_0) \xleftrightarrow{FFT} X(\omega)e^{-j\omega t_0} \quad (4)$$

hence:

$$x(t - t_{01}) \xleftrightarrow{FFT} |X(\omega)| \quad (5)$$

and

$$x(t - t_{02}) \xleftrightarrow{FFT} |X(\omega)| \quad (6)$$

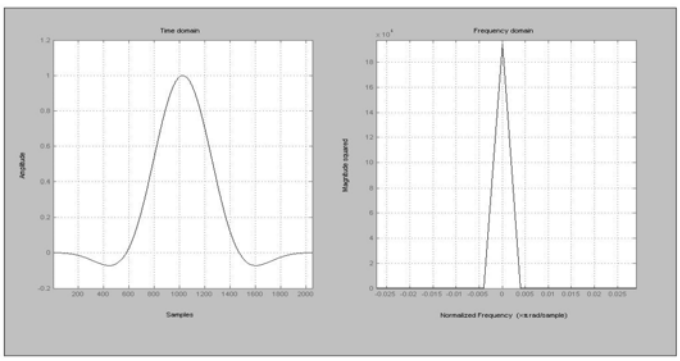

Fig. 10. Flap-top window in time and frequency domains

The above feature, thanks to which after the Fourier transformation (FFT) the spectral module is insensitive to time sample shift (5), (6), forms the basis of the proposed diagnostic method. There is no need to search for the same measuring point in each sample, i.e. for the top dead centre (TDC).

Since the spectral module is insensitive to the shift a decision was made to use the finite pulse response (FPR) filter design method. It is a very popular method of designing filters (except phase filters) [11].

In order to obtain the current output signal sample, FPR filters use only the previous samples and the current sample, which shortens and simplifies the analysis. As a result the method is suitable for real diagnostic systems.

The low-pass filter generated by the Remez method (also called the Parks-McClellan method) was amplified (fig. 11).

Since the spectrum of the filter was characterized by considerable damping and low stability, the obtained filter samples were multiplied in the time domain by the Blackman window (7):

$$\omega(k+1) = 0.42 - \cos(2\pi \frac{k}{N-1}) + 0.08\cos(4\pi \frac{k}{N-1}) \quad (7)$$

where: N – the number of samples, k – the current sample.

The filter obtained in this way is shown in fig. 12.

The filter samples prepared in this way are multiplied in the time domain by the samples of the frequency spectrum of the vibrations generated by the engine. One should note that windowing and filtering are possible in both the time domain and the frequency domain. However, windowing in the frequency domain would require the convolution of the window frequency spectrum and the signal spectrum and the filtering in the time domain would also require the convolution of the filter time spectrum and the vibration signal spectrum. As a result of the additional transformations and the convolution, the method would become complicated. Therefore the particular operations were performed in their natural domains, i.e. windowing by multiplying the window and the signal in the time domain and filtering by multiplying the filter samples and the signal samples in the frequency domain. Regardless of the path taken, the two operations are equivalent.

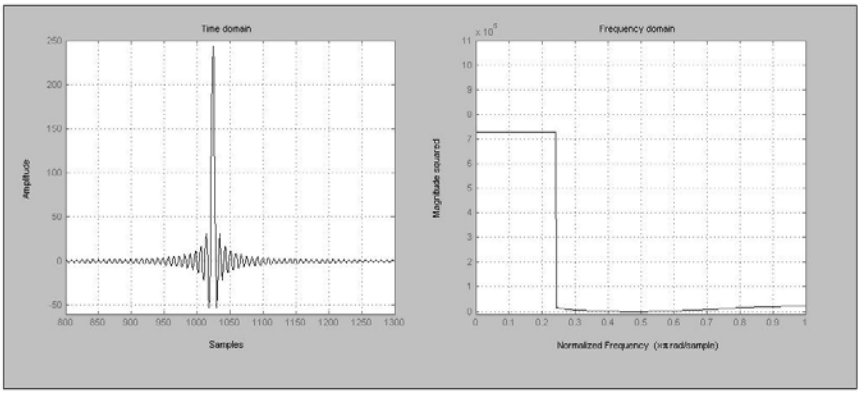

Fig. 11. Spectrum of FPR filter generated by Remez algorithm

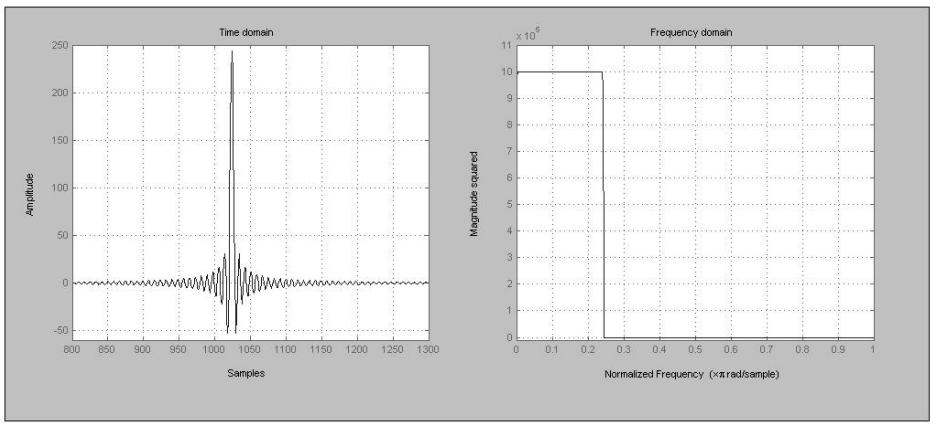

Fig. 12. Spectrum of FPR filter generated by Remez algorithm after windowing with Blackman window

7. ANALYSIS OF RESULTS

The digital signal processing operations were performed multidimensionally. This means that the digital signal processing operations described were performed for all the signals measured at different torques at a constant rotational speed.

In the first step, measurements were performed for the engine in good working order as the reference. The obtained characteristic is shown in fig. 13.

Then the EGR system electrovalve (fig. 3) was switched off and the vibrations generated by the engine were measured again. The obtained signal was processed in the same way as previously. The result is shown in fig. 14. The area in which considerable signal amplitude deviations are observed is circled.

One can notice that the function for the torque of 30 and 40 Nm has a different character. Moreover, the measurement is not fully replicable but characteristic for a given engine when the measurement methodology described here is used. The change here applies to a value of up to -3,5 dB.

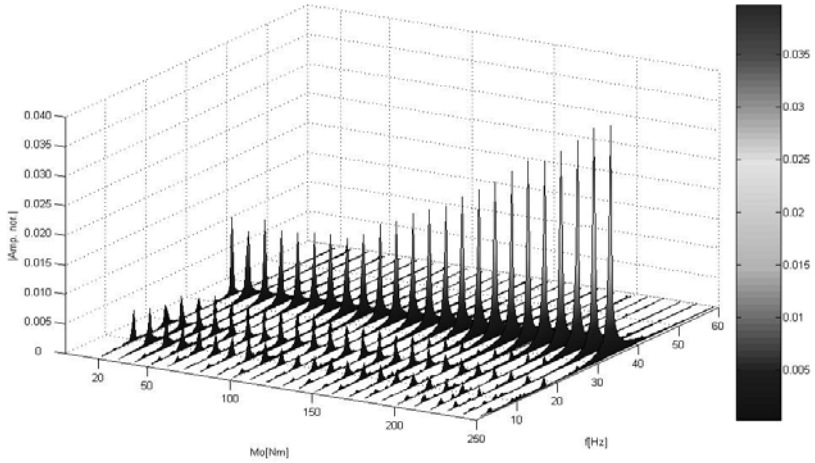

Fig. 13. Vibration versus torque spectrum of engine in good working order; ω = const

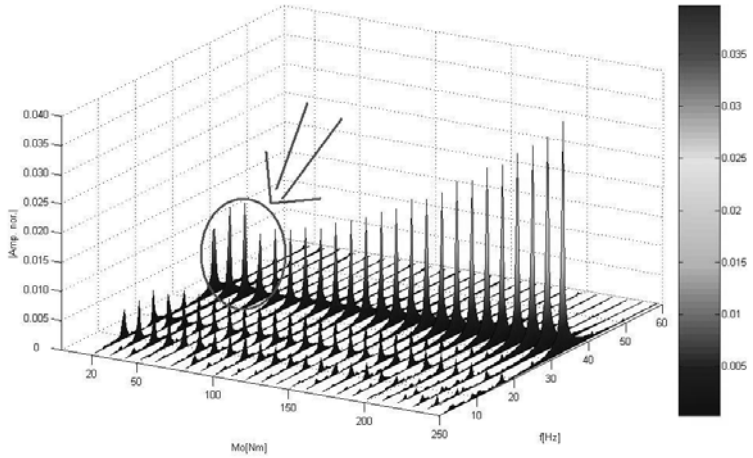

Fig. 14. Spectrum of vibration of engine with switched off EGR electrovalve versus torque; ω = const.

8. CONCLUSIONS

1. In vivo diagnostics of combustion engines, based on the analysis of vibration, is possible. It is desirable to use a laser device for this purpose.
2. Although the method is quite complex, particularly in its digital signal processing aspect, it can be implemented in the widely available diagnostic systems thanks to the increasing popularity of signal processors.
3. Several faults and failures which until now have been considered to have a negligible effect or no effect on the operation of the engine can be immediately detected on the basis of engine vibrations.
4. The multidimensional analysis of engine vibrations allows one to predict failures.
5. In the case of failures which clearly affect the vibrations generated by the engine, the one-dimensional function is sufficient for this type of diagnostics.
6. The proposed method requires that measurements be performed for each model of the engine in good working order as the reference for further measurements. Measurements performed in accordance with the principles of digital processing of signals are replicable.
7. Engine vibrations are not an individual characteristic of each engine, but of the model.

9. REFERENCES

[1] „Engine Technology International" June 1999.
[2] http://en.wikipedia.org/wiki/Exhaust_gas_recirculation
[3] http://www.asashop.org/autoinc/nov97/gas.htm
[4] http://forum.tdi-tuning.pl/viewtopic.php?p=4267
[5] Stefan Myszkowski, „Instalator Polski: Diagnostyka Pokładowa".
[6] http://60degreev6.com/index.php?title=Detailed_Sensor_Descriptions#Exhaust_Gas_ Recirculation _ Valve_.28EGR.29
[7] Merkisz J., Mazurek S.: *Pokładowe systemy diagnostyczne pojazdów samochodowych,* Wydawnictwa Komunikacji i Łączności, Warsaw, 2002.
[8] http://www.avl.com
[9] *The Thrill of Solution: Dynamometers and Drivers,* wyd. AVL, update 12.4.2001.
[10] Stranneby D., *Cyfrowe przetwarzanie sygnałów. Metody, algorytmy, zastosowanie*, Wydawnictwo BTC, Warsaw, 2004.
[11] Zieliński T. P.: *Cyfrowe przetwarzanie sygnałów,* Wydawnictwo WKŁ, Warsaw, 2005.
[12] Lyons R.G.: *Wprowadzenie do cyfrowego przetwarzania sygnałów,* Wydawnictwo WKŁ, Warsaw, 2006.
[13] Szabatin J.: *Podstawy teorii sygnałów,* Wydawnictwo WKŁ, Warsaw, 2003.
[14] http://skoda.autokacik.pl/pages/chtyki/cha%20octavia.htm

SELECTION OF CLUSTERING METHODS FOR WIND TURBINES OPERATIONAL DATA

Mariusz GIBIEC*, Tomasz BARSZCZ*, Marzena BIELECKA**

*AGH University of Science and Technology, Faculty of Mechanical Engineering and Robotics
Department of Robotics and Mechatronics,
Al. Mickiewicza 30, 30-059 Kraków, Polska, e-mail: mgi@agh.edu.pl
**AGH University of Science and Technology, Faculty of Geology, Geophysics and Environmental Protection,
Department of Geoinformatics and Applied Computer Science,
Al. Mickiewicza 30, 30-059 Kraków, Polska, e-mail: bielecka@agh.edu.pl

Summary

Quickly growing number of monitored wind turbines has changed the needs for monitoring and diagnostic algorithms. The data from hundreds of monitoring systems are transferred to the diagnostic centers, where the data should be analyzed. High cost of labor created the need for automated diagnostic methods. The first task in this wide discipline is classification of the data and detection of malfunction states. The paper investigates application of data mining methods for classification of operational data from wind turbines. It is shown, that combination of the agglomeration method with the C-means clustering yields very good results and can be used for automated diagnostics of wind farms.

Keywords: machine diagnostics, wind turbine, data mining, clustering.

DOBÓR METOD GRUPOWANIA DANYCH PROCESOWYCH DLA TURBIN WIATROWYCH

Streszczenie

Szybko rosnąca liczba monitorowanych turbin wiatrowych zmieniła potrzeby w zakresie algorytmów monitorowania diagnostyki. Obecnie dane z setek systemów monitorowania przesyłane są do centrów diagnostycznych, gdzie muszą zostać przeanalizowane. Wysokie koszty pracy ekspertów spowodowały potrzebę zautomatyzowania metod diagnostycznych. Pierwszym zadaniem stała się automatyczna klasyfikacja danych i wykrywanie stanów niesprawności. Artykuł przedstawia zastosowanie metod „data mining" do klasyfikacji danych procesowych z turbin wiatrowych. Pokazano, że połączenie metody aglomeracji danych z metodą K-means daje bardzo dobre wyniki i może być zastosowane do zautomatyzowanej diagnostyki farm wiatrowych.

Słowa kluczowe: diagnostyka maszyn, turbina wiatrowa, eksploracja danych, grupowanie.

1. INTRODUCTION

In recent years wind energy is the fastest growing branch of the power generation industry. The average yearly growth in the years 1997-2003 achieved 32% in the United States and 22% in the European Union [1]. This branch of power generation industry is also quickly developing in Poland. In July 2010 the installed capacity exceeded 1000 MW. Wind farms currently being built will increase this number to 2500 MW in next 3 years [2]. it The distribution of costs during the lifecycle of the unit for wind energy is significantly different from that of traditional, fossil fired units [3]. First of all, initial investment costs are relatively higher, whereas in traditional units cost of fuel plays important role (usually it is the second largest cost). After commissioning, the largest cost for the wind turbine is maintenance. With proper maintenance policies, wind turbines can achieve the highest level of availability in the power generation sector – even up to 98%.

The basis of proper maintenance is continuous monitoring of the transmission of the wind turbine. The most successful monitoring methods use vibration signals [4, 5], but due to a very high number of monitored machines, other methods are also needed. Quickly growing number of monitored wind turbines has changed the needs for monitoring and diagnostic algorithms. Numerous companies develop monitoring methods, which often include remote monitoring. The data from hundreds of monitoring systems are transferred to the diagnostic centers, where the data need to be analyzed. Traditionally, such a work was performed by experts, who used advanced monitoring tools (usually based on vibration analysis) to assess the technical state of the machinery. High cost of labor created the need for automated diagnostic methods. Significant amount of expert time can be saved when an automated tool would be able to browse the

data and to detect "suspicious" or simply novel data, which are next reported to the expert. Thus, the time can be spent only on these interesting cases.

The first task in this activity is the classification of the data and detection of malfunction states. Even before vibration methods are applied, the more basic methods are required. The fundamental operational data for the wind turbine are: wind speed, rotational speed and generated power. Further data should also be investigated, but these three are the most important and are able to detect several malfunctions [6]. Such a selection is also convenient, as the dimensionality of the problem is relatively low and results can be presented in
a human readable form.

The amount of current research in the field of automated wind turbine data classification is not too large. One of first research were devoted to the environmental impact in one of the first Polish wind farms [7]. There were a few works pointing at the importance of the application of artificial intelligence methods, like e.g. [8]. Example of such a classification with ART type networks was presented in [9]. The authors has showed that ART networks can operate automatically, though they are vulnerable to configuration parameters. Another interesting direction of research is application of data mining methods. There are several high quality textbooks on this subject, like e.g. [10, 11]. The data mining methods were successfully applied for another machinery, like e.g. coal harvesters [12].

The paper investigates application of data mining methods for classification of listed operational data from wind turbines. The goal of the work was to obtain clusters, which would represent typical operational states of the wind turbine. Next, the data from normal operation would be tested if they belong to one of found clusters. If not, the expert would be notified about the detected situation.

2. CLUSTERING ALGORITHMS

2.1. Classification – a formal approach

In order to introduce a classification algorithm, a set of interesting objects, say X, should be divided into separate subsets, called classes, and a method of assign a considered object to the proper class should be given. The division of a given set into classes formally corresponds to specification an equivalence relation, denote it by REL, i.e a relation which is reflexive, symmetric and transitive on the space X\Z, where the set Z, being a subset of the space X, is small in comparison with it. In particular, sometimes Z= Ø, but in the opposite case it is necessary to introduce a nonempty set Z because, in practice, there are usually objects which cannot be classified according to the introduced criteria. The property that Z is small should be explained. To do this, a certain mathematical structure on the space X must be introduced. The most convenient one is a measure. Then, it is said that the set is small in the space (X, μ), where μ is the introduced measure, if μ(Z) = 0. Sometimes, however, it is difficult or even impossible to constitute a measure consistent with the considered classification problem. In such a case other structure should be taken into account. Thus, if X is a topological space, the set Z is small when X\Z is open and dense according to the topology established on X. If X is a metric space then Z is small if its diameter is equal to zero.

The equivalence relation REL is introduced consistently to the studied classification problem if the equivalence classes of REL are also recognized classes of the classified objects. The equivalence class of $x \in X \setminus Z$ is denoted by $[x]$ and is defined in the following way: $[x] := \{y \in X \setminus Z : xRELy\}$.

The following describes very basic properties of equivalence classes - see [13]:

(a) $x \in [x]$

(b) $[x_1] = [x_2] \;\Leftrightarrow\; x_1 RELx_2$

(c) $[x_1] \neq [x_2] \Rightarrow [x_1] \cap [x_2] = \emptyset$

The simple implication of the specified properties is that

$$X \setminus Z = \bigcup_{x \in X \setminus Z} [x].$$

The item (c) and (1) means that equivalence relation founds division of the set $X \setminus Z$. On the other hand, every division of a set constitutes an equivalence relation on it. The classifying algorithm realizes the canonical mapping

$$F : X \setminus Z \to (X \setminus Z)/_{REL},$$

where $(X \setminus Z)/_{REL}$ is a quotient set and $F(x)=[x]$.

2.2. Clustering algorithm

In this paper a two-stage approach to a classification problem is applied. Agglomeration method, allowing us to establish a number of classes, is the first stage, whereas a c-means clustering, being the second stage of the algorithm, gives us the representative of each class.

Considering agglomeration method in the most general way, we can specify the following algorithm:

1. Create *n* classes, each consists of one object.
2. Compute the value of the chosen measure of similarity for each pair of classes.
3. Merge two most similar classes.
4. Finish if all objects belong to one class, otherwise go to 2.

In this paper the distance is used as a measure of similarity. This means that on the space X a metric, say *d*, is defined. Let us recall that

$$d:XxX\rightarrow[0;\infty)$$

has the following properties:

1. *d(x,y)=0 if and only if x=y,*
2. *d(x,y)=d(y,x),*
3. *d(x,y)+d(y,z)≥d(x,z).*

There are infinitely many functions satisfying the above metric axioms (1)-(3). In the case of the n-dimensional Euclidean space, the following ones are most often used in clustering tasks.

1. The generalized Euclidean metric:

$$d(\vec{x},\vec{y}) = \sqrt{\sum_{i=1}^{n}\left[\lambda_i \cdot \left(x_i - y_i\right)\right]^2}$$

In the case of the classical Euclidean metric all λ_i are equal to 1.

2. The generalized Manhattan metric

$$d(\vec{x},\vec{y}) = \sum_{i=1}^{n}\lambda_i \cdot \left|x_i - y_i\right|$$

In the case of the classical Manhattan metric all λ_i are equal to 1.

3. The maximum metric

$$d(\vec{x},\vec{y}) = \max\left|x_i - y_i\right|,$$

where $n \geq i \geq 1$.

4. The Minkowski's metric

$$d(\vec{x},\vec{y}) = \left[\sum_{i=1}^{n}\left|x_i - y_i\right|^t\right]^{\frac{1}{t}}$$

The choice of a metric is a crucial point for a correct performance of a classification task – see [14], page 44, Table 4.1.

The representative methods, to which the c-means algorithm belongs, consists in postulation a mapping

$g:X\backslash Z\rightarrow X$, provided that the classes are established. The *g(A)* is an object representing the class (cluster) *A*.

3. CASE STUDY

3.1. Data overview

The data set was recorded on a real wind turbine. The set consisted of three measurement channels: wind speed, rotational speed and generated power. These values were recorded every 10 minutes. The investigated set covered 20 days of data and had 2960 samples. The first test was to analyze basic dependencies in the data (Fig. 1, situated at the end of the paper). It is visible that the data do not follow the Gaussian distribution – see histograms of each channel at the diagonal of the plot. On the other hand, some dependencies can be seen. They are nonlinear, since the speed can be achieved only when the wind is above certain level. Also, in this case the speed does not rise linearly but reaches 1000 rpm in a short time. The data should be grouped into clusters, which would represent typical operational states.

3.2. Agglomeration method

First, the aim of work was to determine number of groups appearing in data. Number of groups can suggest how many patterns are hidden in data, but it does not have to be equal the number of states. Some data qualified into the same group can identify different states. If there are more groups than states, some of them identify the same states or characterize unrecognized state. If there are less groups then states, some of them can not be distinguished. In both cases testing examples or expert validation are necessary to perform the state assessment.

For such a defined clustering task the Ward method was chosen. It is one of the hierarchical agglomeration methods. This type of methods allows specifying hierarchical tree of elements of the analyzed set. The tree is being built via step by step joining of operational taxonomic units into subsets. At the beginning each element of the set is a single unit and a matrix of distances between units is created. Distances are calculated using one of metrics mentioned above.

Then the minimum value among elements of the diagonal is found. It is the minimum agglomeration distance in local sense. Units associated with this distance are joined into the new unit. Next a new matrix of distances is created and the procedure is repeated until all units are joined into a single one.

Ward method differs from other hierarchical methods in the way of estimation of the distance between taxonomic units. Variance analyses is applied – towards minimizing the sum of squared distance between each two groups that are created at each step of agglomeration.

The important advantage of the proposed method is lack of arbitrary defined number of groups in the analyzed data and 40% better efficiency of right detection of data structure than in other methods [15]. Results of Ward clustering of considered data, with the use of the generalized Euclidean metric, are shown in the Fig. 2.

The Ward tree can be cut on the level where bond distance (distance between clusters) equals 10% of maximum cluster to cluster distance. Number of cut branches corresponds to the number of clusters. This way the number of groups in data was identified as 4. It is possible to read from the tree which samples of data belong into particular group, but due to problems with automatic implementation on classification purposes only the number of clusters is useful result of this method.

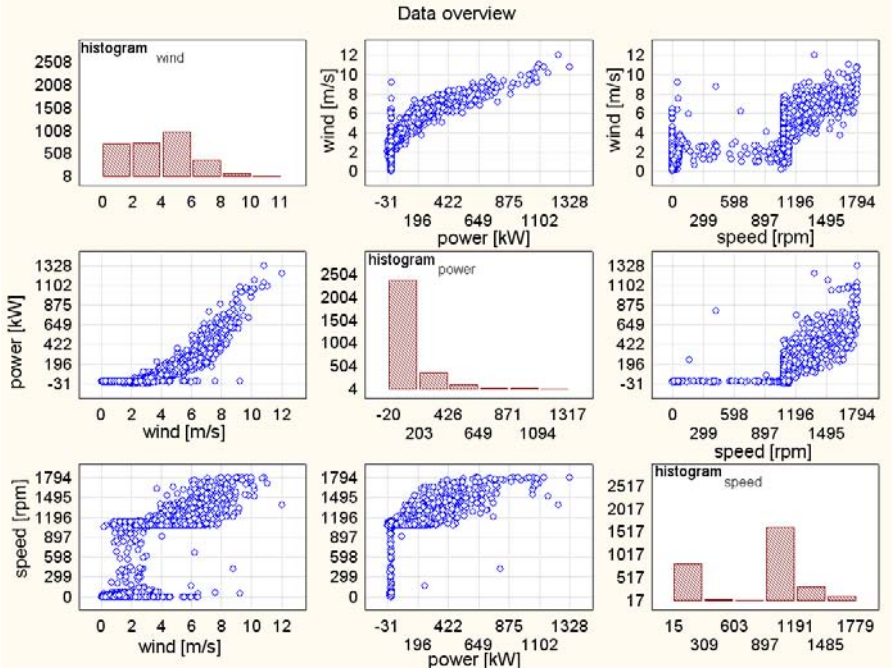

Fig. 1. Basic statistical analysis of the investigated set of data

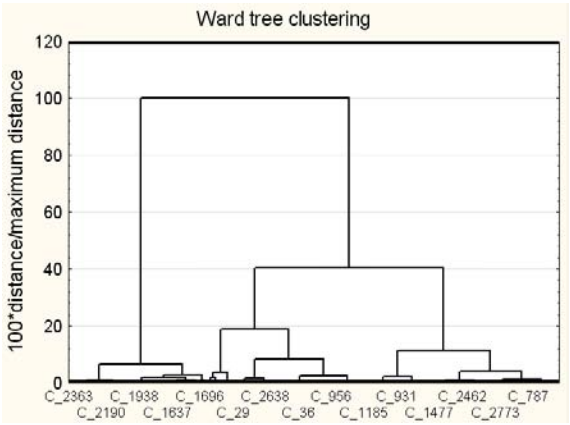

Fig. 2. Result of the agglomeration method

3.3. C–means clustering

The result of Ward clustering was utilized as parameter of non hierarchical method of clustering – c-means clustering. This method requirement is to specify number of clusters the data has to be divided into. The aim of the method is to create specified number of groups, in the considered case 4, that are as different as possible in the distance sense. It can be stated that the method is inverse with respect to variance analyses. At the beginning clusters are created randomly. Then elements of the set are being moved from one cluster to another to assure minimum variety within each cluster and maximum variety between clusters. In the considered case study the aim of c-means method application was to determine which samples of data can be grouped together and what are reference values characteristic for each cluster.

Results of c-means clustering are presented in the figure Fig. 3 and 4 and in Tab. 1. The identified reference values characteristic for each operational state can be used in automatic classification. Results of such a classification with the use of minimum distance method are presented in the Fig. 5 situated at the end of the paper. Classified data samples formed clusters corresponding to four operational states.

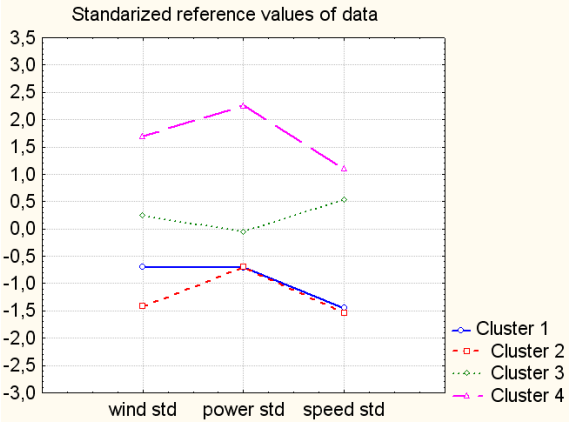

Fig. 3. Result of C-clustering algorithm (normalized values)

Table 1. Reference values of data (cluster centers)

Cluster	Wind [m/s]	Power [kW]	Speed [rpm]
1	2,59	-4,78	80,13
2	1,16	-4,25	31,83
3	4,47	100,03	1117,81
4	7,39	475,83	1417,87

The location of generated clusters is very interesting, as it is very close to the natural grouping used by human experts. The following states were detected:

– idle (weak wind, machine turning, no power)

- stopped (no wind, machine is stopped or turning very slowly)
- low power (average wind, speed 1000 rpm, low power)
- high power (strong wind, speed 1500 rpm, high power)

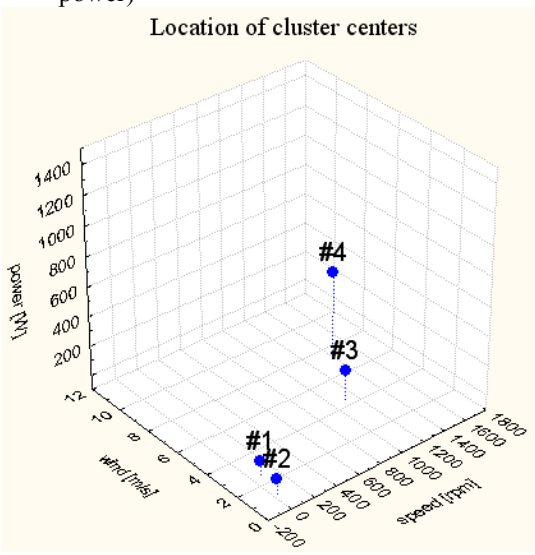

Fig. 4. Location of cluster centers

It is important to note that negative power values in states 1 and 2 are correct values measured from the wind turbine control system, which clearly has a systematic error. Nevertheless, the error is in the range of a few promiles, which is often the case in real installations. Also note, that the order of clusters is not "natural", or as the human expert would list it, because clusters 1 and 2 would have changed order. Nevertheless, in automatic clustering it is a common case and has no influence on the performance of the method.

4. CONCLUSIONS

The paper presents application of data mining methods for clustering the operational data from wind turbines. It is shown, that combination of the agglomeration method with the C-means clustering yields very good results and can be used for the automated diagnostics of wind farms. Obtained results are the important starting point for automated monitoring of wind farms. Further research should be focused on implementation of the method in a software tool, which would periodically run on a real data and detect abnormal pattern in the data.

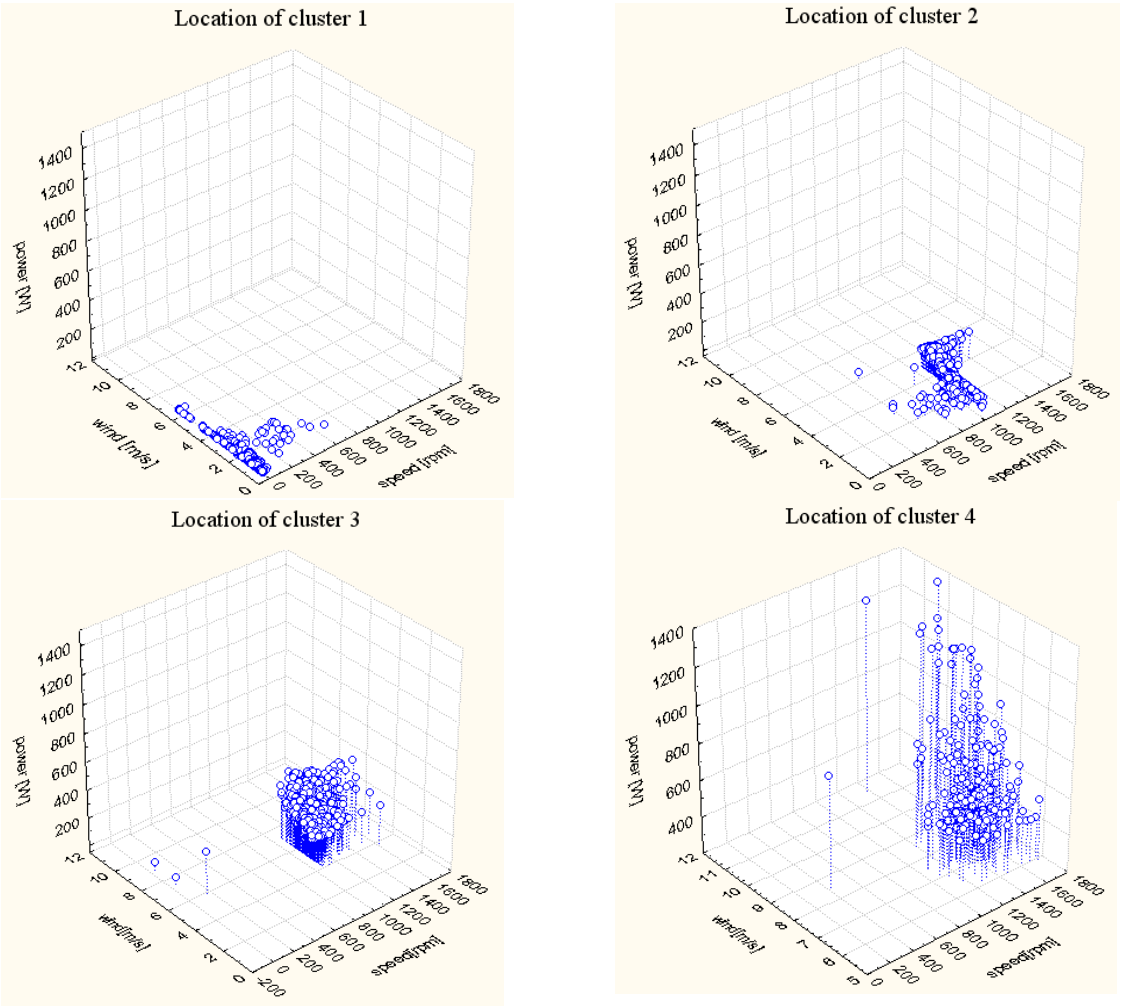

Fig. 5. Results of data clustering

REFERENCES

[1] European Wind Energy Association, *Wind power continues to grow in 2004 in the EU*, EWEA, 2005
[2] European Wind Energy Association, *Wind Energy. The facts. An analysis of wind energy in the EU-25*, EWEA, 2005
[3] Polskie Stowarzyszenie Energetyki Wiatrowej. www.psew.pl
[4] T. Barszcz, *Selection of diagnostic algorithms for wind turbines*, Diagnostyka, vol. 50, 2009/2, pp. 7-12
[5] Z. Hameed, Y.S. Hong, Y.M. Cho, S.H. Ahn, C.K. Song, *Condition monitoring and fault detection of wind turbines next term and related algorithms: A review*, Renewable and Sustainable Energy Reviews, vol. 13, 2009/1, pp. 1-39
[6] E. Hau, *Wind Turbines*. Fundamentals, Technologies, Application, Economics. 2nd Edition, Springer, Heidelberg, 2006
[7] M. Golec, Z. Golec, C. Cempel, *Noise of wind power turbine VESTAS V80 in a farm operation*, Diagnostyka, vol. 37, 2006/1, pp. 115-120
[8] J. Dybała, S. Radkowski, *Use of cp neural network in vibroacoustic diagnostics of toothed gears failure*, Diagnostyka, vol. 31, 2004, pp. 58-66
[9] T. Barszcz, A. Bielecki, M. Wójcik, *ART-type artifcial neural networks applications for classifcation of operational states in wind turbines*, Lecture Notes on Artificial Intelligence, vol.6114, 2010, pp. 11-18
[10] B. Mirkin, *Clustering for Data Mining*. *A Data Recovery Approach,* Chapman & Hall, London, 2005
[11] I.H. Witten, E. Frank, *Data Mining. Practical Machine Learning Tools and Techniques*. 2nd Edition, Elsevier, San Francisco, 2005
[12] M. Gibiec, *Application of selected Data Mining methods to machinery operation*, Diagnostyka, vol. 51, 2009/3, pp. 69-72
[13] Rasiowa H. *Introduction to Contemporary Mathematics*, PWN, Warszawa, 1998.
[14] Tadeusiewicz R., *Flasiński M., Rozpoznawanie obrazów*, PWN, Warszawa 1991.
[15] Grabiński T., Sokołowski A.: *The Effectivness of Some Signal Identification Procedures, Signal Processing: Theories and Applications*, North-Holland Publishing Company, EURASIP, 1980.

Dr hab. inż. **TOMASZ BARSZCZ** pracuje w Katedrze Robotyki i Mechatroniki AGH. Zajmuje się diagnostyką maszyn oraz systemami monitoringu i diagnostyki. Jest autorem 4 książek i ponad 70 publikacji. Opracowane przez niego systemy pracują na stu kilkudziesięciu instalacjach.

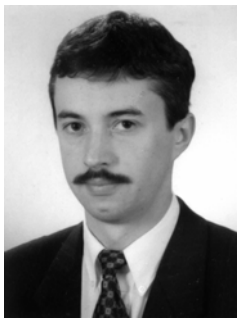

Dr inż. **Mariusz GIBIEC** jest adiunktem w Katedrze Robotyki i Mechatroniki AGH. Jego zainteresowania dotyczą zastosowań metod eksploracji danych oraz sztucznej inteligencji (sieci neuronowych i zbiorów rozmytych) w Diagnostyce Technicznej. Jest autorem prac nad wykorzystaniem powyższych technik w systemach monitorujących do realizacji zadań filtracji, predykcji oraz klasyfikacji stanu maszyn.

Dr **Marzena BIELECKA** jest adiunktem w Katedrze Geoinformatyki i Informatyki Stosowanej AGH. Zajmuje się systemami sztucznej inteligencji. Jest autorem publikacji dotyczących medycznych i inżynierskich zastosowań sztucznej inteligencji

IMAGE CHANGE DETECTION AS A SUPPLEMENT FOR ADAPTIVE CRUISE CONTROL WITH STOP&GO FUNCTIONALITY

Jakub KOMODA[1], Jacek DYBAŁA[2]

[1]e-mail: kuba.komoda@gmail.com
[2]Politechnika Warszawska, Wydział Samochodów i Maszyn Roboczych, Instytut Pojazdów,
ul. Narbutta 84, 02-524 Warszawa, e-mail: jdybala@simr.pw.edu.pl

Summary

The theme of the project was to develop algorithms for image sequence analysis, allowing for improved functionality of adaptive cruise control equipped with Stop & Go function. Using Doppler radar could cause that on the small distances the object that crosses the path of the vehicle may not be detected. This is particularly important because of the Stop & Go function that allows the host vehicle to stop when preceding vehicle stops, and start automatically when the preceding vehicle pulls away. In such a situation collision with an undetected object located between the vehicles can occur. The requirement was to propose such algorithms that will work in real time and ensure compatibility with the existing system architecture.

Keywords: adaptive cruise control, image sequence analysis, change detection, image processing.

WYKRYWANIE ZMIANY OBRAZU JAKO UZUPEŁNIENIE SYSTEMU TEMPOMATU ADAPTACYJNEGO Z FUNKCJĄ STOP&GO

Streszczenie

Tematem projektu było opracowanie algorytmów analizy sekwencji obrazów pozwalających na polepszenie funkcjonalności tempomatu adaptacyjnego wyposażonego w funkcję stop&go. Wykorzystanie dalekosiężnego radaru Dopplera może spowodować, że na małych odległościach nie zostanie wykryty obiekt przecinający trasę pojazdu. Ma to szczególne znaczenie ze względu na funkcję stop&go, która pozwala na zatrzymanie pojazdu, gdy pojazd poprzedzający się zatrzyma, oraz automatyczne ruszenie, gdy pojazd poprzedzający odjedzie. W takiej sytuacji może dojść do kolizji z niewykrytym obiektem znajdującym się pomiędzy pojazdami. Wymaganiem było zaproponowanie takich algorytmów, które pozwolą na pracę w czasie rzeczywistym oraz zapewnią kompatybilność z dotychczas wykorzystywaną architekturą sprzętu.

Słowa kluczowe: tempomat adaptacyjny, analiza sekwencji obrazów, rozpoznanie zmian, przetwarzanie obrazów.

1. INTRODUCTION

In the modern environment one can observe growing congestion in urban areas. This happens mainly because of rapidly growing number of cars, which leads to increase in the number of accidents happening every day. To prevent such situations, number of solutions were developed and introduced in the automotive field – majority of them can be related to as the Driver Assistance Systems. One of such is Adaptive Cruise Control with Stop&Go functionality. Adaptive cruise control in relation to classical cruise control device is additionally equipped with sensor allowing the system to adapt host vehicle speed based on the condition of surrounding environment. Stop&Go feature allows the host vehicle to brake to a complete stop when the preceding vehicle slows down to a halt by using long-range narrow beam Doppler radar to detect velocity of the preceding vehicle. Additional "automatic go" function allows the host vehicle to start driving again without driver intervention once the preceding vehicle pulls away.

As mentioned above, to estimate velocity of the proceeding vehicle long-range narrow beam radar is used. Due to limitations of radar technology and their associated field of view exist possibility that pedestrian, pushchair, bicycle or other object cross the vehicle pathway whilst it is stopped and not be detected by the radar. If the preceding vehicle pulls away under such condition, automatic acceleration of the host vehicle could result in a collision with the object. To overcome this problem most commonly augmenting the main sensor with short range wide-angle radar or laser scanner was used. However, such combination can result in a system that is prohibitively too expensive.

An alternative was proposed to use video sensor instead. Use of the video image processing to detect object that may enter the host vehicle pathway when it is a stopped condition can be used and therefore provide both required support for the narrow beam

long range radar and solution to associated field of view problem. Over the years cost of video sensor has dropped dramatically and thus the integration of video technology into vehicle for functions such as lane detection has become more widespread. Combined with the fact that video technology is becoming inexpensive, especially when multiple functions and algorithms can be integrated within the same camera unit, makes the use of this technology very attractive.

1.1. Cruise Control Systems

Cruise control systems were initially introduced to make driving experience more comfortable and pleasurable rather to make it safer. Vehicle driver was able to set desired cruising speed which will be kept by the device. However, because no additional sensors were applied this system needed continuous driver attention. Only the addition of front-end sensors allowed for more autonomous system introduction. First mass production car equipped with ACC (sometimes also referred to as ICC – Intelligent Cruise Control) was introduced by Toyota in 1998. ACC uses radar, microwave or laser technology to detect approaching vehicle and adjust the speed automatically [2]. This allows to set desired cruise speed which will be reduced if any object will appear in sensor field of view and to automatically accelerate when conditions will allow.

1.2. Technical constrains and requirements

For the solution for the problem of radar associated field of view image processing and analysis algorithms were proposed. The main requirement was to develop such algorithms that will provide real time environment change detection. However as such an algorithm was intended to run simultaneously with other algorithms and functions within one camera unit, constrain of platform compatibility was imposed.

To provide robust sensing covering the entire road surface for all kinds of driver assistance systems the video sensor needs to provide high temporal rate, good resolution, wide angle and high dynamic range. Therefore considerably big amount of data needs to be processed. Traditionally suitable system architecture consist of one or more Digital Signal Processing devices or custom ASIC (Application-Specific Integrated Circuit), both of this approaches states numbers of advantages and limitations. DSP is hard to program due to low-level assembly language and can be easily overloaded by the algorithm and as such prevent any further system development. ASIC circuits posses high performance, low power consumption and low unit price. However, ASIC development process is very difficult and expensive and may be reasonable only for mass production. What is more ASIC, similarly to DSP, is not convenient for algorithm and system development, as it is purpose-designed and hard to extend.

As the best solution for development processes regarding cost and performance balance use of an FPGA array was proposed. Field Programmable Gate Array allows for project specific configuration after unit production.

However FPGA provides very good performance use of this particular technology puts additional constrain on proposed algorithms. Because of small amount of FPGAs internal memory algorithms cannot use image frame buffer. That implies need for the feature based approaches development.

To summarize three main constrains were recognized:

- real time change detection;
- architecture compatibility for multi functional system;
- feature based approach to overcame limited amount of FPGAs internal memory problem.

2. SOLUTIONS

As mentioned above to the problem of associated field of view of radar sensor, use of wide range video sensor was proposed together with application of image sequence processing and analysis in order to detect environment change [3]. During the project two main sets of algorithms were developed, each of them oriented on solution of separate problem. First set was aimed to solve the problem of redundant data amount due to use of the wide range video sensor. Algorithms from second set were aimed at robust scene change detection.

2.1. Image area trimming

To ensure the possibility of using a single optical sensor, allowing it to be used up to a large number of tasks it was necessary to use wide-angle camera. However in situation described in the project, data only in considerably close distance to the proceeding vehicle is relevant. Movement or changes taking place in the extreme corners posses no significant information and can be treated as a noise, and as such needs to be filtered. In fact processing area may be limited only to the preceding vehicle and its closest vicinity. Boundaries should be stretched in order to comply with geometrical relations between host and preceding vehicle and to improve safety.

For detection of preceding vehicle position and orientation following algorithm was modeled. First step was to threshold base image and perform Hough transform to obtain set of lines based on scene edge and boundaries [4, 7]. However majority of acquired lines are not relevant to vehicle area marking and thus need to be filtered. Due to its memory limitations FPGA is unable process whole image and robustly detect near-horizontal lines. To model this feature all near to horizontal lines were filtered out.

Fig. 1. Relevant image area

Next step was based on dividing line segments into those lying on the left and right part of the scene. Basing on the regular symmetric property of vehicles further filtering was imposed by rejecting right leaning lines lying in the right image section and left leaning lines in the left image section. By this step only those line segments are present that can create vehicle contour. However still considerable amount of data can be present in the line segment set, i.e. building edges, lanterns or other cars. To dispose of those false edges line segments were paired basing on their geometrical position in the image. This was done iteratively and with subject to threshold.. The last step contained choosing the most center-scattered lines as possible vehicle boundaries. Basing on their position in the overall image decision is made:

- use whole image when lines lie too close and can be considered as false edges;
- use whole image when lines lie too far from each other and can be considered as false edges;
- use trimmed image when lines lie in the area including correct tolerance.

2.2. Scene change detection

Developing set of algorithm for scene change detection was the main aim of the project. Five algorithm were developed and compared:

- Direct Frame Comparison;
- Image Feature Extraction and differencing;
- Image Feature Extraction and direct matching;
- Neighboring frames feature comparison;
- Optical Flow change detection.

Frame differencing is the most popular method for image change detection [6]. This approach is based on direct subtraction of image frames to reveal their difference and its usefulness was widely investigated. Despite potential high efficiency this method cannot be used for FPGA due to the need of at least two frames buffer. This method was developed to obtain good comparison background.

Second algorithm was based on two main steps: image feature calculation and extraction followed by direct frame subtraction. Despite number of noise reduction techniques (i.e. background features averaging, comparison kernels) it was revealed that this technique is not robust and can result in irregular change detections.

Two next algorithms are based on the same general idea to detect, recognize and collect image features [9]. Because of that whole change detection algorithms are performed exclusively on the feature sets and thus are perfectly suitable for FPGA arrays. The main difference is the source of basic information for the algorithm – background image. While for the Image Feature Extraction and direct matching background image is collected at the beginning of the process, for the Neighboring Frames Feature Comparison background frames are changing iteratively over time [8]. Following image feature comparison and matching is similar for both approaches and involves cascade filtering. Firstly direct matching is performed whilst all features lying in the same image geometrical positions are filtered out. Secondly, features are compared by their position in relation to other features lying in the closest vicinity (based on the kernel), thanks to this noise due to camera lateral movements is removed. Third filtering step consist of filtering isolated features. This is done by iteratively calculating Euclidean distance between all resulting features. By doing this image clusters are recognized. Such clusters can be referred to as significant image change.

The last step is based on calculation of temporal moving average – averaged change in relevant features number over time. By calculating this, noise spikes in feature number can be filtered. Those spikes are due to irregular lightning conditions, camera movement or irrelevant and uneven environment changes.

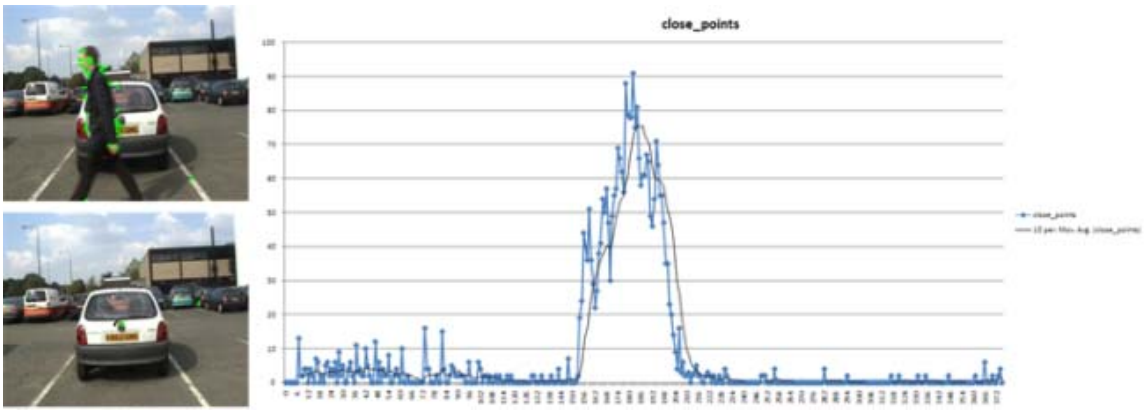

Fig. 2. Temporal features spectrum

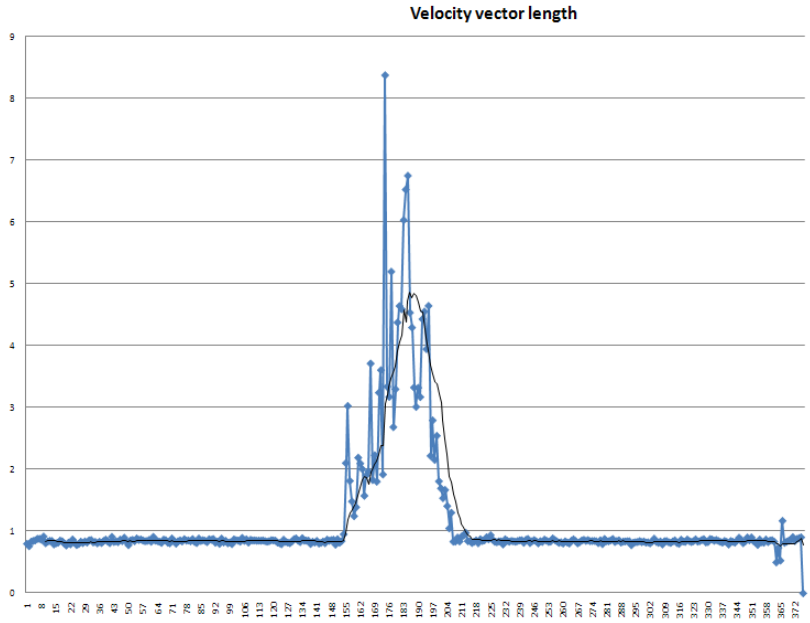

Fig. 3. Temporal optical flow velocity vector length

The last algorithm is purely based on the optical flow method [1, 5]. As an output from this function set of vectors determining corners position change is returned. Those vectors may be referred to as a corner velocity vectors. Under normal conditions vector length is very small and exists only due to the noisy lateral movement of the camera. When the change occurs vector length rises significantly.

3. RESULTS

It was shown that by use of the firstly captured frame, feature extraction, their filtering and matching based on the symmetry property, preceding vehicle area could be correctly estimated. One has to remember that there are two failures possibilities. First one is that too narrow area is obtained. Because of that area in which proper object is situated (or moving) will not be considered as area for which breach detection algorithms will be performed. This situation carries a possible serious health and safety issue and because of that feature span condition was applied. The second one is that significant features will not be recognized. This is trivial case as leads to full area processing and will not state safety problems. To improve area-trimming algorithm following steps are proposed:

- use of adaptive thresholds;
- filtering process verification by altering sequence steps;
- feature detector parameters tuning.

It was also shown that it is possible to obtain good results in change detection thanks to the algorithms based purely on feature comparison. All three methods (Optical Flow, Image Feature Extraction and Direct Matching, Neighboring Frames Feature Comparison) allow detecting image change, thus possible pathway breach, reliably and robustly. The noisiest output is obtained from neighboring frames feature comparison but in the same time this algorithm is the fastest proposed. Optical flow is the most complex and advanced measure not only to detect but also track occurring changes. Each velocity vector carries information

about its space location and direction. Because of that not only change position may be obtained but also direction of movement of possible threat.

For the further work integration of Image Feature Extraction and Direct Matching and Neighboring Frames Feature Comparison algorithms is considered. Such an approach can utilize strengths of both approaches. Background comparison method allows to reliably detecting all changes in the scene but is sensitive to any camera movements and background displacements. Instantaneous change detection allows capturing all fast occurring changes but is not able to detect static obstacles. Combination of those approaches may create one resistant to most of the problems encountered during this project.

REFERENCES

[1] Barron J. L., Fleet D. J., Beauchemin S. S.: *Performance of Optical Flow Techniques.* IJCV, 12(1), pp. 43-77, 1994.
[2] Gajek A., Juda Z.: *Czujniki.* Warszawa, Wydawnictwo Komunikacji i Łączności, 2008. ISBN 978-83-206-1672-9.
[3] Gonzales R. C., Woods R. E.: *Digital Image Processing.* New Jersey, Prentice-Hall, 2002. ISBN 0-201-18075-8.
[4] Harris C., Stephens M.: *A combined corner and edge detection.* Proceedings of The Fourth Alvey Vision Conference, pp. 147-151 1988.
[5] Horn B. K. P., Shunck B. G.: *Determining Optical Flow.* Artificial Intelligence, vol. 17, pp. 185-203, 1981.
[6] Lillestrand R. L.: *Techniques for change detection.* IEEE Transactions on Computers, vol. 21, no. 7, pp. 654-659, 1972.
[7] Marr D., Hildreth E.: *Theory of Edge Detection.* Proceedings of the Royal Society of London. Series B, Biological Sciences, vol. 207, no. 1167, pp. 187-217, 1980.
[8] Shapiro L. S.: *Affine Analysis of Image Sequences.* Cambridge, Cambridge University Press, 1995. ISBN 0-521-55063-7.
[9] Wang H., Brady M.: *Real-time corner detection algorithm for motion estimation.* Image and Vision Computing, vol. 13, no. 9, pp. 695-703, 1995.

Jakub KOMODA, MSc – graduate of the Faculty of Automotive and Constru-ction Machinery Enginee-ring of the Warsaw University of Technology (in 2009) and of the School of Engineering of the Cranfield University (in 2008).
Research interests include image processing and analysis, intelligent transport systems, autonomous navigation, machine vision. Associate of the Integrated Laboratory of the Mechatronics Systems of Vehicles and Construction Machinery.

Jacek DYBAŁA, Ph.D., D.Sc. (Eng.) – graduate of the Faculty of Automotive and Construction Machinery Engineering of the Warsaw University of Technology (in 1988) and of the Institute of Production Systems Organisation of the Warsaw University of Technology (in 1990).
He received the Ph.D. and Habilitate Doctorate (D.Sc.) degrees, all in mechanical engineering, from the Warsaw University of Technology (Poland) in 2000 and 2010, respectively. He is an associate professor in Institute of Automotive Engineering of the Warsaw University of Technology. His research interests include vibroacoustic, technical diagnostics, mechatronics systems of vehicles, processing and analysis of signals and images, feature selection, pattern recognition, data mining, artificial neural networks and genetic algorithms. He is member of Polish Society of Technical Diagnostics.

DETERMINING THE OPTIMAL LOAD OF MACHINES AND DEVICES IN THE PRODUCTION SYSTEM

Justyna BERLIŃSKA

Zachodniopomorski Uniwersytet Technologiczny w Szczecinie, Instytut Technologii Mechanicznej
al. Piastów 19, 70-310 Szczecin; justyna.berlinska@zut.edu.pl

Summary

A company operating nowadays is subject to constant pressure from methods aiming at optimizing processes and minimizing costs. An efficient use of resources such as business assets, human labour, know-how and management of material resources offers a possibility of obtaining a competitive advantage.

The paper examines a production system of bath sponges, for which, in order to properly use its technical infrastructure, a model was simulated in eM-Plant environment. The data from the accepted variant were transferred over to MS Project, in order to schedule work and appropriately allocate the plant's employees. The resulting schedule is used to monitor progress of the plant's operation and for efficient communication between resources in the production system.

Keywords: analysis of resource load, use of resources, simulation of the manufacturing process.

WYZNACZANIE OPTYMALNEGO OBCIĄŻENIA MASZYN I URZĄDZEŃ W SYSTEMIE PRODUKCYJNYM

Streszczenie

Współcześnie działające przedsiębiorstwo poddawane jest ciągłej presji związanej z optymalizacją przebiegu procesów oraz minimalizacją kosztów. Odpowiednie wykorzystanie posiadanych zasobów w postaci aktywów przedsiębiorstwa, pracy ludzkiej, know how oraz zarządzania zasobami materiałowymi daje możliwość uzyskania przewagi konkurencyjnej.

W artykule przeanalizowano system produkcyjny gąbek kąpielowych, dla którego w celu odpowiedniego wykorzystania posiadanej infrastruktury technicznej zasymulowano model w eM-Plant, a następnie dane z zaakceptowanego wariantu przetransportowano do MS Project, celem zaplanowania prac i odpowiedniej alokacji pracowników. Tak przygotowany harmonogram posłużył, jako podstawa do monitorowania postępu prac oraz sprawnej komunikacji między zasobami w systemie produkcyjnym.

Słowa kluczowe: analiza obciążenia zasobów, wykorzystanie zasobów, symulacja procesu produkcyjnego.

1. INTRODUCTION

From today's businesses, due to their size, capabilities and complexity, requires that management functions were an integral part of an organization [1].

Business success depends on proper management of its resources. The aim is to increase work efficiency and reduce manufacturing costs of the product, while maintaining an appropriate level of quality. To meet these objectives, a company should be subject to continuous improvement and elimination of inefficiency.

In a smooth running operation of a production system the elimination of non-technological breaks should occur immediately and should be combined with an analysis of the use of workstations

The basic production factors, such as human labour and technical infrastructure complement each other. Proportions between these factors should be such as to ensure their efficient use.

The use of modeling and simulation mechanisms of production processes makes it possible to optimally use their technical infrastructure and to select necessary staff, so as to balance the available means of production [2]. Such planning can be performed using the methodology of ERP systems. However, such systems are not always available, and the implementation costs are very high [3].

The paper presents a study of how corporate resources are used by means of two computer programs: eM-Plant and Microsoft Project.

The proposed solution does not generate significant costs for the company. On the contrary, owing to the method it is possible to quickly and easily diagnose how efficiently machinery, equipment and personnel are used in the process of calculating production costs, scheduling and controlling the workflow.

Exchanging data between the programs makes it possible to analyze the impact of a specific production task on the entire production process. It

is possible to analyze different models of the system by simulating connections of several work packages.

Proper selection of the factors of production, selection of an adequate flow of data in the system, maintain the principle of Just In Time, and continued to motivate staff to work effectively is necessary for the operation and competition in dynamically changing environment of internal and external business.

2. METHODS FOR SELECTING RESOURCES IN THE PRODUCTION PROCESS

To effectively control a production system it is necessary to analyze how its resources are used. This task must be considered in terms of hardware, material and human resources.

Machines' performance is determined by analyzing the performance of a specific machine, including its depreciation which is the reason for its stoppages due to breakdowns or technical inspections.

The reason for not meeting production plan deadlines could be an inadequate number of machines used for a given task or else too many machines used at another working station [4].

Another threat of failing to meet the deadline of a production plan is bad allocation of resources. While overloaded resources can be a problem, resources not loaded enough can also generate unnecessary costs.

There are many coefficients that describe the use and performance of a system. However, these coefficients do not consider all the features, which in some cases makes them inapplicable [5][6].

The solution is to use modeling and simulation, which makes it possible to analyze the functioning of a given system .

In the eM-Plant simulation environment it is possible to build a hierarchical, fully object-oriented structure of a manufacturing process and dynamically seek the best solutions of the preset criteria [7]. The environment provides tools for optimizing material flow, resources utilization and logistic processes both at a basic detail level and at the level of global enterprises.

The designed simulation model of the production system shows its behavior without the need of conducting expensive experiments on real objects [8].

Microsoft Project is an application supporting management of projects, resources, time and finances. It is a tool to develop and manage schedules.

After the allocation of resources to respective tasks it is possible to balance that and analyze the use of workers in view of scheduled tasks and the use of machinery in view of its availability. It also provides the ability to coordinate the progress of work checking for deviations from the plan and respond to-date on emerging risks associated with their jobs.

3. SIMULATION OF MANUFACTURING LINE IN EM-PLANT ENVIRONMENT

The purpose of the analysis is to develop a simulation model of a production system characterized with a high use of its machinery and devices.

The load of machinery and devices as well as processes were simulated in eM-Plant environment. This is a utility object which can simulate discrete events.

A sponge bath production line has been analyzed. The production is divided into three shifts. The flow of material in individual slots in the system is pipelined.

Polyurethane foam block is cut into slabs on a rotary saw, and then it is transported to the production station, where an automatic spray of glue and connection of the bottom and top layers of sponge take place. After gluing is completed the slab is cut into individual sponges on a vertical saw.

The basis for modeling the production system and for the harmonization of scheduling tasks is a operation diagram of the system presented in Figure 1.

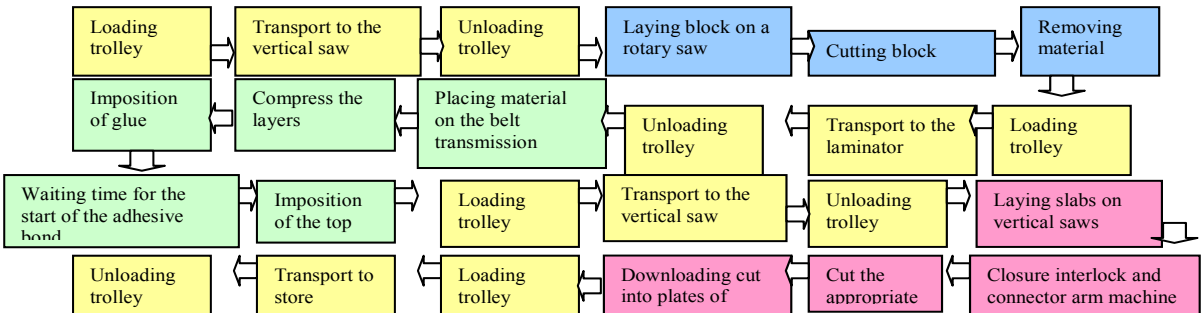

Fig. 1. Production process of bath sponges

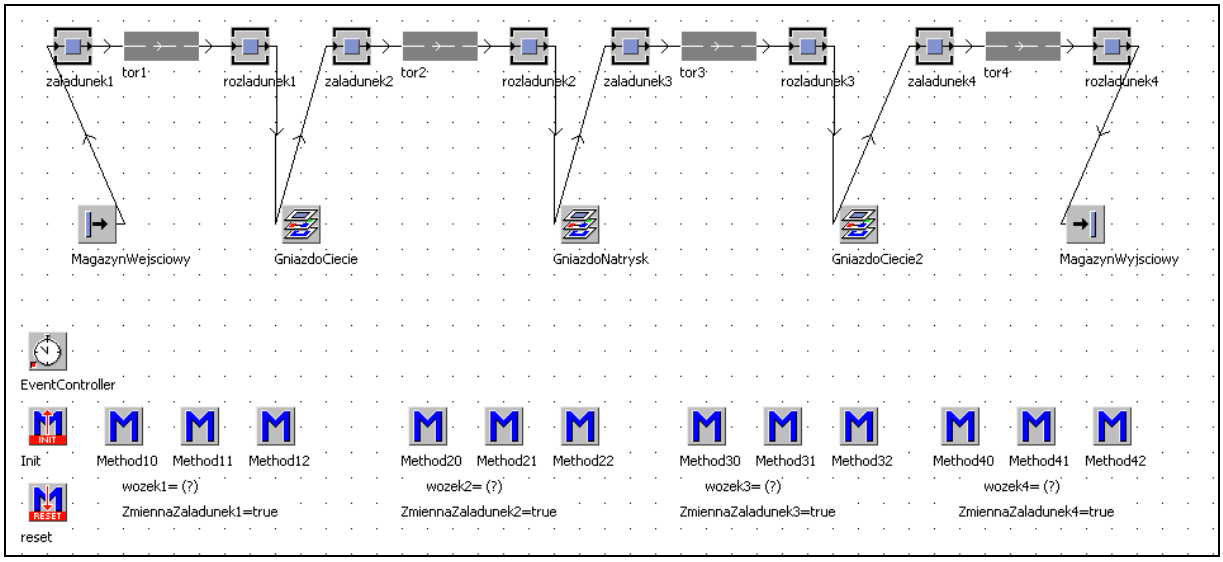

Fig. 2. Simulation model of production line implemented in eM-Plant program

Assumptions for the construction of the model:

- Simulation of the process will be carried out for one shift, i.e. 8 hours of work,
- Time duration of various phases of the process (Table 1) was adopted according to data provided by the manufacturer,
- Truck after unloading returns to fetch another element,
- Ready-made components are transported to an external storage.

Table 1. Characteristics of the manufacturing process

Process Step	Object Model **eMplant**	Working time **[min]**
Loading trolley No 1	*zaladunek 1*	5
Transport to the vertical saw	*tor 1*	5
Unloading the truck No 1	*rozladunek 1*	5
Laying block on a rotary saw	*G1*	4
Cutting block	*G2*	3
Removing material from the machine	*G3*	5
Loading trolley No 2	*zaladunek 2*	5
Transport to the laminator	*tor2*	6
Unloading the truck No 2	*rozladunek 2*	5
Placing material on the belt transmission	*G4*	5
Compress the layers and downloading from the machine	*G5*	4
Imposition of glue	*G6*	4
Waiting time for the start of the adhesive bond	*G7*	5
Imposition of the top layer	*G8*	5
Loading trolley No 3	*zaladunek 3*	5
Transport to the vertical saw	*tor 3*	6
Unloading the truck No 3	*rozladunek 3*	2
Laying slabs on vertical saws	*G9*	5
Closure interlock and connector arm machine	*G10*	5
Cut the appropriate	*G11*	3
Downloading cut into plates of sponge	*G12*	5
Loading trolley No 4	*zaladunek 4*	5
Transport to store	*tor4*	6
Unloading the truck No 4	*rozladunek 4*	3

The model has a two-layer structure. The second layer is formed by a frame-type model objects known in the model as: Gniazdo Cięcie, Gniazdo natrysk, Gniazdo Ciecie2, which model various stages of manufacturing processes: cutting on the
rotary saw, gluing the sponge layers and cutting individual products out of the sponge slab on the vertical saw.

The model of the system is shown in Figure 2.

During the simulation characteristic parameters for a given process (transportation, facilities utilization rates, number of items produced, etc.) are generated and calculated. Several simulation experiments with different number of transportation batches were carried out. For further analysis in MS Project the organizational variant was selected ensuring the most efficient use of the technological stations.

An analysis of the system operation is possible owing to statistics produced in eM-Plant environment, which are generated for each individual object. A sample statistics is presented in Figure 3.

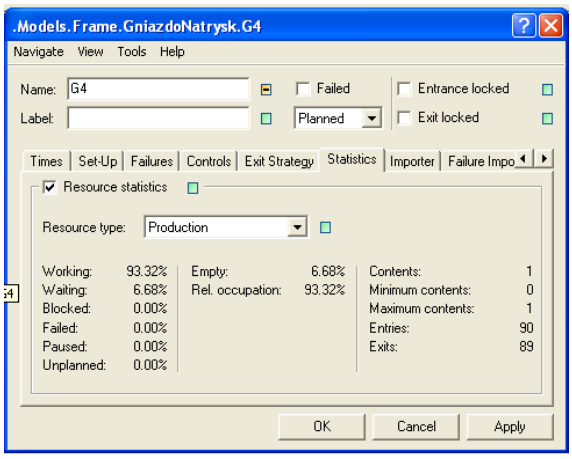

Fig. 3. Statistic for neck „natrysk"

Statistics include information about the number of items that were sent over to a machine or device, the efficiency level of its use and its stoppages. For example, an average use of machinery of the slot "natrysk" amounted to 84.2%. The summary of statistics of the technical resources of the manufacturing system is presented in Figure 4.

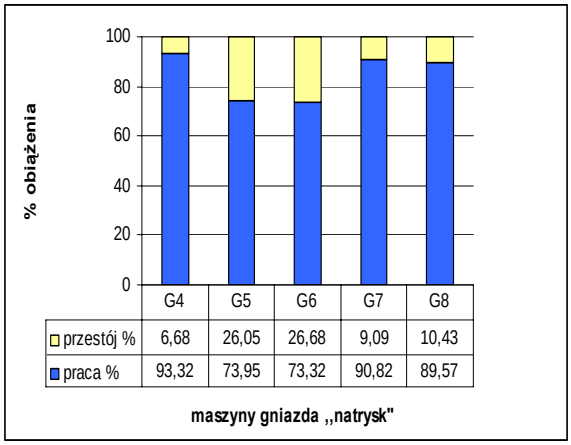

Fig. 4. Characteristic of using technical resources for 'natrysk" neck

4. ANALYSIS OF THE USE OF HUMAN RESOURCES IN MICROSOFT PROJECT

Having a model which can efficiently use machinery and equipment, the allocation of human resources was conducted.

MS Project was used for the purpose. This is a commonly used planning tool, allowing to generate a Gantt chart, balance resources and analyze critical tasks of the project. For the scheduled operations human resources had been assigned, and then the performance of their work was examined.

In the production of sponge baths four employees are employed: a warehouse employee, a vertical saw operator, a rotary saw operator, an operator of the laminator. The employees are assigned to their respective tasks, bearing in mind that when it is necessary they will be delegated to perform other tasks.

High productivity can be achieved owing to the generated allocations. The average workload of human resources assigned to all the tasks was 85.9%.

Figure 5 shows the workload of human resources for this process.

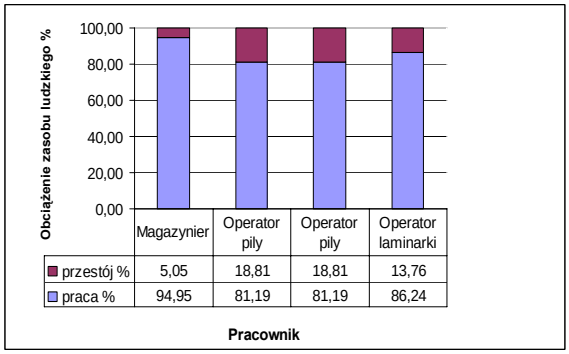

Fig. 5. Use of human resources

The resulting schedule provides a basis for monitoring the implementation of production, rapid response to errors and allows changes in the functioning system.

Resource management involves tracking progress, identifying and solving problems of allocation, management of shared resources, and creating reports of its progress.

MS Project is a helpful tool in managing the system. It shows a current status of a given task, differences between the work done and planned, the estimated time of completion of each task and the entire project.

5. CONCLUSION

Management of a production system relies in seeking optimal solutions for a given machinery and performance of its employees. Taking into consideration an appropriate use of the available resources it is possible to shorten a production cycle and reduce the costs.

An implementation of the model in eM-Plant environment provided a solution to the presented problem. The machinery and devices were simulated using batches of a size that would ensure obtaining the highest degree of using the machines. Following on from that, the data were exported to MS Project. MS Project was used in the study because the manufacturing firm had this very program. So far, planning data were imported as values of Microsoft Excel. Their treatment did not ensure a proper balancing of resources, which was the cause of discrepancies between the planned and actually obtained values.

The allocation of staff was conducted using MS Project. A schedule prepared in this way was a basis for monitoring progress of work and use of resources. The schedule also made it possible to

generate reports and statistics to be used both on the production line and used as the summary and control material available for senior managers.

The analysis of the production system conducted by means of the above described programs shows that both the machine utilization, and human resources at specified conditions, is at a high level.

LITERATURE

[1] Muhlemann A. P., Oakland J. S., Lockyer K. G.: *Zarządzanie - produkcja i usługi*. Warszawa, PWN, 1995.
[2] Korzeń Z.: *Informatyczne systemy badań symulacyjnych i wizualizacji w logistyce*. Politechnika Wrocławska; 2001.
[3] Chlebus E.: *Techniki CAX w inżynierii produkcji*. WNT, Warszawa, 2000.
[4] Pasieczna A.: *Analiza wydajności parku maszynowego*. Encyklopedia Zarządzania, http://mfiles.pl/pl/index.php/Analiza_wydajno%C5%9Bci_parku_maszynowego;
[5] Brzeziński M. (red): *Organizacja i sterowanie produkcją. Projektowanie systemów produkcyjnych i procesów sterowania produkcją*. Warszawa, Agencja Wydawnicza Placet, 2002.
[6] Duraj J.: *Podstawy ekonomiki przedsiębiorstw*. Warszawa, Polskie Wydawnictwo Ekonomiczne, 2004.
[7] www.emplant.de/english/index.html;
[8] Ciszak O.: *Komputerowo wspomagane modelowanie i symulacja procesów produkcyjnych*. Zeszyty Naukowe Politechniki Poznańskiej, Budowa Maszyn i Zarządzanie Produkcją, 6/2007.

Justyna BERLIŃSKA, Ph.D. a lecturer in Institute of Mechanical Technology of Department of Mechanical Engineering and Mechatronics at the West Pomeranian University of Technology, Szczecin. Main area of research are computer technology in production engineering, planning and simulation of manufacturing systems, production systems management.

SELECTION OF EFFICIENT MONITORING METHODS FOR MACHINERY GENERATING HIGH VIBRATION SIGNAL DISTURBANCE

Tomasz BARSZCZ*, Jacek URBANEK*, Łukasz SZUMILAS**

*Katedra Robotyki i Mechatroniki, Akademia Górniczo-Hutnicza
Al. Mickiewicza 30, 30-059 Kraków, tbarszcz@agh.edu.pl
**EC Systems sp. z o.o., ul. Lublańska 34, 31-476 Kraków, lszumilas@energocontrol.pl

Summary

Monitoring and diagnostics systems of machinery are increasingly used in many industries. Generally, these systems are responsible for such a machinery like steam turbines, pumps, fans, etc. The increase in efficiency as well as the growing interest of diagnostics systems has expanded the potential markets to other related industries such as mining or metallurgy.

This paper presents efficient monitoring methods of machinery generating high vibration signal disturbances. The results have been developed by a diagnostic team, monitoring a reciprocating compressor, which is located on the Baltic Sea oil rig. Important feature of the compressor is existence of strong impacts in the vibration signals. These impulses introduce strong distortion to the signal spectrum.

The paper shows that different faults require specific diagnostic methods. The paper shows example of selection of such a method. It is the application of the enhanced resolution envelope analysis for detection of the bearing faults.

Keywords: diagnostics, reciprocating compressor, narrow band envelope analysis.

DOBÓR EFEKTYWNYCH METOD MONITORINGU DLA MASZYN GENERUJĄCYCH SILNE ZAKŁÓCENIA SYGNAŁÓW DRGANIOWYCH

Streszczenie

Systemy monitoringu i diagnostyki maszyn są coraz powszechniej stosowane w wielu gałęziach przemysłu. Są odpowiedzialne za pracę takich maszyn jak turbiny parowe, pompy, wentylatory i wiele innych. Powiększająca się skuteczność oraz wzrost zainteresowania systemami diagnostycznymi spowodował poszerzenie grona odbiorców na inne pokrewne gałęzie przemysłu takie jak przemysł wydobywczy i hutniczy.

Niniejszy artykuł przedstawia efektywne metody monitorowania stanu technicznego maszyn charakteryzujących się silnymi zakłóceniami sygnału drganiowego. Wyniki opracowane zostały przez zespół diagnostów monitorujących kompresor tłokowy, który znajduje się na platformie wiertniczej na Morzu Bałtyckim. Charakterystyczną cechą pracy kompresora jest obecność bardzo silnych impulsów. Impulsy te wprowadzają silne zakłócenia widma sygnałów drgań.

W artykule pokazano, że w zależności od typu uszkodzenia konieczny jest dobór specyficznych metod diagnostycznych. Artykuł przedstawia przykłady zastosowania analizy obwiedni o podwyższonej rozdzielczości do wykrywania uszkodzeń łożysk tocznych.

Słowa kluczowe: diagnostyka, kompresor tłokowy, analiza obwiedni.

1. INTRODUCTION

Monitoring and diagnostics systems of machinery are increasingly used in many industries. Generally, these systems are responsible for such machinery like steam turbines, pumps, fans, etc. The increase in efficiency as well as the growing interest of diagnostics systems has expanded the potential clients body to other related industries such as mining or metallurgy.

Modern machines, ubiquitous in our daily life, are characterized by a complex structure and a challenging technical state assessment. Monitoring and diagnostics systems are generally dedicated to rotating machinery with a relatively simple design (e.g. steam generators, fans, pumps). Such systems take advantage of commonly known vibration analysis in the time domain as well as in the frequency domain, which are prone to extraneous disturbances. Those disturbances can be results of both: external sources, operation of supporting machinery and the object nature of work.

One of the examples of machines, which require a custom diagnostic algorithms is gas compressor explored by the authors. The presence of strong impacts excited by the compressor's pistons causes the characteristic frequencies to be masked, and ultimately unrecognizable.

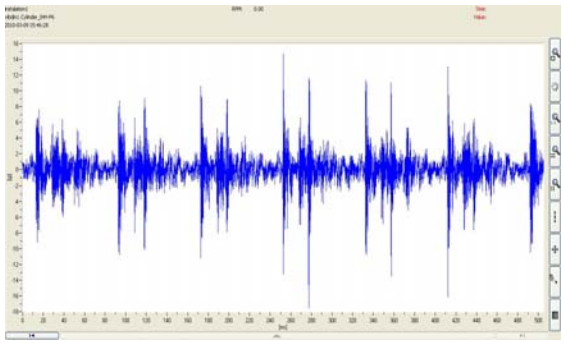

Fig. 1. Vibration signal from the gas compressor

Fig. 1 illustrates a fragment of a time vibration signal of the investigated large-dimension piston compressor. As stated above, a number of strong several impacts can be observed. Due to the number of compression levels, these disturbances occur at the rate of 0.04 s. Such a high impulse repetition rate totally hinders the analysis of signal's fragments recorded between the impulses, since these signals become too short. Therefore, in order to enable vibration analysis, a number of custom algorithms should be engaged.

2. OBJECT DESCRIPTION

The studied gas compressor of a type Dresser Rand C-VIP Compressor is 1000kW, operating between 600-1000 rpm, is a four-stage compression machine. Fig. 2 illustrates the layout of the compressor.

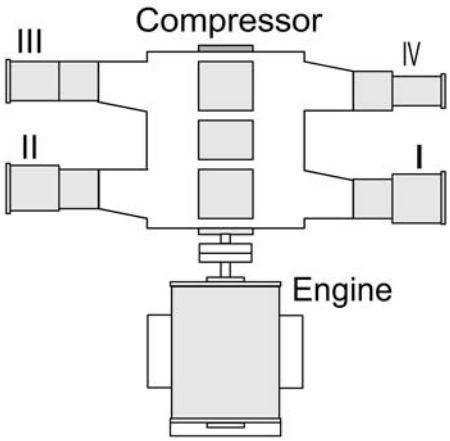

Fig. 2. Layout of the gas compressor

The machine is located on an oil rig in the Baltic Sea, and is responsible for a natural gas compression and transport (to the power plant 70 km away). Supporting machinery (hydrocarbon pumps, oilers, coolers etc.) has a strong influence on operational conditions of the described object. Due to very important function of the reciprocating compressor and high security requirements it is necessary to provide proper operation by scheduling repairs effectively. Location of the facility and the difficult weather conditions is the serious obstacle for frequent visit of maintenance team. This implies the need to reduce repairs to the minimum. Therefore, the decision of condition monitoring system has been made.

3. SYSTEM DESCRIPTION

The installed system of monitoring and diagnostics includes 20 vibration channels, four on every compression level. The remaining channels monitor rolling bearings, supporting the shaft. For every channel, a set of standard analysis has been defined. Apart from typical broadband analysis, a set of frequency analysis corresponding to particular machine parts has been configured in the system. Additionally, a phase reference sensor has been mounted, in order to obtain the speed information. Moreover, a set of process values is monitored, including pressures, temperatures, and flows. The highly-hazardous working environment (salt vapors, ATEX zone) has forced the designers to implement special solutions.

4. TYPICAL VIBRATION SIGNALS GENERATED BY GAS COMPRESSOR

The compressor operation is characterized by the generation of relatively strong vibrations, among which the piston and valves related impacts are the most dominant. These impacts in turn produce impulse responses, which induce vibrations in numerous machine components. It makes typical usage of frequency analysis almost impossible. Fig. 3 shows Fourier spectrum of vibration signal of gas compressor. Strong harmonic components of rotational speed caused by mentioned impacts can be seen.

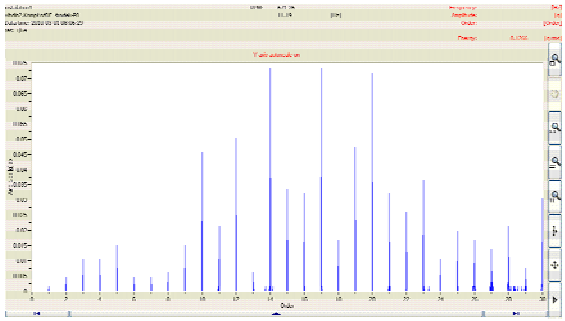

Fig. 3. Fourier spectrum of vibration signal of gas compressor

They are present in the whole range of analyzed frequencies (12kHz), which masks characteristics signals of other machine components. Another obstacle in vibration analysis is the influence of process parameters on the vibration signal generated by the machine. Fig.4 presents trends of the rms and the parameter of pressure at the inlet to the pipeline at constant speed operational conditions.

The installation tracks 22 process values, which together with aforementioned 20 vibration channels (about 6 analyses per channel, what gives altogether 120 analysis results), creates a complex correlation net.

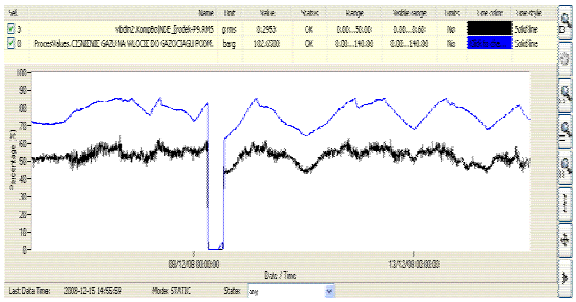

Fig. 4. Trends of the rms and pressure

5. BEARING FAULT DETECTION

Over a several years of the compressor continuous monitoring, a number of malfunctions was experienced by the authors. Generally, the malfunctions concerned bearings' races, raptures of elements connecting mid-chambers with the body, and breakage of bolts mounting cylinders' covers.

Due to harsh operating conditions, in all of these cases, the classical vibration analysis din not meet the customer's expectations.

In order to enhance the risk assessment efficiency, a number of extra vibration algorithms has been developed and implemented (including order analysis and custom envelope analysis). Typical method for detecting bearing faults is wideband envelope analysis, insufficient in describe case. Envelope spectrum calculated in tradition method shows only rotational speed components. It is necessary to apply more selective diagnostic methods.

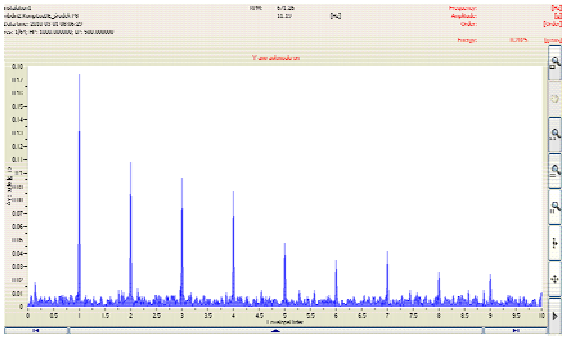

Fig. 5. Envelope order spectrum

The first method was the high resolution envelope analysis. In this method, we have calculated the envelope spectrum after signal resampling, which improves peakidness of spectral lines from synchronous sources. Then, the spectrum had sufficient line resolution to detect spectral lines from the sought bearing fault. The fig. 6 presents the high resolution envelope spectrum. As shown, the sought fault signature is visible, but the magnitude of the responsible spectral lines is low and the fault is still hard to detect.

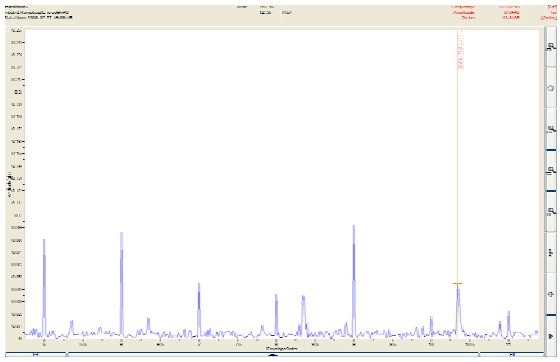

Fig. 6. High-resolution envelope spectrum. Two lines caused by the innerring bearing fault are visible

The second method was the narrowband envelope analysis (NEA) based on the Hilbert transform [1]. For a proper parameters selection, the method enables identification of rolling-element bearings' characteristic components.

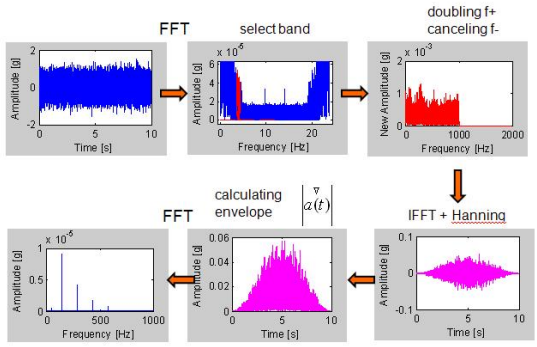

Fig. 7 The algorithm of envelope spectrum generation [1]

The principle of the NEA algorithm is the selection of the band, in which the vibration signal is to be demodulated. The band selection problem was discussed in a number of contributions [2] of which the kurtogram proposed by Antoni [3] deserves a special attention. This powerful method is based on the kurtosis of the vibration signal processed by several filterbanks, modifying both, the center frequency (*CF*), and the filter bandwidth (*dF*). Nevertheless, this approach is sensitive to strong impulsive noises, which are present in the case of the reciprocating compressor. The Fig. 8 presents the Fast Kurtogram calculated for the vibration signal with the bearing fault. The presence of such disturbances may cause the kurtogram to miss the optimal solution, which in fact results in magnifying impulses not related to the fault.

Since the aforementioned method of the optimal band selection did not yield useful results, the authors have started to investigate the problem thoroughly starting from the basic approach. On one hand, a number of cases has been encountered, when "trial & error" approach gave relatively satisfactory results. On the other hand, it is obvious that such approach is (to a degree) based on pure luck. Moreover, it would require to assess a number of combinations manually. Therefore, another methods

have been used in order to limit the number of possible *CF-dF* [1].

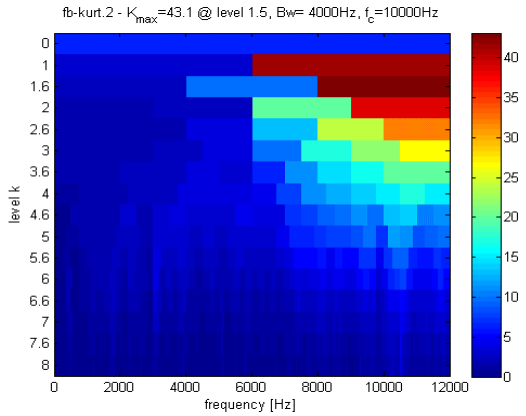

Fig. 8. Fast Kurtogram obtained from the signal with the fault. Detected maximum is not related to the fault, but to the operation induced impacts

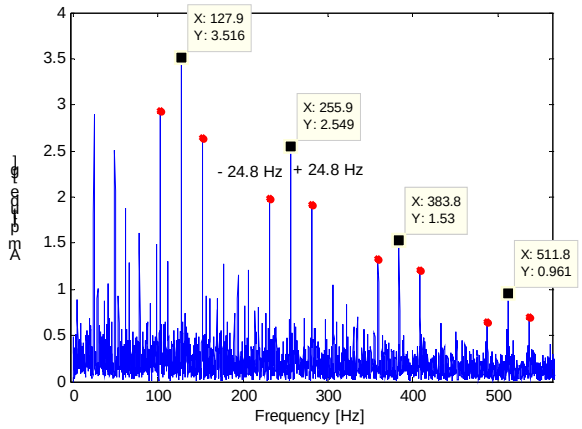

Rys. 9. Narrowband envelope spectrum (CF=8900 Hz, dF=600 Hz)

Fig. 9 illustrates the narrowband envelope spectrum with marked bearing inner race characteristic component. The figure was calculated for the center frequency *CF* equal 8900 Hz, and the bandwidth *dF* 600 Hz. The first four harmonics from the bearing fault BPFI are clearly visible along with the sideband components spaced at 2 times the machine speed.

6. CONCLUSIONS

The proposed methods have enabled to extract diagnostic information from the vibration signals, despite of the high disturbances. However, the selection of the optimal parameters for the developed algorithms is yet to be improved. The further work of the authors will also be directed towards signal separation. Even though the latter topic is popular topic in the signal processing literature, the high repetition rate of the impulses remains a challenge to both, scientists and engineers.

REFERENCES

1. T. Barszcz, A. Jabłoński: *Analysis of Kurtogram performance in case of high level non-Gaussian noise*. Proc. of ICSV 2009, Kraków, Poland
2. Ho D., Randall R. B.: *Optimization of bearing diagnostic techniques using simulated and actual bearing fault signals*. Mechanical Systems and Signal Processing (2000), 14(5), 763-788
3. Antoni J.: *Fast computation of the kurtogram for the detection of transient faults*. Mechanical Systems and Signal Processing, vol. 21, 2007, 108-124.
4. Bartelmus W., Zimroz R.: *Optimal frequency range for amplitude demodulation for local fault detedtion*. Diagnostyka vol.37,2006,141-150
5. Vance J. M.: *Rotordynamics of turbomachinery*. John Wiley & Sons, New York, 1988.
6. Żółtowski B., Cempel Cz. (red.), *Inżynieria diagnostyki maszyn*. Instytut Technologii Eksploatacji PIB, Warszawa 2004.

dr hab. inż. **Tomasz BARSZCZ**. Graduate of Electronic Eng at Politechnika Gdańska (1993r.). Received PhD in mechatronics in 1997r. (AGH). Has long experience of working with companies like ABB Zamech and ALSTOM Power. Author of many papers and books on machinery diagnostics. Monitoring systems developed under his supervision were installed on several hundred machines worldwide.

mgr inż. **Jacek URBANEK** PhD student in the Department of Robotics and Mechatronics, AGH University of Science and Technology, Kraków, Poland. His scientific interests are focused on practical application of machine diagnostics. Co-author of hand book on vibrodiagnostics (2008).

mgr inż. **Łukasz SZUMILAS**. Graduate of Department of Robotics and Mechatronics, AGH University of Science and Technology, Kraków, Poland. (2008). Currently working as a diagnostics engineer in EC Systems in Kraków. His scientific interests are focused on difficult cases of fault detection in compressors, wind turbines and printing machines.

PLD AIDED DEMODULATION, CASE OF NAVAL TURBO ENGINE

Witold CIOCH, Piotr KRZYWORZEKA
AGH University of Science & Technology in Cracow
Institute of Mechanics & Vibro-acoustics
cioch@agh.edu.pl, krzyworz@agh.edu.pl

Summary

It's widely known that proper investigation of vibration signal modulation VSM can provide a variety of diagnostic information in the early stage of fault evolution. However, variable loading rate, run-up and run-out generally cause some difficulties in VSM real-time demodulation procedures. The methods of angle demodulation, created and optimized for carrier-signals in a specified form and constant frequency, turn out to be inefficient. To overcome these problems the authors proposed PLD pre-processing to customize and improve asynchronous PM and AM demodulator. Some conclusive examples and practical results are presented, discussed and quantitively compared.

Keywords: diagnostics, vibrations, modulations PLD.

PLD WE WSPOMAGANIU DEMODULACJI DRGAŃ SILNIKA OKRĘTOWEGO

Streszczenie

Od dawna znane jest i doceniane znaczenie modulacji niezamierzonych jako źródła informacji o wczesnych stanach ewolucji uszkodzeń. Jednak w systemach czasu rzeczywistego monitorujących maszyny pracujące stale w warunkach dużych zmian obciążenia prędkości obrotowej demodulatory optymalizowane dla stałej częstotliwości nośnej okazują się nieskuteczne. Rozwiązaniem może okazać się *preprocessing* zmieniający skalę czas lokalny przy zachowaniu modulacji kąta, PLD zdaniem autorów nadaje się tu najlepiej.

Słowa kluczowe: diagnostyka, drgania, modulacja, PLD.

1. PLD PREPROCESSING

Original authors procedure of linear decimation called PLD, converts universal (dynamic) time - '*t*' to local time scale 'η' synchronized with $\Psi(\Theta)$, straight-line approximation of instantaneous cycle changes Θ, monotonous in observation window T. Properly applied PLD tends to equalize temporal intervals of recalculated cycles derived from $\Psi(\Theta)$ in 'η domain (see [3] for details). Nevertheless on-line phase demodulation of machine vibration signal brings some specific problems [1, 5]. Even if equalization of harmonic spectra is being carried out correctly, demodulation procedure could fail, especially an asynchronous demodulation. Without getting into operational details [3, 4] it should be pointed out that efficient DPM is already required to detect, track and recover the carrier signal or some of its parameters, at least carrier cycle, or carrier frequency $f_C = 1/\Theta_C$. In practice, mentioned parameters are usually not so easy to be recovered or measured. Fortunately, the only aproximative PLD equalization preserve PM and all at once reduces spectral leakage just enough for improve lines legibility [2, 4] Fig 1 shows the rules of accepted solution.

2.EXPERIMENT

The subject of study was naval turbo-engine L2500 (see Fig. 2) working in situ in conditions of strongly variable both load and rotational speed.. Experiment aimed at verification of practical advantages and limits of short time PLD version in on-line PM and AM demodulation of VMS. PLD was based on marker sequences captured every $\pi/6$ of reference shaft revolution angle. Realization of PLD assistance was arranged according to the diagram on Fig. 1

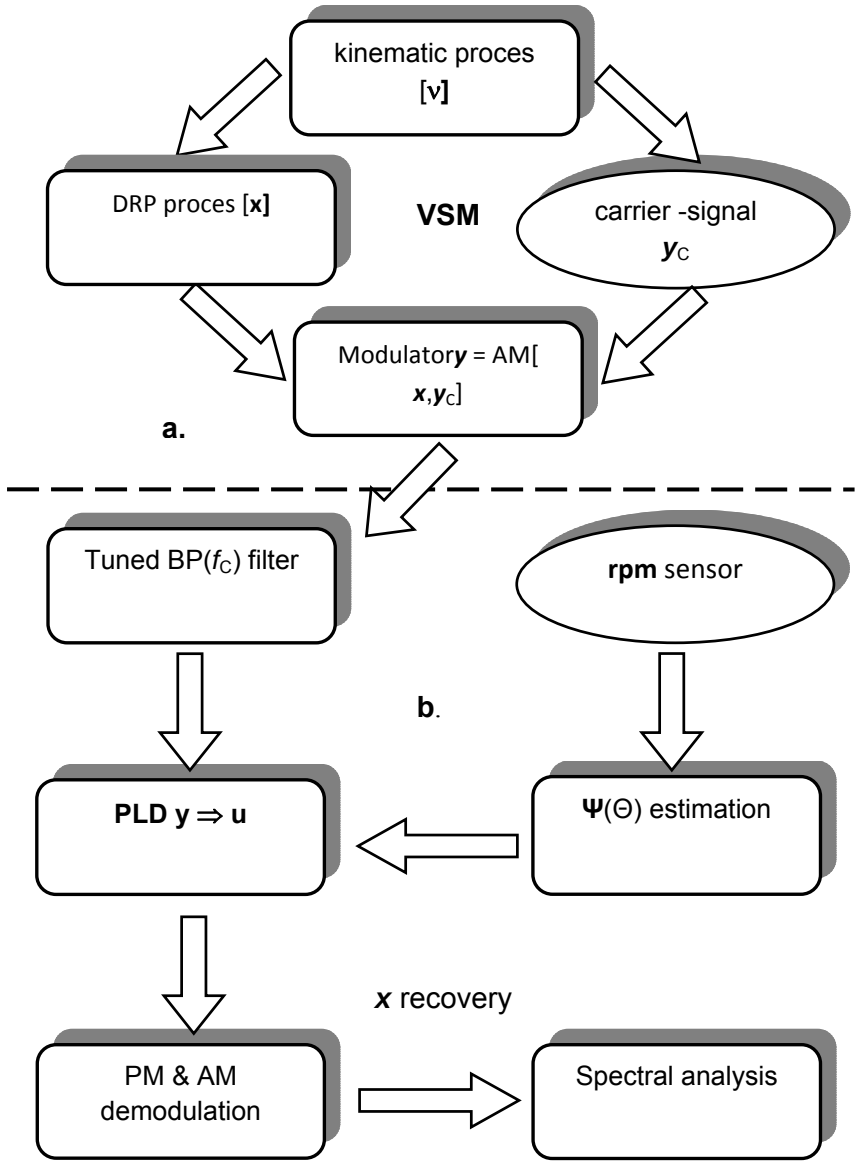

Fig. 1. PM & AM demodulation procedure
a) vibration signal PPM modulation – L2500 turbo-engine,
b) PM AM demodulation after PLD time scale conversion

Some run-up and run-out has been examined in order to:

- detect traces of modulation even in perfect technical state (presented case);
- evaluate efficiency of PLD in standard asynchronous procedure APMD based on generalized phase or generalized amplitude;
- tune PLD synchronization.

None at all VSM detailed model have been taken into account, as well as the number of existing VSM[3]:

- these may differ by;
  - VSM category;
  - carrier frequency f_C;
  - modulation band width Δ_M.
  - nature of message signal (synchronous or not witch referential kinematic process)

Note, that close proximity of similar VSM could seriously disturbed APMD, so that situation need more advanced demodulator. However, practical skills in sensor emplacement are often sufficient to select chosen VSM using BPF.

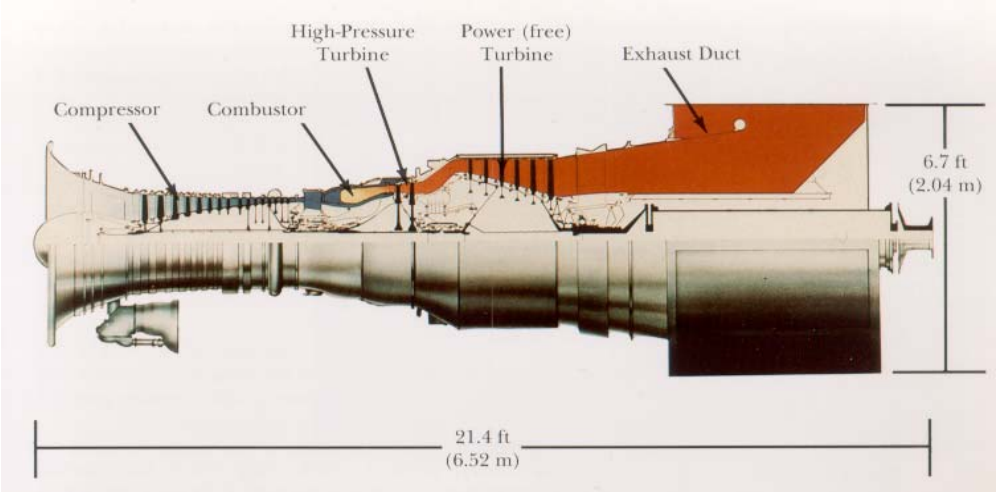

Fig. 2. Longitudinal cross-section of examined L-2500 engine

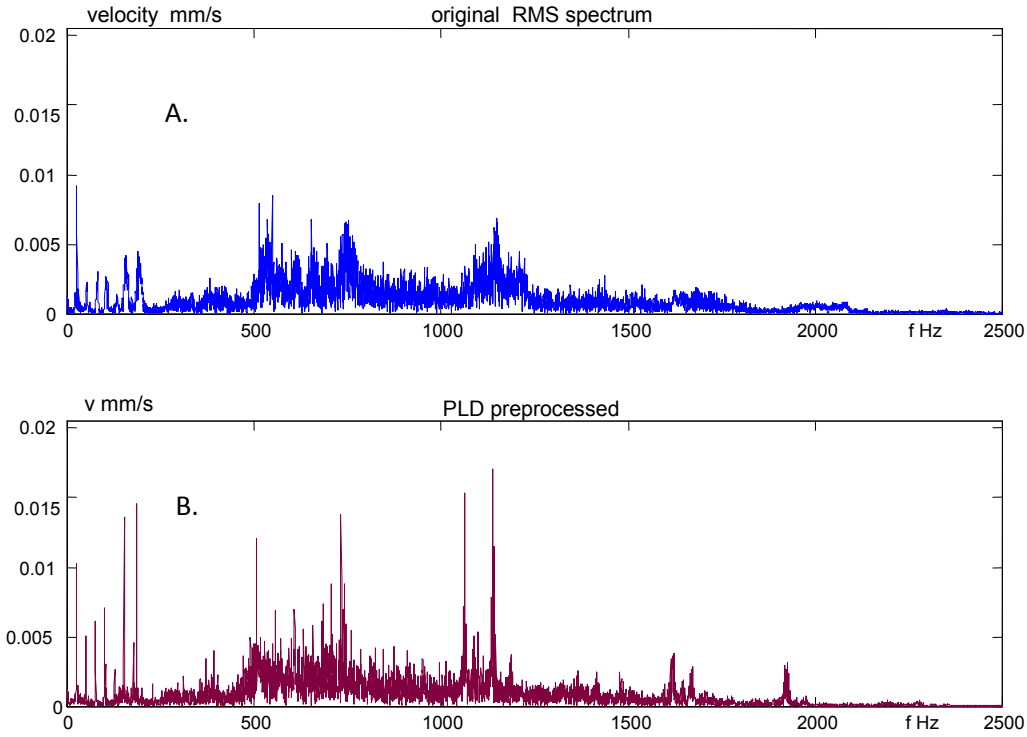

Fig. 3. Run – out of L-2500 ,vibration spectraPLD equalized:
A. original signal B. PLD preprocessed

3. EXAMPLES

Some typical realizations of VSM before and after PLD (Fig. 3) and the same for selected modulation band (Fig. 3) show distinct improvement of spectral lines legibility [2]

Comparison of PM and AM demodulation spectra (see Fig. 5.) show essential qualitative difference confirmed in time domain par intercorrelation before and after PLD – example on Fig. 6.

- Case PM – Usually some parasite fluctuation appear, disturbing low frequency segment of recovered PM spectra – these should be HP filtered (see Fig. 4).
- Case AM – Lack of distinctive spectral lines suggests the initial state of possible failure evolution.

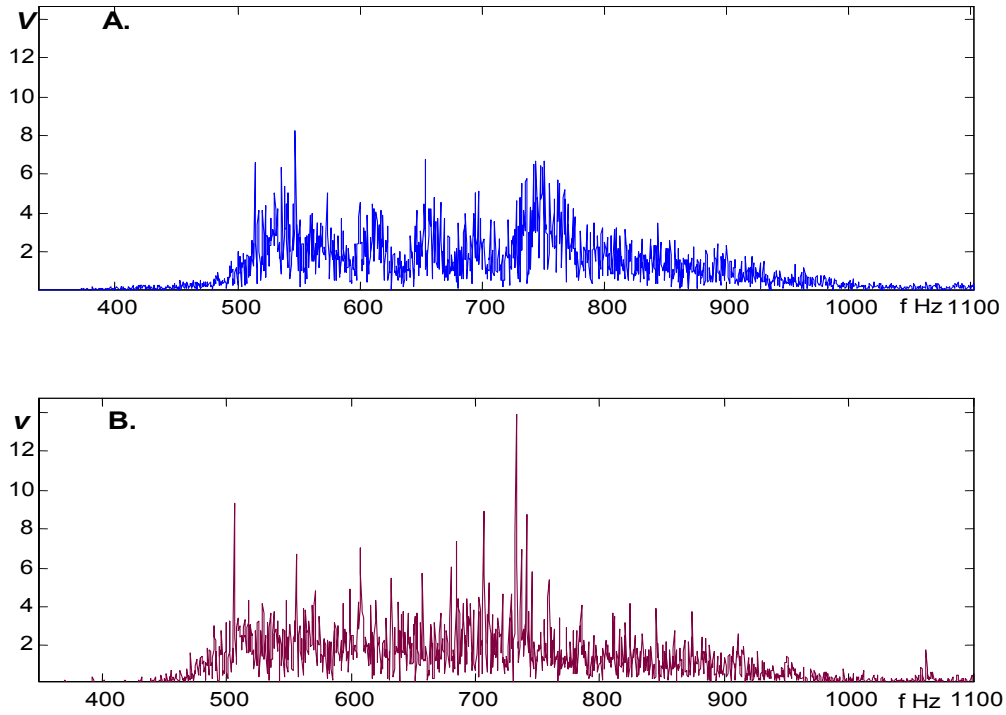

Fig. 4. Spectral area of modulation, BPF filtered
A) Measured signal, B) PLD applied

4. EVALUATION OF PREPROCESSING EFFICIENCY

4.1. Indexes

Any unique index of PE has been never found. Biasing factor of final estimate, although conclusive, requires the original message signal to be known, or APMD calibration with appropriate PM models. Indexes tested below aim to reveal specific PLD action on PM or AM. These are:

- **Intercorrelation** based index (for PM) defined as: $CC(\boldsymbol{u},\boldsymbol{x}) = \max\{abs[corr(\boldsymbol{u},\boldsymbol{x})]\} \in [0,1]$.
- **RMS** based index (for AM).

4.2. Results

Some typical results are presented in Table 1. and configured in Fig. 7 as follows:
RMS values on Fig. 7A

– PM: $X_P \Rightarrow (1)$, $U_P \Rightarrow (2)$, $U_{fP} \Rightarrow (3)$

– AM: $X_A \Rightarrow (4)$, $U_A \Rightarrow (5)$, $Uf_A \Rightarrow (6)$

CC values on Fig. 7B

– PM: CC $(\boldsymbol{u},\boldsymbol{x})$ (1), CC $(\boldsymbol{u}_f,\boldsymbol{x})$ (2), CC $(\boldsymbol{u}_f,\boldsymbol{u})$ (3)

– AM: CC $(\boldsymbol{u},\boldsymbol{x})$ (4), CC $(\boldsymbol{u}_f,\boldsymbol{x})$ (5), CC $(\boldsymbol{u}_f,\boldsymbol{u})$ (6)

(k) – number of consecutive bar.

4.3. Remarks

- Case PM – Relatively high value of $CC(\boldsymbol{u},\boldsymbol{v})$ (Fig 7.1). seems to suggest some common factor as residual low frequency fluctuations due to approximative nature of PLD synchronization [4]– the more so as HP filtering of $\boldsymbol{u}$ reduces inter-correlation.
- Case AM – insignificant difference among X_A,, U_A & Uf suggests that neither PLD nor HP filtering affect RMS of recovered AM [3].
- For quantitative interpretation of demodulation results one should refer to prior scaling results.

Table 1

	PM			AM		
Conf. nr.	1	2	3	4	5	6
CC	0.681	0.157	0.226	0.132	0.137	0.139
RMS*)	11.94	10.66	3.106	0.399	0.393	0.381

*)RMS data interpretation in mutual comparison only

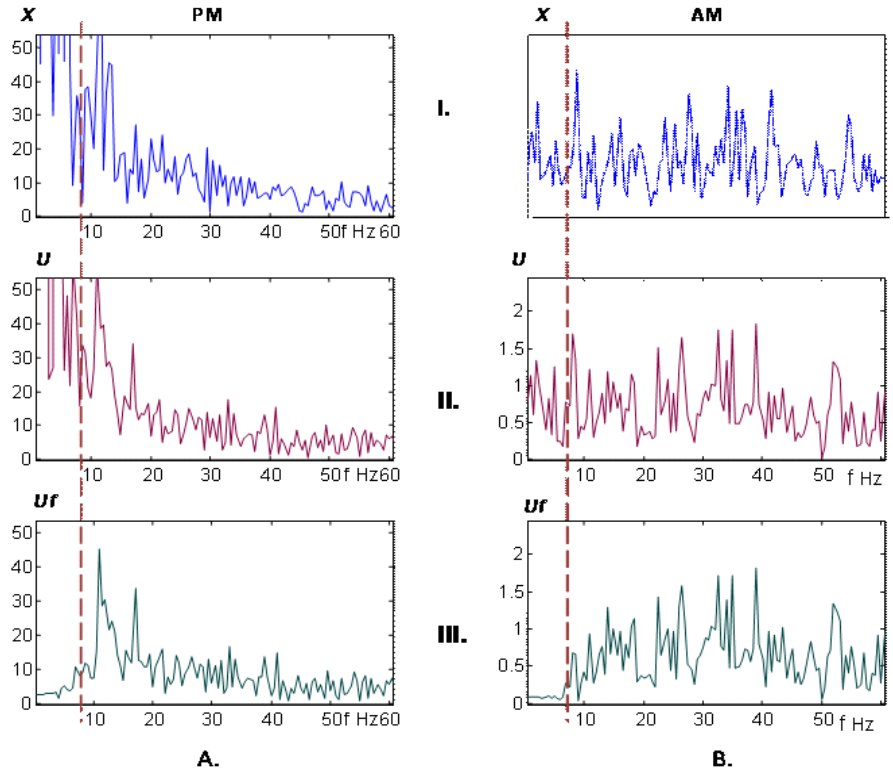

Fig. 5. PM (A) and AM (B) demodulation results, in frequency domain;
I. original signal, II. PLD preprocessed, III. low frequency fluctuation removed

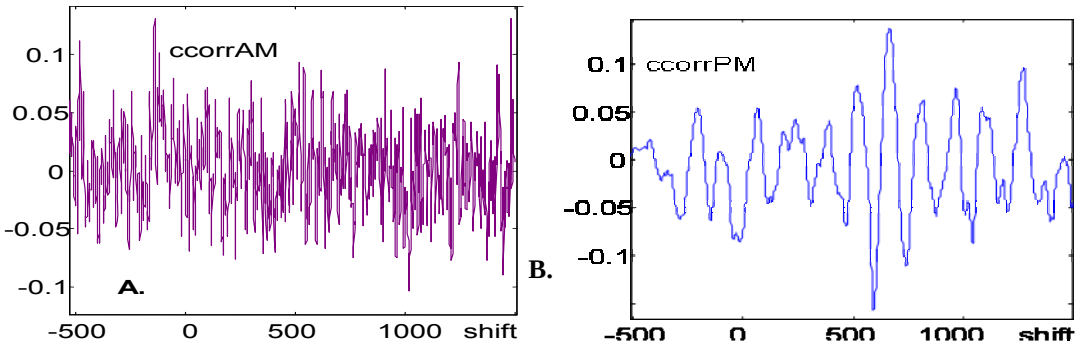

Fig. 6. The natures of AM (A) and PM (B) cross-correlation functions differ significantly

4. CONCLUSIONS

- Procedure is efficient and easy to use in real-time monitoring system;
- To avoid mismatch, selected modulation zone should be pre-filtered
- Spectra of amplitude modulations whose message signal is synchronized with carrier cycle, are insensitive to PLD
- Recovery of carrier signal is not necessary

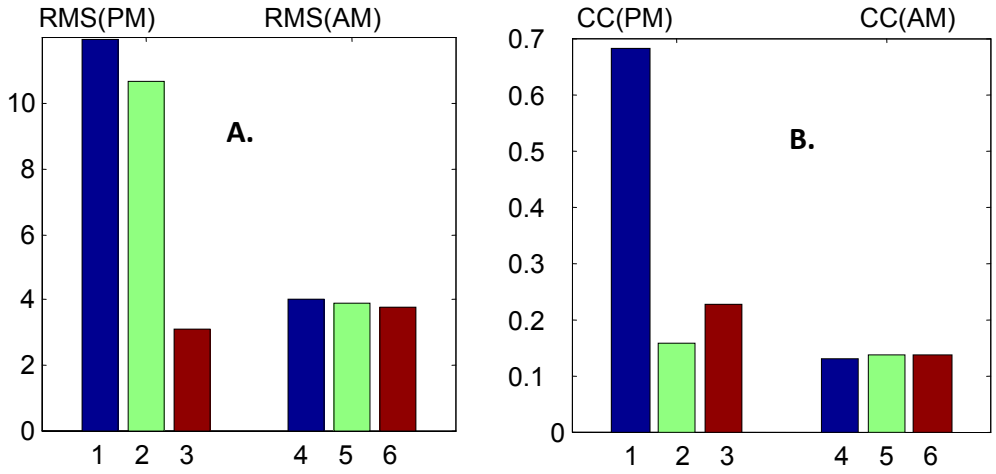

Fig. 7. Evaluation and comparison of demodulation results , both PM (bars 1,2,3) and AM (bars 4,5,6) see Tab. 1 for details
A.) RMS values, B) inter-correlation indices CC

5. REFERENCES

[1]. Bartelmus W., Zimroz R.: *Vibration condition monitoring of planetary gearbox under varying external load.* Mechanical Systems and Signal Processing, Volume 23, Issue 1, January 2009, Pages 246-257.

[2]. Cioch W, Jamro E., Krzyworzeka P.: *Accuracy of machine vibrations approximated analysis in nonstationary states.* Diagnostyka, vol. 40/4, 2006, 203 – 208.

[3]. Krzyworzeka P.: *Wspomaganie synchroniczne w diagnozowaniu maszyn.* monografia, s. 204, Radom Wyd. ITE 2004.

[4]. Krzyworzeka P.: *Synchronizm aided recoveryof phase modulation nonstationary signal – comparison of two methods*. Diagnostyka, vol. 48/4, 2008, 31 – 35.

[5]. Gębura A. Tokarski T. *The diagnostic of technical condition of turbine engine's bearing by means of method of alternator frequency modulation.* pp123-131 V – Int. Sc. Journal of Polish CIMAC Gdansk– Stockholm 2007.

6. SYMBOLS & ABBREVIATIONS

AM – amplitude modulation
APMD – asynchronous PM demodulator
DP – demodulation procedure
DPM – angular demodulation
PE – preprocessing efficiency
PM – phase modulation
TSC − time scale conversion
VSM – vibration signal modulation

$\psi(\Theta)$ – synchronizing cycle
Θ – instantaneous cycle
η – cycle related time
t – dynamic time
$\boldsymbol{x}_h$ – demodulation result, original VSM
$\boldsymbol{u}_h$ – demodulation result, PLD aided
$\boldsymbol{u}_{fh}$ – demodulation result, HPF filtered
$\boldsymbol{y}$ – modulated vibration signal carrier
$\boldsymbol{y}_C$ – carrier signal

Supported by Project nr: N R03 0061 06

SIGHTING THROUGH AS PART OF SHAFT ALIGNMENT PROCEDURE

Eliza JARYSZ-KAMIŃSKA

West Pomeranian University of Technology, Szczecin, Institute of Manufacturing Engineering,
Al. Piastów 19, 71-310 Szczecin, ejarysz@zut.edu.pl

Summary

This paper presents chosen activities of the ships propulsion system shafting alignment procedure. The main focus in this paper was put on sighting through (bore sighting) which can be done with three different types of measurement equipment: piano were, optical instruments and laser instruments. The analysis of measurement equipment allows selection of most optimal measurement solution for company. The matter of this selection is to avoid hazard to the shaft line due to shafts misalignment. Presented in paper measuring techniques and measurement equipment which is being used for sighting trough the elements of ships propulsion system meet technological requirements requested by the client and by the ship classification society.

Keywords: shaft, alignment, ships propulsion system.

WYZNACZANIE LINII ODNIESIENIA JAKO ELEMENT PROCEDURY OSIOWANIA WAŁÓW

Streszczenie

W artykule przedstawiono zagadnienie procedury osiowania układu napędowego statku. Skoncentrowano się na ustawianiu bezpośrednim z wykorzystaniem trzech różnych przyrządów pomiarowych. Do pomiarów wykorzystano strunę stalową, urządzanie optyczne i urządzenie laserowe. Przedstawienie trzech różnych grup przyrządów pozwala na wybór najbardziej optymalnego rozwiązania dla przedsiębiorstwa. Istotą tego doboru jest uniknięcie zagrożenia dla linii wałów wynikającą z przekroczenia parametrów współosiowości. Omawiane techniki i przyrządy pomiarowe służące do bezpośredniego ustawiania elementów okrętowego układu napędowego spełniają wymagania technologiczne stawiane zarówno przez klienta jak i towarzystwa klasyfikacyjne.

Słowa kluczowe: wał, współosiowość, okrętowy układ napędowy.

1. INTRODUCTION

The alignment procedure is part of the alignment process where alignment is performed in accordance with the requirements defined by the alignment designer. It is executable part of the propulsion shaft alignment process which consists of design, analysis and measurement. Every part must be performed in accordance with the requirements defined by standard requirements of the propulsion systems, the rules of classification societies and producers elements of the ship propulsion system, shipbuilders and designers.

Activities to comply with shaft alignment procedure depends of many problems. Moreover, it must be verified by the alignment criteria and guidelines, parts of the propulsion system like bearings, shafts, couplings, depend on experiences and practices and of the production schedule in shipyards.

2. SHAFT ALINGMENT PROCEDURE

2.1. Requirement of shaft alignment

Every of shipyards must to meet the recommendations to prevent or minimize disturbances of the engine position, established bearing location, stern tube bearing inclination. The shaft alignment procedure is not expected to start before:

- temperature of the vessel's structure is stable and as even as possible (normally procedure is conducted in early morning)
- structural part like superstructure, main engine etc. shall be installed on the vessel,
- all elements of the hull structure and equipment are in place,
- vessel stern blocs are fully welded,
- leak tests have been completed.

2.2. Elements of shaft alignment

Among the activities which are carried out during the propulsion shafting alignment procedure can be summarized in the following activities [1]:

- sighting through,
- bearing slope boring and bearing inclination

- engine bedplate deflection measurements and pre-sagging,
- Sag&Gap procedure,
- reactions measurement,
- bearing-shaft misalignment evaluation,
- intermediate shaft bearing offset readjustment,
- gear-shaft bearings reaction measurements.

3. SIGHTING THROUGH

3.1 Sighting through procedure

Sighting through is a process of establishing the reference line. The another name for this process is bore sighting. When the sighting through is finished, the established shafting reference line is rectified by slope boring or inclination of stern tube bearing. By this part of the alignment process is time to put the shaft were it is positioned, connecting the engine and gearbox, propeller installation and other elements of ship propulsion.

The sighting through is normally conducted before sunrise in the early morning hours to ensure an even temperature distribution throughout the structure. Conducting this process under certain thermal condition affects on the bearing offset because reaction measurement may be significantly different in another thermal condition

Sighting through procedure is conducted by piano wire, by optical or laser instruments. The measurement equipment is positioned in front of the after stern tube bearing. Target points are defined at the location of the intermediate shaft bearings, gearbox flange or main engine flange and these are offsets for values corresponding to the prescribed bearing offsets for the dry dock condition.

When the vessel is launched the initial alignment is expected to be disturbed by hull girder deflections. Alignment of the waterborne vessel needs to be verified and adjusted. It is not possible to accurately predict the extent of hull deflections and without knowledge of offset the alignment process may not be verified with the desired accuracy.

3.1.1 Piano wire application

Figure 1 shows a piano wire application in sighting through procedure.

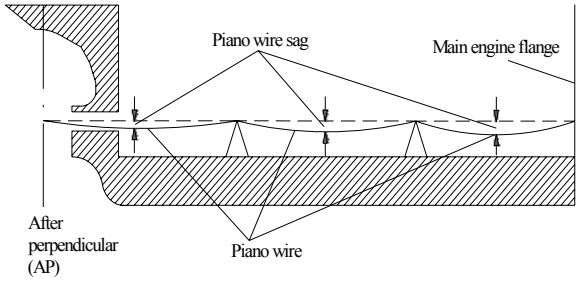

Fig. 1. Example of shafting alignment using piano wire

The application of a piano wire in sighting through procedure is used to establish a center line of the shafting. The piano wire is pulled straight from the aft stern tube bearing from the stern to the main engine flange (Fig. 1).

Fig. 2 shows screen with co-ordinate system (0÷30 mm) which is mounted on the wooden board inside the stern tube (Con-ro vessel).

Fig. 2. View of the piano wire stretched in stern tube

The screens are mounted on brackets and wooden boards in purpose of minimize piano wire sagging. The piano wire is applied with load at least 40 kg.

Measuring the vertical distance from the piano wire to the location of the particular intermediate shaft bearing is applied to the prescribed bearing offset. When the piano method is used positions of the bearings and a slope boring angle are defined as the reference.

Using piano wire the theoretical data must be corrected for piano wire sagging which depends on the piano wire diameter (0.5, 0.6 and even 0.7 [mm] diameter wire may be applied), gravity constant, gravity of the piano wire material and distance between points of its support.

3.1.2 Optical and laser instruments application

The sighting through procedure could be conducted by optical instruments, for example like:

- telescope,
- collimator,
- autocollimator,
- theodolite.

Optical instruments can be used in two ways of measurement process: to define exact position of elements of propulsion or define their angular offset.

The optical line of reference (Fig.3) is established while the vessel is in the dry dock. After the vessel is launched this line is distorted due to the hull deflections.

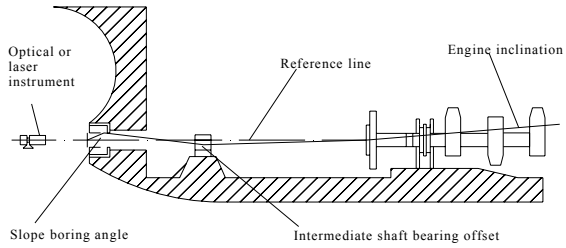

Fig. 3. Example of sighting through using optical or laser instrument

Fig. 4 presents example of using the optical instrument. It is aliniometer during concentricity measurements on the shaft bracket on the Con-ro vessel.

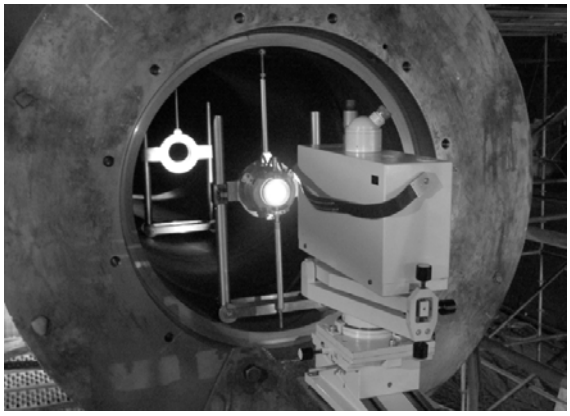

Fig. 4 Alignment using aliniometer

In the eighties, the first laser instruments were set measure the machines. This allowed to significantly increase the accuracy and simplicity of implementation of the alignment.

Laser instruments allow to receive:

- precise alignment without manual input of data and subjective interpretation,
- a graphical presentation of results of alignment,
- possibility of shaft alignment for the large distance between their flange,
- is not necessary to disassembly the couplings or the flanges,
- saving data and printing reports with the results,
- accurate and repeatability results, while ensuring their transparency to the user
- short time needed for training of the personnel,
- obtained misalignment results are projected on the screen of the instrument and compared with the tolerance limit for the coupling.

The impact of air temperature located between the laser and detector, as well as other environmental factors (dust) are affecting the stability of the measurements can be minimized by using a filter. Laser equipment made by Easy-Laser or Prüftechnik is implemented with such filters. Example of such instrument is shown on the Fig. 5. Numerous software features in the laser instruments allow to deal with different cases of measurement.

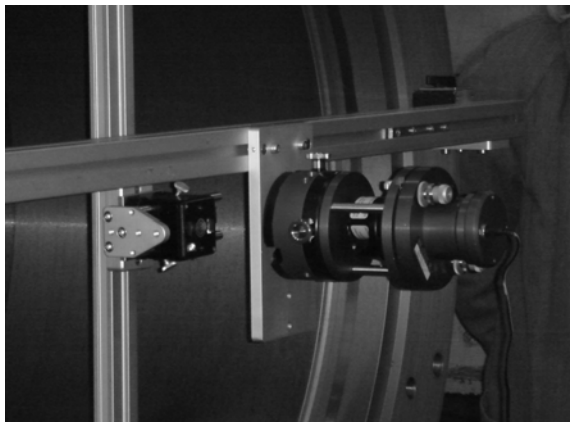

Fig. 5. Alignment using laser instrument for ex ample Easy-laser

4. DATA ANALYSIS

The problem of shafting alignment of components in propulsion system is described on the example of sighting through process on stern tube. The process of establishing the reference line has been done with three kinds of equipment: piano wire, optical instrument and laser instrument.

The figure 6 presents the scheme of stern tube alignment in order to better understanding of the problem. Measurements were performed on Con-ro vessels built the Stocznia Szczecińska "Nowa" Sp. z o.o..

Measurements on the stern tube were made in subsequent sections A, B, C in the direction from stern to fore.

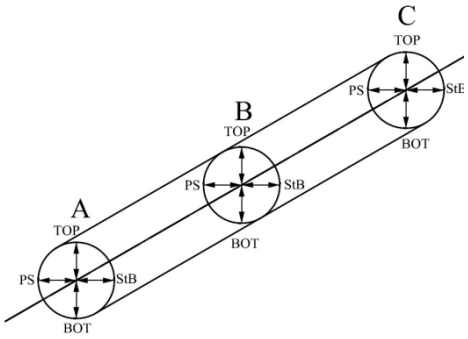

Fig. 6. Scheme of stern tube alignment

Data used for analysis allowed statistical analysis to compare the errors of measurements obtained using three equipment (piano wire, aliniometer made by Zeiss Company and laser instrument made by Easy-Laser S.L.)

The fig. 7 presents the distribution of measurements errors in successive measuring points (A, B, C). For results obtained by the optical instrument received measuring error at the order of 0,03 [mm] and for the laser instrument is at level of 0.003 [mm]. In turn measurements received by using the piano wire required further analysis due to the measuring error which is in range of 3,6÷6,6 [mm].

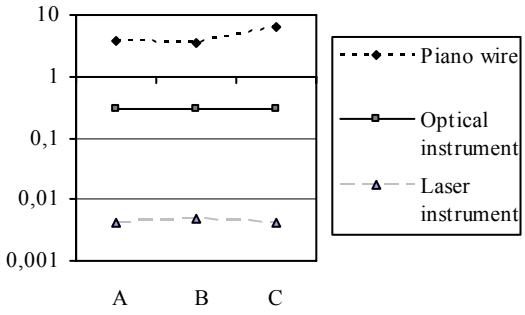

Fig. 7. Graphical presentation of the distribution of measurement errors for the selected measuring instruments

Designated error of measurement at such a high level gives a large dispersion of the value of measurand and the results obtained in measurements by this method requires further analysis.

For further analysis of measurement method using piano wire used method for evaluating the stability of measuring systems for measuring performance of specific tasks which an analysis of repeatability and reproducibility R&R (Repeatability and Reproducibility Study) was used. Results of this analysis are presented in tabele1.

Tab. 1. The results of the R&R analysis for the measurement of stern tube using piano wire

	Measurement using piano wire	
	Value	% process variability
Repeatability EV (equipment variability)	64,5708	24,6307
Reproducibility AV (operator variability)	38,3803	14,6403
Part variability PV	251,1636	95,8071
R&R	75,1161	28,6533
Total Variation TV	262,1557	100,0000

The value of % R&R below 30% [2, 3, 4] (28.65% in Tab. 1.) in the case of measurements made by piano wire allows for conditional acceptance of the measurement system.

5. CONCLUSIONS

The analysis of the results of measurements carried out on board a Con-ro vessels series B-201 produced by the Stocznia Szczecińska has demonstrated the possibility of measuring misalignment of various kinds of measurement equipment. The analysis of measurement systems shows that both a piano wire and optical and laser instruments can be used in sighting through process. However, for measurements carried out using the piano wire it is advisable to check the measurements, carried out for confirmation of quality through the application of measurement methods using optical or laser instruments.

The results obtained during measurements are satisfactory and they are within the tolerances and acquire the implementation of technical specifications related to the process of assembly of ships propulsion systems. Precise measuring instruments used in process of sighting through on stern tube (piano wire, optical instrument, laser instrument) are adequate in the existing work in the technical conditions.

BIBLIOGRAPHY

1. American Bureau of Shipping (ABS), *Guidance notes on propulsion shafting alignment*. ABS Houston TX 2006.
2. Automotive Industry Action Group - Daimler Chrysler Corporation, Ford Motor Company and General Motors Corporation: Measurement *Analysis System MSA*. Third Edition, Carwin Limited 2002.
3. Pajzderski P.: *Metodyka badania powtarzalności i odtwarzalności systemów pomiarowych.* Metrologia w systemach jakości-3. VI Sympozjum Klubu Polskie Forum ISO 9000, Politechnika Świętokrzyska 2000.
4. Tabisz R.: *Zapewnienie wiarygodności analizowanych danych – podstawy analizy MSA.* StatSoft Polska 2004.

dr inż. **Eliza JARYSZ-KAMIŃSKA** is an assistant in Institute of Manufacturing Engineering on Faculty of Mechanical Engineering and Mechatrinics in West Pomeranian University of Technology in Szczecin. In her scientific work (doctor's thesis) she deals estimate of shaft misalignment ships propulsion system evaluation.

TRAJEKTORIA FAZOWA JAKO NARZĘDZIE OCENY PROCESÓW DEGRADACYJNYCH POMPY WYPOROWEJ

Wojciech BATKO*, Tomasz KORBIEL*, Jerzy STOJEK**

Akademia Górniczo-Hutnicza, Katedra Mechaniki i Wibroakustyki*, Katedra Automatyzacji Procesów**
al. Mickiewicza 30, 30-059 Kraków, email: batko@agh.edu.pl

Streszczenie

W artykule podjęto próbę oceny przydatności obrazów trajektorii fazowych dla procesu diagnozowania zmian stanu pomp wyporowych. Przedstawiono przesłanki realizacyjne podjętych badań i ich laboratoryjną realizację. Dotyczyły one eksperymentalnego sprawdzenia zmian obrazów trajektorii fazowych sprawnej pompy wyporowej - pracującej z stałą wydajnością, z pompą w której element tarcz rozrządczych pompy wielotłoczkowej uległ procesom degradacji. Wykazały one ich informacyjną przydatność do rozpoznawania zmian degradacyjnych w pompie wyporowej. Artykuł sygnalizuje celowość rozważenia wprowadzenia portretów fazowych monitorowanych sygnałów drganiowych do procedur nadzoru diagnostycznego stanu elementów konstrukcji pompy wyporowej.

Słowa kluczowe: trajektorie fazowe, pompa wyporowa, diagnostyka techniczna, hydraulika siłowa, analiza sygnału.

PHASE TRAJECTORY AS A TOOL FOR ASSESSING DEGRADATION PROCESSES IN A DISPLACEMENT PUMP

Summary

A test of assessing a suitability of the phase trajectory pattern for diagnostics of condition changes of displacement pumps - is undertaken in the presented paper. Accomplishment reasons of investigations together with their laboratory realizations are given. They concerned the experimental comparison of changes in the phase trajectory patterns of the efficient displacement pump – working with a constant output – with the multi-piston pump, in which an element of the gear disc plate was degraded. The performed tests confirmed the suitability of phase trajectories in the recognition of degradation changes in displacement pumps.

The paper signals the usefulness of considering the introduction of phase trajectory patterns of the monitored vibration signals into processes of the diagnostic inspection of the displacement pump structural elements.

Keywords: phase trajectories, displacement pump, technical diagnostics, forced hydraulics, signal analysis.

1. WSTĘP

Badania stanu degradacji elementów pompy wyporowej można przeprowadzać na wiele sposobów. Powszechnie stosowane jest pomiar podstawowych parametrów eksploatacyjnych pompy takich jak: pomiar ciśnienia wyjściowego, pomiar wydajności pompy, określenie współczynnika nierównomierności wydatku czy też oszacowanie chwilowej wartości sprawności ogólnej pompy. Innym sposobem rozpoznawania stanu degradacji pompy wyporowej jest zastosowanie tak zwanej diagnostyki wibracyjnej bazującej na pomiarze sygnałów drganiowych (przyspieszenia, prędkości, przemieszczenia) w miejscach charakterystycznych korpusu pompy. Na uzyskanych tą drogą przebiegach czasowych monitorowanych sygnałów drganiowych wyznaczane są estymaty punktowe lub funkcyjne, które mogą być określane zarówno w dziedzinie czasowej, jak i częstotliwościowej. Wybór właściwych związany jest z analizą wrażliwości, czyli ocenami zmian degradacyjnych wywołanych nieskończenie małymi zmianami wybranego symptomu.. Istotnym warunkiem tej drogi postępowania jest związany z nią wymóg małej wrażliwości wyróżnionego symptomu na możliwe zakłócenia wymuszeń stanów ustalonych diagnozowanego obiektu, najczęściej oscylujące w granicach błędu wartości wejściowej. Przykładem takim może być wartość prędkości obrotowej wału wejściowego dowolnej maszyny wirnikowej, która oscyluje wokół założonej wartości. Obecność w procesach rozpoznań diagnostycznych zakłóceń; związanych z dopuszczalnymi zaburzeniami, na które składają się: dopuszczalne błędy parametrów struktury diagnozowanych obiektów, zaburzenia wymuszające działające na ich wejściach, jak i błędy powstające w systemie pomiarowym; jest przesłanka

dla poszukiwań nowych symptomów diagnostycznych, o lepszej jakości odwzorowania relacji degradacyjnych w diagnozowanym obiekcie na podstawie odpowiednio zdefiniowanych miar ich zmienności. Prace w tym zakresie prowadzą do odkrywania i definiowania różnych relacji diagnostycznych, na bazie których budowane są systemy monitorujące zmiany stanu diagnozowanego obiektu i stanowią podstawę do wnioskowania o jego stanie.

W artykule zaprezentowano badania nad przydatnością obrazów trajektorii fazowych dla procesu rozpoznawania zmiany stanu wybranych elementów pomp wyporowych. Mają one odniesienia do idei budowy systemów monitorujących bazującej na teorii stateczności technicznej [1], [2]. Zgodnie z jej ideą, trajektorie fazowe analizowanych sygnałów diagnostycznych stanowią element wykonawczy budowy systemu monitorującego. Mają walor użytecznego, prostego w obserwacji narzędzia kontrolnego, odwzorowującego oddziaływania dynamiczne występujące w diagnozowanych maszynach, określone prawami fizyki opisujących ich funkcjonowania.

Weryfikacja tej tezy w odniesieniu do oceny degradacji elementów pomp wyporowych jest przedmiotem badań przedstawionych w artykule. Ich ilustracją jest opis czynnego eksperymentu diagnostycznego dotyczącego oceny procesu degradacji płaskiej tarczy rozrządczej wielotłoczkowej pompy wyporowej o stałej wydajności z wykorzystaniem obserwacji zmian obrazów fazowych sygnałów drganiowych poddanych kontroli.

2. OBIEKT BADAŃ

W hydraulicznej pompie tłokowej rozdzielanie cieczy roboczej do i od cylindrów wirnika odbywa się na ogół za pomocą nieruchomej płaskiej tarczy rozdzielczej (rozrządem pompy), prostopadłej do osi obrotu wału pompy (rys. 1). Tarcza ta posiada otwory o kształcie nerek łączące cylindry z objętościami niskiego i wysokiego ciśnienia. Czoło wirnika współpracuje z tarczą rozdzielczą ślizgając się po jej powierzchni podczas ruchu obrotowego.

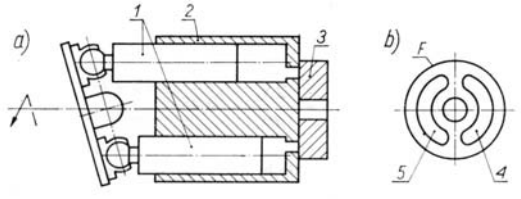

Rys. 1. Uproszczony schemat pompy wielotłoczkowej osiowej: a) przekrój poprzeczny, b) widok tarczy rozdzielczej (rozrządu pompy), 1. tłoczki, 2. wirnik, 3. tarcza rozdzielcza,4. otwór ssawny, 5. otwór tłoczny

Powierzchnia styku tych elementów narażona jest na zużycie, a nawet niebezpieczeństwo zatarcia spowodowane min. zanikiem filmu olejowego. Wypracowanie tarcz rozrządczych związane jest z pojawianiem się mikro-kanałów przepływowych pomiędzy otworem ssawnym pompy a otworem tłocznym na powierzchniach stref przejściowych tarczy (tzw. mostków) (rys. 2). Powstałe kanały powodują przepływ czynnika roboczego co prowadzi do braku szczelności między strefą ssawną i tłoczną pompy, obniżenia jej sprawności wolumetrycznej oraz ciśnienia eksploatacji.

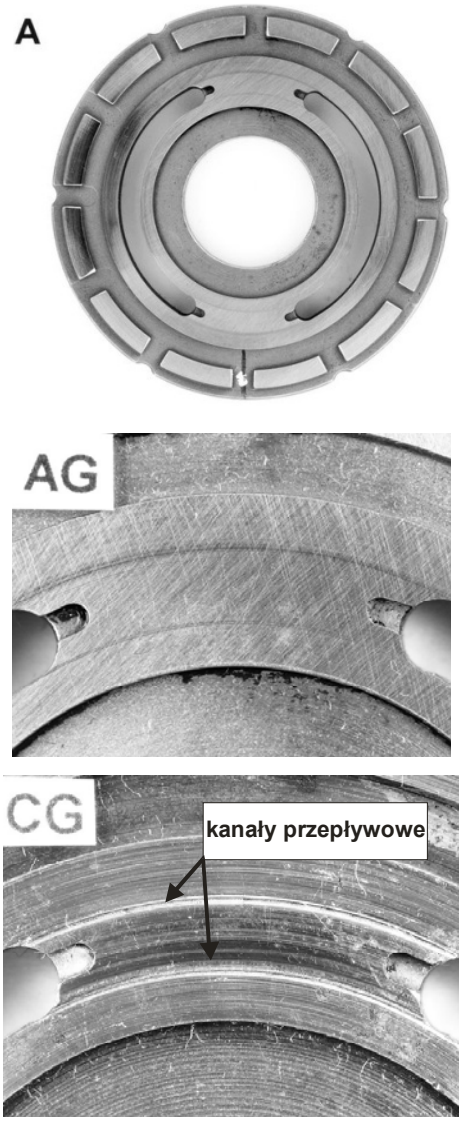

Rys. 2. Widok tarczy rozrządczej wraz z strefami przejściowymi: A) ogólny widok tarczy, AG) strefa przejściowa tarczy sprawnej, CG) strefa przejściowa tarczy wypracowanej

Rozwój wypracowania tarczy rozrządczej, związany z powiększeniem geometrii kanałów przepływowych w przeprowadzonych badaniach zamodelowano wykonując nacięcia kanałów przepływowych na powierzchniach tarcz rozrządczych o głębokościach odpowiednio: 0.01 mm (rozrząd typu B) i 0.05 mm (rozrząd typu C).

3. OPIS METODY TRAJEKTORII FAZOWYCH

Wykrycie wstępnej fazy uszkodzenia poszczególnych elementów pompy (tarczy rozrządczej, wirnika czy tarczy wychylnej), powinno być niezależne od zakłóceń związanych z pracą pozostałych elementów składowych. Jednakże niemożliwe jest wyodrębnienie z dostępnego sygnału diagnostycznego składowych informacyjnych związanych z konkretnym jej elementem (np. tarczą rozrządczą). Zatem mamy do czynienia z maszyną, urządzeniem, elementem pracującym w otoczeniu innych maszyn, urządzeń czy elementów. Oddziaływania otoczenia na badany element, niezależnie od charakteru zjawisk mogą zostać opisane funkcjami zwanymi dalej zaburzeniami stale działającymi. Tak sformułowane zagadnienie w literaturze fachowej opisane jest jako stateczność w sensie Lapunowa oraz stateczność techniczna [2].

Rozpatrując konkretny element pompy wielotłoczkowej, na który działają siły pochodzące od innych elementów pompy lub obiektów układu hydraulicznego, równanie ruchu badanego elementu można sformułować następująco:

$$\ddot{x} = f\left(\dot{x}, x, t\right) \tag{1}$$

gdzie: $\ddot{x}$ - przyspieszenie elementu badanego,
$\dot{x}$ - prędkość badanego elementu,
x - przemieszczenie badanego elementu,
t – czas.

Równanie to posiada jednoznaczne rozwiązania określone przez warunki początkowe. Uwzględniając oddziaływanie na badany element otoczenia opisanego w postaci równania zaburzeń „R" stale działających, otrzymujemy:

$$\ddot{x} = f\left(\dot{x}, x, t\right) + R\left(\dot{x}, x, t\right) \tag{2}$$

Rozwiązanie powyższego równania przeprowadza się poprzez podstawienie i redukcję jego rzędu otrzymując:

$$\dot{x} = f\left(x, t\right) + R\left(x, t\right) \tag{3}$$

Biorąc pod uwagę to, iż funkcja *R(x,t)* uwzględnia dopuszczalne odchyłki od stanu ustalonego oraz zmianę warunków początkowych i przewidziane zaburzenia zewnętrzne i wewnętrzne działające na rozpatrywany element (obiekt, układ) o charakterze stochastycznym oraz periodycznym można określić stan dynamiczny obiektu poprzez pojęcie stateczności technicznej [2].
Proponowane podejście nie wymaga pełnej identyfikacji struktury układu, czyli ścisłego określenia funkcji *f(x,t)*, skupiając się jedynie na rozwiązaniach równania (3). Skutecznym narzędziem do badania rozwiązań układów równań różniczkowych jest analiza trajektorii w przestrzeni fazowej. Z definicji układu statecznego technicznie wynika, ze jeżeli dla warunków początkowych zawartych w obszarze ω przestrzeni fazowej, rozwiązania układu (3) pozostają w obszarze Ω, to badany element (układ, obiekt) jest statyczny technicznie (rys. 3).

Badając rzeczywisty obiekt jakim jest pompa wielotłoczkowa mamy do czynienia z wieloma jej elementami składowymi oddziaływującymi między sobą. Stateczność układu możemy określić poprzez pomiar parametru ruchu poszczególnych elementów. Fizycznie dostępne są tylko elementy związane z obudową pompy.

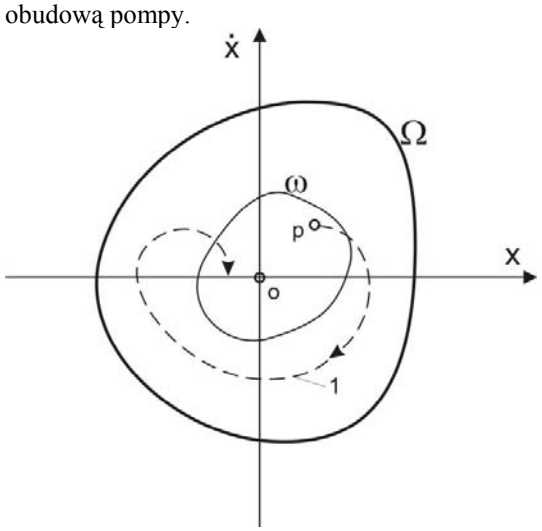

Rys. 3. Ilustracja pojęcia stateczności technicznej: 1 – trajektoria fazowa, Ω - obszar dopuszczalnych odchyleń od stanu równowagi, ω – obszar warunków początkowych, p –stan początkowy układu po wytrąceniu, ze stanu równowagi „o"

Parametry drganiowe obudowy są powiązane z ruchem elementów składowych pompy. Zatem należy wybrać odpowiednie miejsce na obudowie, geometryczne powiązane z badanymi elementami pompy. Pomiary przemieszczenia i prędkości drgań wybranego punktu odniesione do przestrzeni fazowej będą charakteryzowały klasę rozwiązań równań cząstkowych związanych z poszczególnymi elementami pompy. Problem określenia obszaru Ω, można rozwiązać na kilka sposobów. W przypadku pomp wielotłoczkowych preferowanym podejściem będzie określenie obszaru Ω na podstawie analizy dynamiki pompy niewypracowanej. Badanie trajektorii fazowej dla pompy sprawnej z uwzględnieniem zakłóceń zewnętrznych pozwoli na określenie tego obszaru. W przypadku analizy drgań korpusów pomp wyporowych mamy odczynienia, ze zjawiskiem drgań nietłumionych wokół położenia równowagi. Obrazem przestrzeni fazowej dla takiego obiektu będzie wówczas płaszczyzna fazowa z tzw. cyklem granicznym. Występuje ona wówczas gdy trajektoria fazowa nie

dochodzi do punktu równowagi lecz przechodzi w krzywą zamkniętą otaczającą ten punkt (rys. 4).

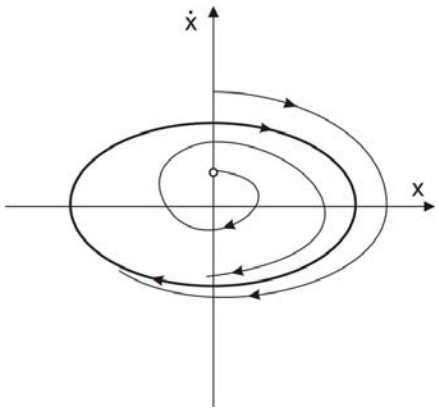

Rys. 4. Przykładowa trajektoria fazowa z cyklem granicznym

Obserwacja zmiany obszaru zawierającego trajektorie posłuży stworzeniu symptomu diagnostycznego, a następnie doprowadzi do postawienia hipotezy diagnostycznej. Z rozważań teoretycznych [1] wynika, że nie wiadomo jak obszar Ω uznany jako statyczny technicznie będzie się zmieniał w wyniku degradacji badanego elementu. W przestrzeni fazowej ujęta jest informacja o zmagazynowanej energii (sumie energii kinetycznej i potencjalnej) badanego obiektu. Z modelu maszyny jako procesora energii [3], wynika, że w przypadku wzrostu sumarycznej energii badanego elementu pole powierzchni obszaru Ω będzie się zwiększać. Ta przesłanka umożliwi identyfikację struktury energetycznej badanego obiektu. Obserwując elementy związane z procesem roboczym pompy (wytworzenie wydatku Q) w przypadku spadku sprawności energetycznej można spodziewać się zmniejszenia obszaru Ω. Dla elementów, gdzie nastąpi destrukcyjne sprzężenie energii dyssypowanej obszar ten powinien się zwiększać.

4. CZYNNY EKSPERYMENT DIAGNOSTYCZNY

Badania stopnia wypracowania tarcz rozrządczych pomp wielotłoczkowych zostały przeprowadzone na stanowisku laboratoryjnym, którego głównymi elementami była pompa wielotłoczkowa o stałej wydajności wraz z zamontowanymi przetwornikami pomiarowymi (wibracji, natężenia przepływu ciśnienia statycznego i dynamicznego). Widok układu badawczego pomp wraz z zamontowanymi przetwornikami wibracji przedstawiono na rys. 5.

Umieszczając w pompie tarcze rozrządcze o różnym stopniu wypracowania dokonywano pomiaru wibracji jej korpusu w miejscu bezpośredniego ich zamontowania. Do pomiaru wibracji użyto piezoelektrycznych przetworników przyspieszenia, usytuowanych w trzech osiach pomiarowych X, Y oraz Z. W pomiarach wykorzystano 16 bitową kartę pomiarową współpracującą z układem kondycjonującym i programowaną, za pomocą pakietu LabView. Przykładowy przebieg przyspieszeń wibracji przypadający na jeden pełny obrót wału pompy zaprezentowano na rys. 6.

Rys. 5. Widok badanej pompy w na stanowisku badawczym

Zmierzone sygnały zostały archiwizowane na dysku twardym komputera poczym poddano je analizie numerycznej.

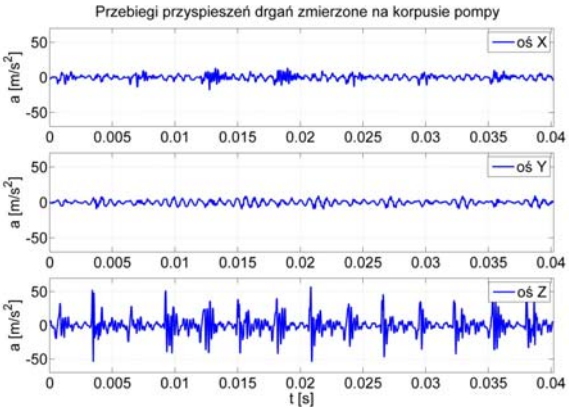

Rys. 6. Przebiegi przyspieszeń drgań korpusu pompy mierzone w osi X, Y, Z

5. WYBRANE WYNIKI BADAŃ

Prowadzone badania polegały na wyznaczeniu trajektorii w przestrzeni fazowej dla pompy z niewypracowana tarczą rozrządczą (typ A) oraz pomp wyposażonych w wypracowane tarcze rozrządcze (typu B i C). Metodyka wyznaczania trajektorii fazowych oparta była o całkowanie numeryczne przebiegów przyśpieszeń drgań korpusu pompy w jej punktach charakterystycznych. Uzyskane wykresy trajektorii fazowych wyznaczone w trzech osiach pomiarowych przedstawiono na rysunkach poniżej.

a)

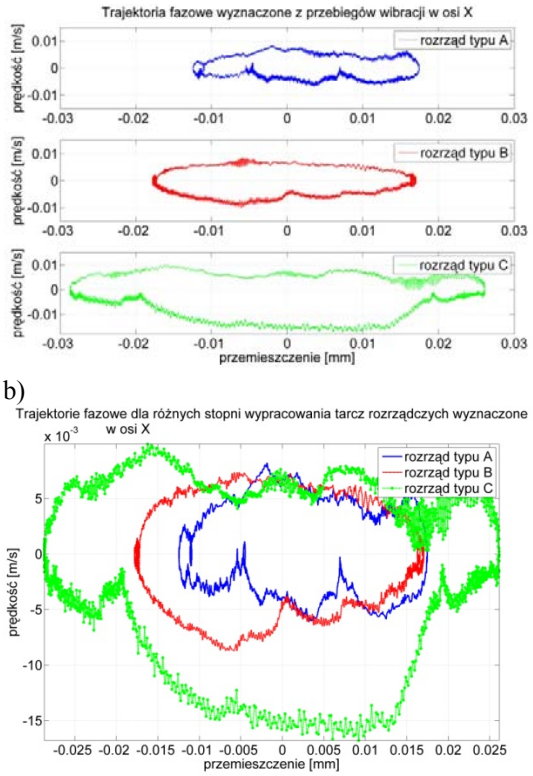

Rys. 7. Trajektorie fazowe wyznaczone z przebiegów wibracji zmierzonych w osi X: a) przebiegi indywidualnych trajektorii dla tarczy typu A, B, C, b) zestawienie porównawcze

a)

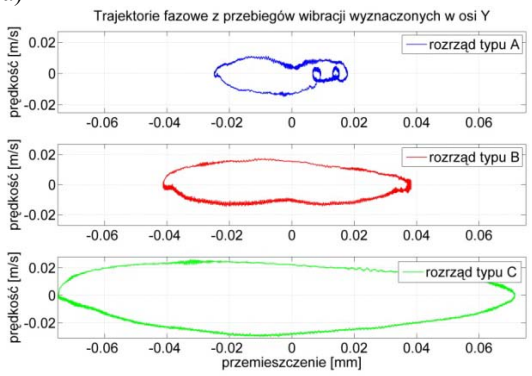

b)

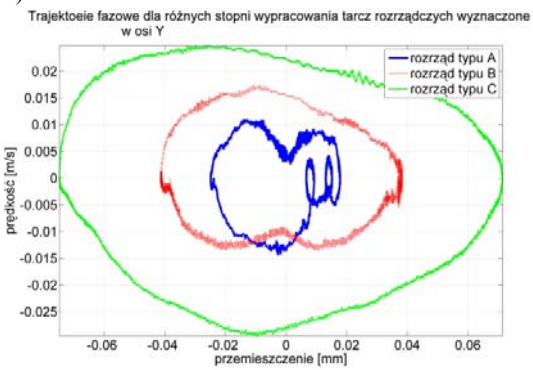

Rys. 8. Trajektorie fazowe wyznaczone z przebiegów wibracji zmierzonych w osi Y: a) przebiegi indywidualnych trajektorii, dla tarczy typu A, B, C, b) zestawienie porównawcze

a)

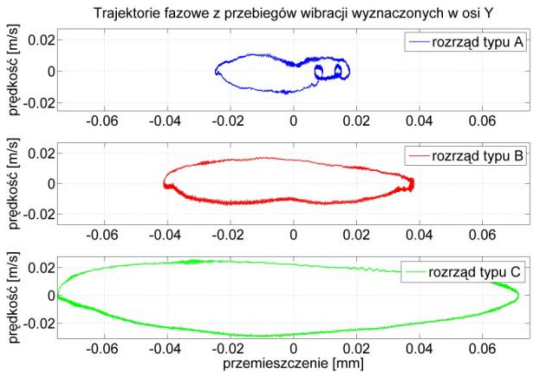

b)

Rys. 9. Trajektorie fazowe wyznaczone z przebiegów wibracji zmierzonych w osi Z: a) przebiegi indywidualnych trajektorii, dla tarczy typu A, B, C, b) zestawienie porównawcze

6. UWAGI KOŃCOWE

Wyniki badań czynnego eksperymentu diagnostycznego pompy wyporowej z tarczą rozrządczą (typ A) w dobrym stanie technicznym oraz pomp wyposażonych w tarcze rozrządcze (typu B i C) uszkodzone, którymi symulowano proces ich degradacji; poprzez pogłębianie rowków przepływowych w strefie przejściowej miedzy kanałem ssawnym tarczy, a jej kanałem tłocznym; wykazały dużą wrażliwość trajektorii fazowych; na wszystkich trzech osiach pomiarowych; na uszkodzenie diagnozowanego elementu.

Odwołując się do modelu energetycznego maszyny można wnioskować, że w obszarze pomiaru drgań w miejscu bezpośredniego zamontowania tarczy rozrządczej, następuje wzrost energii korpusu pompy spowodowanej rozpraszaniem całkowitej energii pary kinematycznej, jaką jest „*tarcza rozrządcza-powierzchnia czołowa wirnika pompy*". Szczególnie dobrze ilustruje tę zależność obraz trajektorii uzyskany z przetworników zamontowanych w osi X i Y, w bezpośrednim sąsiedztwie rozrządu pompy. Mniej wyraźnie, ale równie poprawnie można rozpoznawać degradację tarczy, poprzez obserwacje zmian trajektorii przyporządkowanej lokalizacji pomiaru sygnałów drganiowych z przetwornika zamontowano na powierzchni tarczy wychylnej

pompy na kierunku osi Z, co wynikało z braku możliwości pomiaru drgań w bezpośrednim sąsiedztwie badanego rozrządu. Sygnał pomiarowy z tego przetwornika, będąc reprezentantem sygnałów od elementów składowych pompy (min. tarczy wychylnej, wirnika wraz z łożyskowaniem), miał tym samym ograniczoną selektywność do pozyskania właściwej informacji diagnostycznej. Biorąc pod uwagę przytoczone rezultaty można stwierdzić, że trajektorie fazowe monitorowanych sygnałów drganiowych na pompie wyporowej mogą być dobrym wskazaniem do poszukiwania szerszych wdrożeń tych symptomów do diagnostyki i monitoringu zmian stanu różnych jej elementów. Na etapie ich klasyfikacji i powiązań z stopniem rozpoznawanych uszkodzeń możliwe jest zastosowanie różny miar dla opisu ich zmian.

Dalsze prace autorów ukierunkowane będą na rozwiązanie tego problemu, tj. przyporządkowania określonych miar liczbowych dla obserwowanych zmian trajektorii fazowych, który pozwoliłby na ich związanie z parametrami opisującymi stan degradacji analizowanego uszkodzenia.

LITERATURA

[1] Batko W.: *Nowe idee w budowie systemów monitorujących*. Przegląd Mechaniczny, nr 11/ 2007, str. 43-47.
[2] Batko W.: *Technical stability – a new modeling perspective for building solutions of monitoring systems for machine state*. Zagadnienia Eksploatacji Maszyn, z.3 (151), Vol.42, s.147-157, 2007.
[3] Bogusz W.: *Stateczność techniczna*. Państwowe Wydawnictwo Naukowe, Warszawa1972.
[4] Cempel C. Diagnostyka maszyn. Wyd. Międzyresortowe Centrum Naukowe, Radom 1992.
[5] Stryczek S.: *Napęd hydrostatyczny*. Wydawnictwo Naukowo Techniczne, Warszawa 1995.
[6] Żółkiewski B., Cempel C.: *Inżynieria diagnostyki maszyn*. Praca zbiorowa. Wydawnictwo PTDT, Radom 2004.

Prof. dr hab. inż. **Wojciech BATKO**, prof. zw. AGH ur. 1949. Kierownik Katedry Mechaniki i Wibroakustyki AGH, autor i współautor ponad 230 publikacji, w tym 12 książkowych. Zajmuje się zagadnieniami dynamiki i wibroakustyki maszyn oraz zagadnieniami diagnostyki technicznej

Dr inż. **Tomasz KORBIEL** jest adiunktem w Katedrze Mechaniki i Wibroakustyki AGH. Jego zainteresowania związane są z diagnostyką techniczną oraz systemami monitorującymi w technice

Dr inż. **Jerzy STOJEK** jest pracownikiem Wydziału Inżynierii Mechanicznej i Robotyki AGH. W Katedrze Automatyzacji Procesów zajmuje się zagadnieniami napędu i sterowania hydraulicznego ich modelowaniem i symulacją

IDENTYFIKACJA PĘKNIĘĆ ZMĘCZENIOWYCH ELEMENTÓW Z POWŁOKAMI PVD, PRACUJĄCYCH W SYSTEMACH TRIBOLOGICZNYCH

Witold PIEKOSZEWSKI, Marian SZCZEREK
Instytut Technologii Eksploatacji – Państwowy Instytut Badawczy w Radomiu
witold.piekoszewski@itee.radom.pl

Streszczenie

W artykule przedstawiono wyniki badań wpływu nowych technologii (PVD) konstytuowania warstw wierzchnich wysokoobciążonych elementów maszyn na ich powierzchniową trwałość zmęczeniową. Zbadano typowe powłoki stosowane na narzędzia skrawające TiN, CrN oraz powłoki niskotarciowe o złożonej strukturze WC/C, MoS_2, MoS_2/Ti. We wszystkich przypadkach badania skojarzeń powłoka naniesiona była tylko na jeden z elementów testowych (stożek). Badane styki smarowane były olejami: mineralnym wzorcowym, syntetycznym oraz roślinnym. Stwierdzono, że w przypadku smarowania olejem mineralnym praktycznie każdy rodzaj powłoki naniesiony na próbkę obniżał powierzchniowa trwałość zmęczeniową. W przypadku smarowania badanego styku olejami syntetycznym i roślinnym najwyższą trwałość zmęczeniową odnotowano dla węzłów tarcia z elementami z naniesioną powłoka niskotarciową MoS_2/Ti, porównywalną z trwałością węzła stalowego smarowanego olejem mineralnym. Ponadto stwierdzono, że na powierzchniową trwałość zmęczeniową badanych skojarzeń bardzo istotny wpływ miał rodzaj oleju bazowego, którym skojarzenia było smarowane, a także fakt, że w przypadku pokrycia powłoką PVD wysokoobciążonego elementu pittingowi ulega element z powłoką, a nie sama powłoka.

Słowa kluczowe: zużycie, trwałość, powłoki PVD, pitting.

THE IDENTIFICATION OF FATIGUE CRACKS ON PVD COATED PARTS WORKING IN TRIBOLOGICAL SYSTEMS

Symmary

The paper presents the results on the effect of application of new PVD technologies deposited on the surface layer of heavy-loaded machine parts on the rolling contact fatigue life. Two kinds of coatings were tested: single TiN, CrN used for cutting tools and low-friction with multilayer structure WC/C, MoS_2 and MoS_2/Ti. In all tests the coating was deposited only for one rolling element - a cone. The investigated tribosystems were lubricated with mineral base oil, synthetic base oil and refined rapeseed oil. It was stated that for mineral base oil for all coated specimens the fatigue life were shorter than for uncoated parts. In case of lubrication with synthetic oil and vegetable oil the highest fatigue life were measured for MoS_2/Ti coating. The durability of the coating was comparable to uncoated parts lubricated with mineral base oil. It was also stated that in case of coated elements the kind of oil base is very important factor influencing the pitting life. Furthermore, in case of heavy-loaded coated element the pitting wear concerns the whole element not only the coating layer.

Keywords: wear, durability, PVD coatings, pitting.

1. WPROWADZENIE

Artykuł dotyczy badania wpływu nowych technologii (PVD) konstytuowania warstw wierzchnich wysokoobciążonych elementów maszyn na ich powierzchniowa trwałość zmęczeniową (pitting).

Dobre właściwości tribologiczne powłok PVD (mała przewodność cieplna, odporność temperaturowa oraz brak skłonności do tworzenia sczepień adhezyjnych) były czynnikami, które spowodowały ich zastosowanie do zwiększenia odporności na zużycie narzędzi skrawających (noże, wiertła, frezy, wkładki węglikowe[1, 2, 3]) oraz narzędzi do obróbki plastycznej na zimno (wykrojniki, matryce, stemple i formy odlewnicze[4, 5, 6]). W związku z powyższym dane na temat charakterystyk tarcia i zużycia elementów z twardymi powłokami przeciwzużyciowymi dotyczą w głównej mierze tzw. styku obróbkowego. Brak jest natomiast danych tarciowych i zużyciowych dotyczących smarowanego styku skoncentrowanego, występującego w wysokoobciążonych węzłach tarcia, takich, jak: przekładnie zębate, łożyska toczne, mechanizmy typu krzywka-popychacz. Głównymi przyczynami destrukcji takich węzłów tarcia są zacieranie i pitting [7, 8, 9]. Około 80% uszkodzeń przekładni zębatych spowodowane jest tymi formami zużycia.

W praktyce nie ma dostępu do opracowań ujmujących kompleksowo zarówno odporność na zacieranie i jak pitting elementów z naniesionymi powłokami przeciwzużyciowymi. Aby ten problem po części wyjaśnić przeprowadzono badania wpływu rodzaju powłoki na powierzchniową trwałość zmęczeniową.

a)

b)

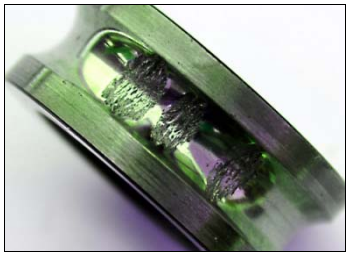

Rys. 1. Główne formy zużycia wysokoobciążonych elementów maszyn: a) ślady zatarcia na zębie koła przekładni, b) pitting na bieżni wewnętrznej łożyska kulkowego

2. METODA BADAŃ

Celem badań było określenie wpływu nowych technologii (PVD) konstytuowania warstw wierzchnich wysokoobciążonych elementów modelowego węzła tarcia na powierzchniowa trwałość zmęczeniową (pitting).

Do badań wykorzystano zmodernizowany aparat czterokulowy opracowany i produkowany w ITeE-PIB. Zarówno zmodernizowany aparat jak i metoda badawcza zostały przedstawione w szeregu publikacjach [10, 11]. Istota modyfikacji metody polega na zastąpieniu górnej, obracającej się kulki próbką w postaci stożka. Zastąpienie kuli stożkiem pozwala na badanie dowolnego materiału, poddanego dowolnej obróbce cieplnej lub cieplno-chemicznej. Jej powierzchnia trąca (testowana) może być konstytuowana dowolną, osiągalną technologią. Jest to szczególnie istotne w przypadku wprowadzania nowych, próżniowych technologii konstytuowania warstw wierzchnich elementów trących, które są najczęściej ostatnimi zabiegami technologicznymi w procesie ich wytwarzania.

Badania polegały na przeprowadzaniu, przy stałym zadanym obciążeniu P i stałej prędkości obrotowej n (Rys. 1a), 24 biegów badawczych elementów testowych współpracujących tocznie w obecności środka smarowego, ciągłym pomiarze amplitudy drgań generowanych w badanym węźle, pomiarze czasu poszczególnych biegów badawczych, sporządzeniu rozkładu Weibulla i na jego podstawie określeniu trwałości węzła tarcia.

a)

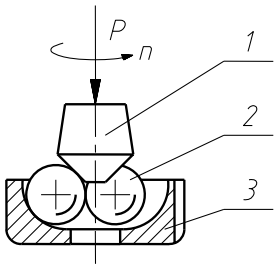

b)

Rys. 2. Węzeł tarcia aparatu T-03 do badania zużycia zmęczeniowego materiałów stosowanych na wysokoobciążone elementy toczne: a) schemat: 1-próbka stożkowa, 2-kulki dolne, 3-bieżnia., b) widok

Trwałość zmęczeniową charakteryzowano za pomocą tzw. trwałości 10%, oznaczonej symbolem L_{10}. Jest to czas eksploatacji tocznych elementów węzła tarcia (smarowanych badanym olejem), w którym 10% ich populacji ulega uszkodzeniu.

Warunki, przy których przeprowadzono biegi badawcze, były następujące:

- obciążenie węzła tarcia 3924 N,
- prędkość obrotowa wrzeciona: 1450 ± 50 obr/min,
- obciążenie wstępne węzła tarcia: 981 N,
- temperatura otoczenia: 23 ± 2ºC.

2.1. Obiekty badań

Do wykonania próbek (stożków) wybrano stal łożyskową 100Cr6, ze względu na to, że charakteryzuje się jednorodną strukturą w całej swojej objętości, a więc nadaje się jako materiał odniesienia i podstawowy materiał do nanoszenia powłok. Ponadto należy zaznaczyć, że stal 100Cr6 stosowana na elementy łożysk tocznych pod względem powierzchniowej trwałości zmęczeniowej została przebadana wszechstronnie [12, 13].

Do badań elementów z powłokami wytypowano powłoki proste jednowarstwowe TiN i CrN oraz niskotarciowe o złożonej strukturze WC/C, MoS_2, MoS_2/Ti. We wszystkich przypadkach powłoka naniesiona była tylko na jeden z elementów testowych.

Wszystkie powłoki osadzono na stalowych elementach testowych w procesach PVD, przy czym powłoki jednowarstwowe (TiN oraz CrN) metodą łukowo-próżniową, powłokę WC/C metodą reaktywnego rozpylania, natomiast powłoki MoS_2 i MoS_2/Ti metodą rozpylania magnetronowego. Wszystkie procesy osadzania zostały przeprowadzone poniżej temperatury wystąpienia przemian w materiale podłoża (poniżej 200ºC).

Do smarowania styku użyto olejów: mineralnego wzorcowego bez dodatków (RL 144), syntetycznego (PAO 8) oraz roślinnego rzepakowego rafinowanego (RzR).

2.2. Wyniki badań

Wyniki badań powierzchniowego zużycia zmęczeniowego modelowego węzła tarcia z elementami pokrytymi powłokami i smarowanego olejem mineralnym przedstawiono na Rys. 3.

Należy zwrócić uwagę, że na wykresie tym oś czasu jest logarytmiczna i różnice w trwałości skojarzeń TiN-100Cr6 i CrN-100Cr6 są przynajmniej o rząd mniejsze od trwałości skojarzeń 100Cr6-100Cr6, WC/C-100Cr6 czy MoS_2/Ti-100Cr6.

Duże zróżnicowanie powierzchniowej trwałości zmęczeniowej L_{10} badanych skojarzeń materiałowych najlepiej obrazują rezultaty ujęte na Rys. 4. Z przedstawionych zestawień wynika, że typowe, najpopularniejsze powłoki przeciwzużyciowe stosowane na narzędzia (TiN, CrN), w drastyczny sposób zmniejszają odporność na pitting badanego węzła tarcia (aż 30 krotnie) w stosunku do stalowego węzła tarcia 100Cr6-100Cr6.

Zdecydowanie odmienne jest zachowanie skojarzeń, w których próbki pokryte są powłokami niskotarciowymi na bazie węglika wolframu (WC/C) i dwusiarczku molibdenu (MoS_2/Ti i MoS_2). Dla powłoki WC/C zaobserwowano tylko ok. 15% obniżenie trwałości L_{10} w stosunku do skojarzenia 100Cr6-100Cr6. Należy przy tym zaznaczyć, że dużo mniejsze trwałości L_{10} wyznaczono dla skojarzeń z pozostałymi

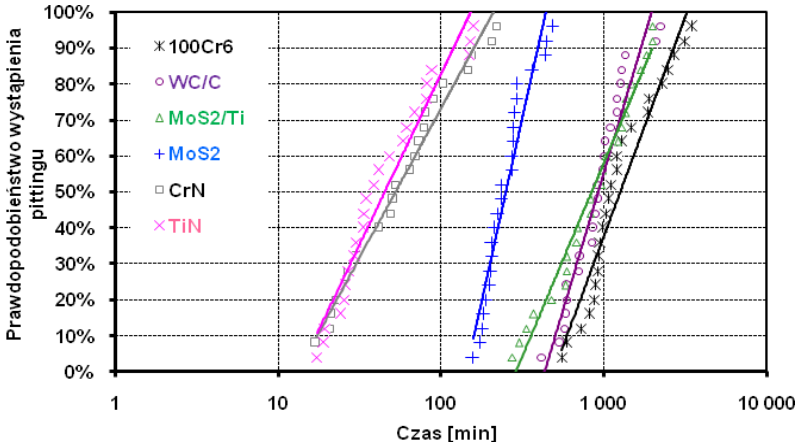

Rys. 3. Wyniki badań zmęczeniowych badanych skojarzeń materiałowych smarowanych olejem mineralnym RL 144

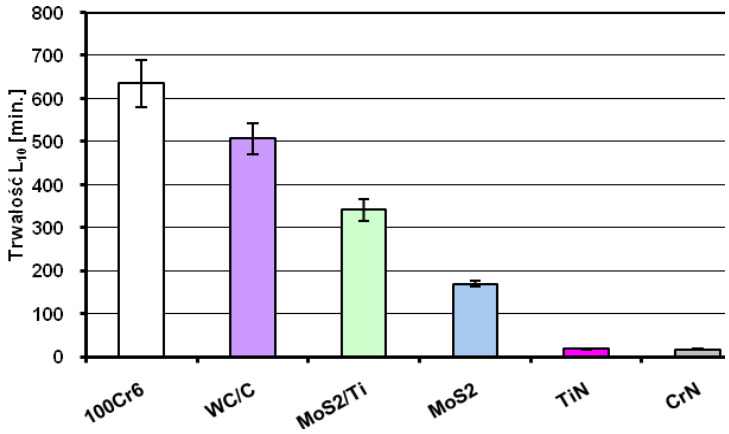

Rys. 4. Powierzchniowa trwałość zmęczeniowa L_{10} badanych skojarzeń materiałowych smarowanych olejem mineralnym RL 144

powłokami niskotarciowymi. Dla elementu z powłoką MoS_2 trwałość L_{10} w stosunku do trwałości elementów ze stali 100Cr6 zmniejszyła się prawie 4-krotnie, natomiast z powłoką MoS_2/Ti ok. 2-krotnie.

Na kolejnych wykresach przedstawiono wyniki badań skojarzeń smarowanych olejem syntetycznym PAO 8. W przypadku tego oleju największą odporność na pitting posiadało skojarzenie, w którym na elementy testowe naniesiono powłokę MoS_2/Ti (Rys. 5).

Z analizy wyników przedstawionych na Rys. 6 wynika, że trwałość L_{10} skojarzenia stalowego 100Cr6-100Cr6 jest mniejsza prawie o połowę. Mniejszą od stalowego węzła trwałością charakteryzują się węzły z próbki z nałożonymi warstwami WC/C. Najbardziej niekorzystnymi powłokami, ze względu na trwałość, okazały się powłoka TiN, CrN oraz MoS_2. W tym ostatnim przypadku (MoS_2) jest to tym bardziej interesujące, że powłoka tego typu dedykowana jest specjalnie na trące elementy maszyn (powłoka niskotarciowa), podobnie jak powłoka MoS_2/Ti, która jak zaznaczono wcześniej, okazała się najlepszą z przebadanych powłok pracujących w styku smarowanym olejem syntetycznym.

Kolejną serię badań przeprowadzono dla skojarzeń smarowanych olejem rzepakowym rafinowanym (RzR). Na Rys. 7 przedstawiono prawdopodobieństwo wystąpienia pittingu elementów z naniesionymi powłokami, smarowanych tym olejem.

Podobnie jak w przypadku oleju syntetycznego (PAO 8), najwyższą trwałością zmęczeniową charakteryzowało się skojarzenie, w którym stożki pokryte był powłoką MoS_2/Ti (Rys.8). Nie zmieniła się również kolejność w hierarchii trwałości pozostałych skojarzeń. Również w tym przypadku

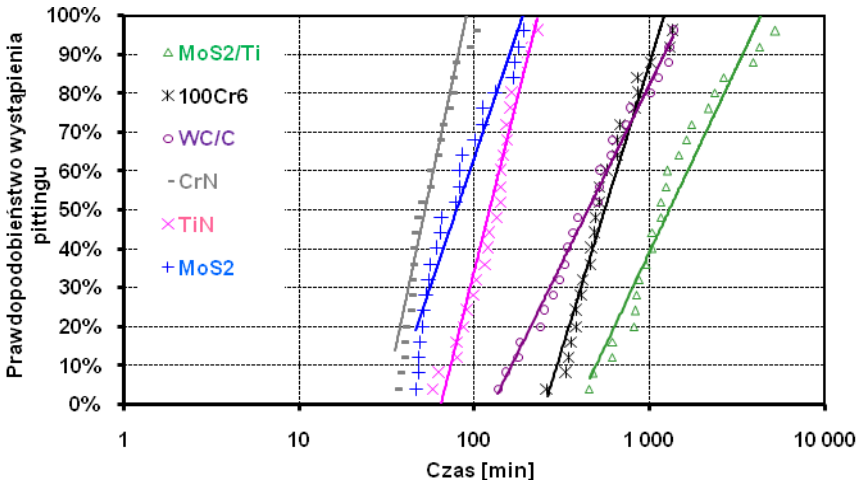

Rys. 5. Wyniki badań zmęczeniowych badanych skojarzeń materiałowych smarowanych olejem syntetycznym PAO 8

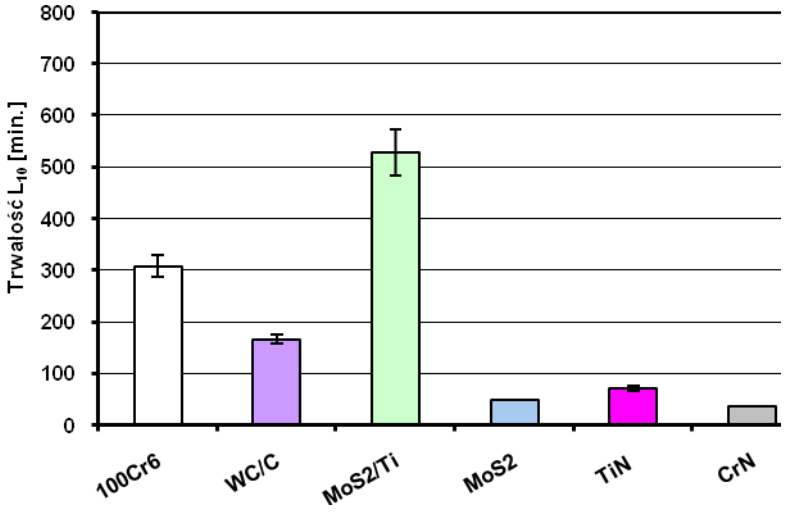

Rys. 6. Powierzchniowa trwałość zmęczeniowa L_{10} badanych skojarzeń materiałowych smarowanych olejem syntetycznym PAO 8

najniższe trwałości L_{10} otrzymano dla skojarzeń z naniesionymi powłokami TiN, CrN oraz MoS_2.

Należy jednak zaznaczyć, że w przypadku tego oleju skojarzenia 100Cr6-100Cr6 i WC/C-100Cr6 charakteryzowały się podobną (w stosunku do siebie) trwałością zmęczeniową, jednak znacznie niższą od skojarzenia, w którym element testowy pokryty był powłoką MoS_2/Ti. Dla pozostałych przebadanych skojarzeń smarowanych olejem roślinnym zaobserwowano ponad dwukrotny spadek powierzchniowej trwałości zmęczeniowej w stosunku do tych samych skojarzeń smarowanych olejem syntetycznym.

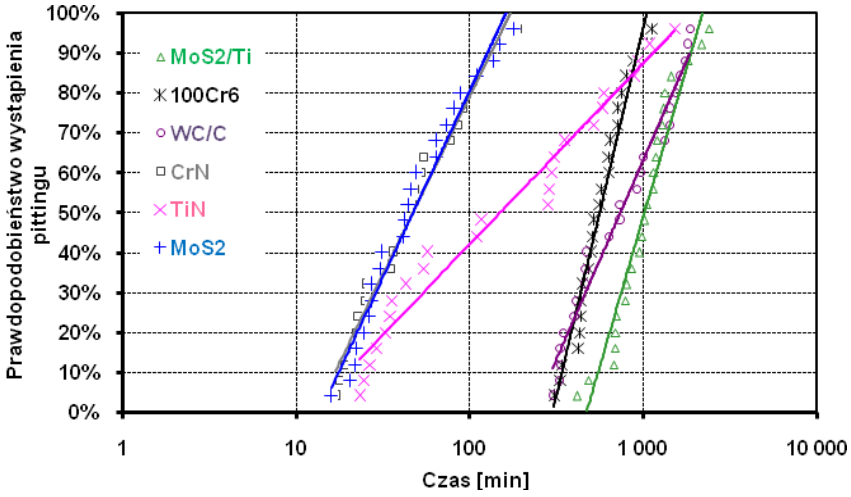

Rys. 7. Wyniki badań zmęczeniowych badanych skojarzeń materiałowych smarowanych olejem rzepakowym rafinowanym RzR

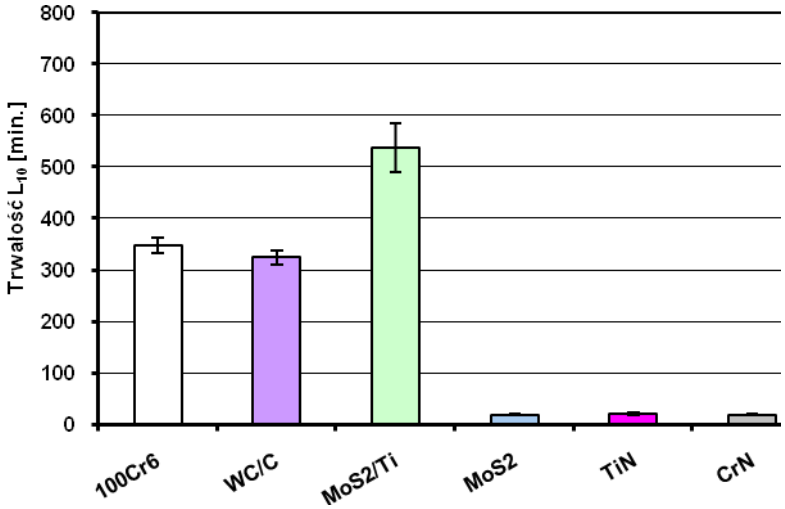

Rys. 8. Powierzchniowa trwałość zmęczeniowa L_{10} badanych skojarzeń materiałowych smarowanych olejem rzepakowym rafinowanym

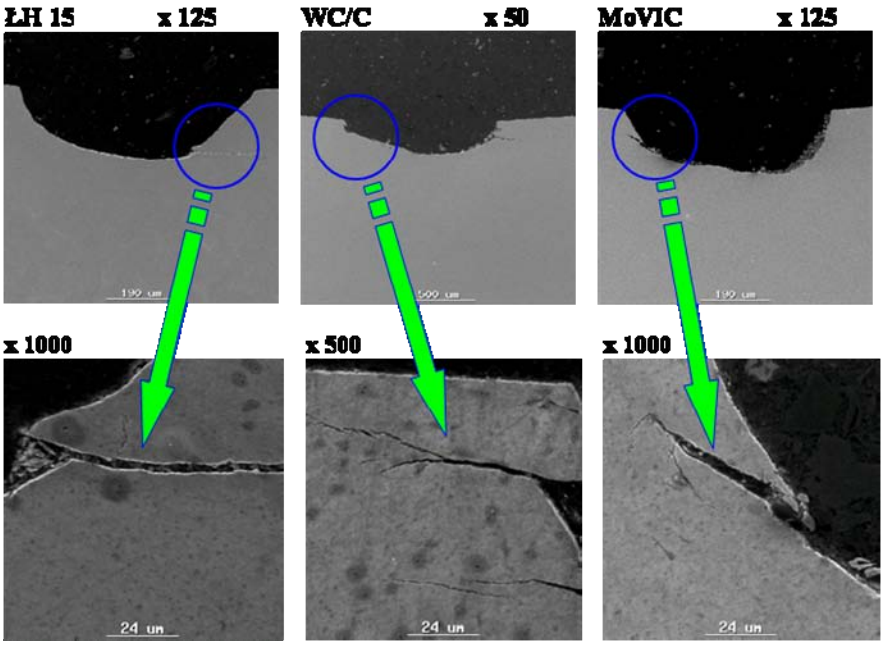

Rys. 9 Przykładowe obrazy pęknięć zmęczeniowych zidentyfikowane na elementach testowych

Z przeprowadzonych przez autorów badań analitycznych wynika jednoznacznie, że pittingowi ulega element z powłoką a nie sama powłoka (grubość powłoki ok. 2 μm a głębokość wyrwy pittingowej ok. 100 razy większa). Te różnice zaprezentowano dla stali i wybranych powłok na Rys. 9.

3. PODSUMOWANIE

Z przeprowadzonych badań wynika, że:

1. W przypadku smarowania olejem mineralnym praktycznie wszystkie powłoki naniesione na powierzchnie elementów wysokoobciążonych obniżają powierzchniową trwałość zmęczeniową:
   - z przebadanych skojarzeń największą trwałość, porównywalną z trwałością skojarzenia 100Cr6-100Cr6, posiadało skojarzenie WC/C-100Cr6,
   - elementy z powłokami niskotarciowymi (WC/C, MoS_2/Ti, MoS_2) smarowane olejem mineralnym posiadały trwałość zmęczeniową o rząd wyższą od typowych powłok nanoszonych na narzędzia (TiN, CrN).
2. W przypadku smarowania olejami syntetycznym i roślinnym najwyższą trwałość zmęczeniową odnotowano dla węzłów tarcia z elementami z powłoką niskotarciową MoS_2/Ti.
3. Skojarzenia 100Cr6-100Cr6 oraz WC/C-100Cr6 smarowane olejami syntetycznym i roślinnym posiadały powierzchniową trwałość zmęczeniową dużo niższą (prawie o połowę) od skojarzenia MoS_2/Ti-100Cr6.
4. W przypadku smarowania badanego styku olejem syntetycznym i roślinnym najniższymi opornościami na pitting charakteryzowały się skojarzenia TiN-100Cr6, CrN-100Cr6 i MoS_2-100Cr6.

Należy podkreślić, że na powierzchniowa trwałość zmęczeniową badanych skojarzeń **bardzo istotny wpływ miał rodzaj oleju bazowego**, którym skojarzenia było smarowane.

4. LITERATURA

[1] Vetter J.: *Vacuum arc coating for tools: potential and application. Surface and Coating Technology*. 1995, t. 76-77, s. 719÷724.

[2] Smolik, J., Walkowicz J., Bujak, J., Miernik, K.: *Badania eksploatacyjne powłok przeciwzużyciowych stosowanych w przemyśle maszynowym*. Problemy Eksploatacji. 1995, nr 2, s. 23÷38.

[3] Lewis, D.B., Bradbury, S.R., Sarwar, M.: *The effect of substrate surface preparation on the wear and failure modes of TiN coated high speed steel circular saw blades*. Wear. 1996, t. 197, s. 82÷88.

[4] Smolik J.: *Rola warstw hybrydowych typu warstwa azotowana/powłoka PVD w procesie zwiększania trwałości matryc kuźniczych*. Studia i Rozprawy, ITeE-PIB Radom, 2007

[5] Walkowicz J., Smolik J., Miernik K., Bujak J.: *Duplex surface treatments of moulds for pressure casting of aluminium*. Surface and Coating Technology. 1997, t. 97, s. 453÷464

[6] Navinsek, B., Panjan, P., Milosev, I.: *Industrial applications of CrN (PVD) coatings, deposited at high and low temperatures*. Surface and Coating Technology. 1997, t. 97, s. 182÷191.

[7] Pytko S.: *Badania mechanizmu niszczenia powierzchni tocznych elementów maszynowych*. Zeszyty naukowe AGH nr 191, Kraków 1967.
[8] Pytko S., Szczerek M.: *Pitting - forma niszczenia elementów tocznych*. Tribologia. 1993, nr 4/5, s. 317-334.
[9] Gawroński Z.: *Technologiczna warstwa wierzchnia w kołach zębatych i mechanizmach krzywkowych*. Politechnika łódzka, Monografie, 2005.
[10] Michalczewski R., Piekoszewski W., Wulczyński J.: *Metoda badania powierzchniowej trwałości zmęczeniowej elementów z powłokami przeciwzużyciowymi*. Problemy Eksploatacji, vol. 51 (4/2003), s. 91 ÷ 99.
[11] Michalczewski R., Piekoszewski W.: *The Method for Assessment of Rolling Contact Fatigue of PVD/CVD Coated Elements in Lubricated Contacts*. Tribologia, Finnish Journal of Tribology, vol. 25/2006 (4), s. 34÷43.
[12] Waligóra W.: *Rozrzut powierzchniowej trwałości zmęczeniowej łożysk tocznych*. Wydawnictwo Politechniki Poznańskiej. Poznań 2002.
[13] Libera M.: *Wpływ wybranych parametrów warstwy wierzchniej na powierzchniową trwałość zmęczeniową węzłów tocznych*. Rozprawa doktorska. Politechnika Poznańska, WMRiT, 2001 r.

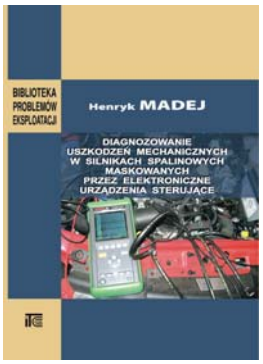

Henryk MADEJ

Diagnozowanie uszkodzeń mechanicznych w silnikach spalinowych maskowanych przez elektroniczne urządzenia sterujące

ITE Radom

W monografii podano przykłady diagnozowania wybranych przypadków uszkodzeń mechanicznych silników na podstawie różnych metod analizy sygnałów drganiowych zarejestrowanych na kadłubie i głowicy.

Przedstawiono ogólne problemy diagnozowania silników podkreślając, że przyczyną maskowania uszkodzeń są współczesne systemy sterowania silników. Niektóre uszkodzenia mechaniczne takie jak: narastające zużycie gniazd zaworowych i przylgni zaworów, przesunięcie faz rozrządu, zużycie gładzi cylindrowej nawet ponad wymiary dopuszczalne dla danego silnika, w wielu przypadkach potwierdzonych w praktyce nie stanowią podstawy do reakcji systemu diagnostycznego. Najczęstszą przyczyną tego stanu są stosowane algorytmy adaptacyjnego sterowania silników spalinowych. Uszkodzenia mechaniczne oraz zużycie eksploatacyjne, szczególnie we wczesnych fazach rozwoju są kompensowane przez adaptacyjne systemy regulacji wskutek przyjętych dopuszczalnych zakresów regulacji.

Podano wyniki analizy uszkodzeń występujących w pojazdach samochodowych ze szczególnym uwzględnieniem uszkodzeń silników, które są niewykrywalne przez systemy diagnostyki pokładowej OBD. Omówiono systemy sterowania silników oraz diagnozowanie silników spalinowych z wykorzystaniem modeli. W rozdziale czwartym przedstawiono zagadnienia związane z diagnozowaniem silników metodami wibroakustycznymi oraz najczęściej stosowane rodzaje analizy sygnałów.

W rozdziale 6 przedstawiono stanowiska, na których wykonywano badania oraz aparaturę użytą do badań. Identyfikację częstotliwości rezonansowych silników za pomocą analizy modalnej oraz charakterystyk rozbiegowych przedstawiono w rozdziale 7. W celu identyfikacji częstotliwości rezonansowych silnika przeprowadzono badania w warunkach pracy nieustalonej (rozruchu lub hamowania). Badania w tych warunkach umożliwiają obserwację odpowiedzi układu na różne, często niestacjonarne wymuszenia. W porównaniu z analizą modalną w tym eksperymencie można wyznaczyć częstotliwości rezonansowe w znacznie szerszym zakresie. Podstawowym celem tego eksperymentu była identyfikacja i rozdzielenie symptomów zjawisk występujących podczas pracy silnika w zmiennych warunkach, na co najmniej dwie grupy. W diagnostyce wyróżnia się grupę symptomów stanu zależnych od zmiennych warunków działania (np. prędkość obrotowa) oraz grupę symptomów związanych z częstotliwościami rezonansowymi, które nie zależą od warunków działania. Sygnał wibroakustyczny rejestrowany podczas badań w zmiennych warunkach działania zawiera często jednocześnie składowe szeroko i wąskopasmowe będące wynikiem zjawisk o znacznie różniących się długościach czasu trwania. Identyfikacja tych składowych wymagał stosowania analizy jednocześnie w dziedzinie czasu i częstotliwości.

W kolejnych rozdziałach przedstawiono wyniki eksperymentów czynnych na podstawie, których określono wpływ wybranych uszkodzeń mechanicznych silnika na generowany sygnał przyspieszeń drgań kadłuba i głowicy. Głównym zadaniem w procesie diagnozowania uszkodzeń mechanicznych silnika była separacja użytecznego sygnału wibroakustycznego oraz wybór charakterystycznych cech przetworzonego sygnału wrażliwych na uszkodzenia. Wczesne fazy rozwoju uszkodzeń w odróżnieniu od stanu zaawansowanego zużycia, nie zawsze wywołują zauważalny wzrost mocy sygnału WA. Początkowe fazy rozwoju uszkodzenia mogą powodować zmiany struktury częstotliwościowej sygnałów wyraźnie widoczne na płaszczyźnie czas-częstotliwość. Chwilowe zaburzenia sygnałów WA związane są między innymi z intensyfikacją zjawisk nieliniowych w trakcie formowania uszkodzeń, Ze względu ma niestacjonarny charakter rejestrowanych sygnałów drgań kadłuba i głowicy w badaniach wykorzystano metody przetwarzania sygnałów w dziedzinie czasu i częstotliwości takie jak transformata Wignera-Ville’a, dyskretna (DWT) i ciągła analiza falkowa (CWT), pakiety analizy falkowej (WPT), empiryczna dekompozycja sygnałów(EMD), oraz cepstrum i współczynniki Hoeldera. Wyniki tych analiz posłużyły między innymi do opracowania danych wejściowych do klasyfikatora neuronowego. W badaniach wykorzystano probabilistyczne sieci neuronowe (PNN). Przeprowadzone badania pozwoliły na budowę poprawnie działającego klasyfikatora neuronowego rozpoznającego różne stany techniczne silnika wywołane uszkodzeniami mechanicznymi.

Opracowano procedury przetwarzania sygnału drganiowego, które umożliwiają określenie miar zużycia eksploatacyjnego lub symulowanych lokalnych uszkodzeń.

W końcowym rozdziale autor przedstawił koncepcję systemu diagnozowania silnika samochodowego na podstawie pomiaru sygnałów wibroakustycznych.

Diagnostyka

Obszar zainteresowania czasopisma to:
- ogólna teoria diagnostyki technicznej
- eksperymentalne badania diagnostyczne procesów i obiektów technicznych;
- modele analityczne, symptomowe, symulacyjne obiektów technicznych;
- algorytmy, metody i urządzenia diagnozowania, prognozowania i genezowania stanów obiektów technicznych;
- metody detekcji, lokalizacji i identyfikacji uszkodzeń obiektów technicznych;
- sztuczna inteligencja w diagnostyce: sieci neuronowe, systemy rozmyte, algorytmy genetyczne, systemy ekspertowe;
- diagnostyka energetyczna systemów technicznych;
- diagnostyka systemów mechatronicznych i antropotechnicznych;
- diagnostyka procesów przemysłowych;
- diagnostyczne systemy utrzymania ruchu maszyn;
- ekonomiczne aspekty zastosowania diagnostyki technicznej;
- analiza i przetwarzanie sygnałów.

Topics discussed in the journal:
- General theory of the technical diagnostics,
- Experimental diagnostic research of processes, objects and systems,
- Analytical, symptom and simulation models of technical objects,
- Algorithms, methods and devices for diagnosing, prognosis and genesis of condition of technical objects,
- Methods for detection, localization and identification of damages of technical objects,
- Artificial intelligence in diagnostics, neural nets, fuzzy systems, genetic algorithms, expert systems,
- Power energy diagnostics of technical systems,
- Diagnostics of mechatronic and antropotechnic systems,
- Diagnostics of industrial processes,
- Diagnostic systems of machine maintenance,
- Economic aspects of technical diagnostics,
- Analysis and signal processing.

Wszystkie opublikowane artykuły uzyskały pozytywne recenzje wykonane przez niezależnych recenzentów.

All the published papers were reviewed positively by the independent reviewers.

Druk:
Centrum Graficzne „GRYF”, ul. Pieniężnego 13/2, 10-003 Olsztyn, tel. / fax: 89–527–24–30

Oprawa:
Zakład Poligraficzny, UWM Olsztyn, ul. Heweliusza 3, 10-724 Olsztyn
tel. 89-523-45-06, fax: 89-523-47-37

Announcement No 1

10th International
Science and Technology Conference

DPS'2011

Diagnostics of Processes and Systems

Zamość, Poland
19-21 September 2011

www: http://iair.mchtr.pw.edu.pl/dps11

Patronage
Committee for Automatic Control and Robotics, Polish Academy of Sciences

Wszystkie opublikowane w czasopiśmie artykuły uzyskały pozytywne recenzje, wykonane przez niezależnych recenzentów.
Redakcja zastrzega sobie prawo korekty nadesłanych artykułów.
Kolejność umieszczenia prac w czasopiśmie zależy od terminu ich nadesłania i otrzymania ostatecznej, pozytywnej recenzji.
Wytyczne do publikowania w DIAGNOSTYCE można znaleźć na stronie internetowej:
http://www.diagnostyka.net.pl

Redakcja informuje, że istnieje możliwość zamieszczania w DIAGNOSTYCE ogłoszeń i reklam.
Jednocześnie prosimy czytelników o nadsyłanie uwag i propozycji dotyczących formy i treści naszego czasopisma.
Zachęcamy również wszystkich do czynnego udziału w jego kształtowaniu poprzez nadsyłanie własnych opracowań związanych z problematyką diagnostyki technicznej. Zwracamy się z prośbą o nadsyłanie informacji o wydanych własnych pracach nt. diagnostyki technicznej oraz innych pracach wartych przeczytania, dostępnych zarówno w kraju jak i zagranicą.